An Endoplasmic Reticulum Junctional Structure Supports Nuclear Protein Quality Control and Viral Pathogenesis

by

Madison Lynn Pletan

A dissertation submitted in partial fulfillment
of the requirements for the degree of
Doctor of Philosophy
(Cellular and Molecular Biology)
in the University of Michigan
2024

Doctoral Committee:

Professor Billy Tsai, Chair
Professor Phyllis I. Hanson
Assistant Professor Shyamal Mosalaganti
Professor Carole Parent
Professor Kristen Verhey

Madison Lynn Pletan

mpletan@umich.edu

ORCID iD: 0000-0002-3603-9180

Dedication

To Dustin and Nate, my favorite guys.

To baby girl Pletan, for keeping me on my toes.

Acknowledgements

Thanks first to Billy Tsai: your enthusiastic (sometimes exhaustingly enthusiastic) love for data is only matched by your genuine care for your trainees. I've always known I can count on you to help me troubleshoot and brainstorm, whip up a recommendation letter within the hour, and support me through many big life changes. You've taught me to give myself one day to be sad about failures, then to get back up and try again. Thanks for being in my corner.

Thank you to all the members of the Tsai lab: Dr. Jay Chen, Jeff Williams, Jeff Knupp, Katy Speckhart, Dr. Tai-Ting Woo, Grace Cha, Ethan Houck, Dr. Riya Sarkar, Renaldo Sutanto, Dr. Chao-Yin Cheng, Whitney Reid, Emily Wang, and Luke Gohmann; and former members: Dr. Mara Harwood, Dr. Chelsey Spriggs, Dr. Xiaofang Liu, Dr. Parikshit Bagchi, Ellen James, Dr. Corey Cunningham, Dr. Allison Dupzyk, and Aaron Chang. You've lent antibodies, helped with ill-timed Western transfers, swapped toddler anecdotes, patiently explained protocols, and split mountains of Pacific Rim appetizers. I always tell Bill I joined his lab "just for the science," but in truth, I joined for the people. I could not have asked for a more supportive and positive lab environment the past five years. A special thanks to my CMB buddies Mara Harwood, Jeff Knupp, and Katy Speckhart—the seminars, retreats, and symposia were far more fun with you.

Thank you to the many passionate, talented science teachers and researchers who have mentored me over the years, especially Dr. Jason Rosé, Dr. Courtney Meyet, Dr. Silas Johnson, and Dr. Steven Triezenberg. Extra thanks to my first research mentor, Dr. Courtney Meyet, whose patience, unflappability, tenacity, and love for her students are unrivaled.

Thank you to all the friends, old and new, who have cheered me on. To Devon Dennison, thanks for the many commiserative lunches and your advice on dissertation writing. To the Ryds, Harmons, and Voyleses: I treasure your loyal friendship and look forward to many more years of sharing parenting, podcasts, and too-long book selections together. To my Grace Group family: thank you for your listening ears, encouraging texts, and wisdom. I am deeply grateful for every one of you.

Thank you to my family: my far funnier and better-at-keeping-in-touch siblings, Kolson and Reagan, and the wonderfully vast and loving Pletan clan. It's easy to get bogged down in experiments, but FaceTimes, Snapchats, and long phone calls with all of you keep me feeling grounded and loved. To my parents: you both (but especially Mom) have sacrificed so much and worked so hard for my education, long before I could notice or appreciate it. I've always known beyond question that you will be here whenever I need you. Thank you for checking in, for praying for me every day, and for spending two months coaxing Nate to take bottles and naps.

To Nathaniel: your infectious laugh and exploratory antics have brightened every long day of manuscript writing. Thanks for being my unwitting in-utero lab buddy and a little hypothesis-testing scientist all of your own.

To Dustin, for acts of unconditional love too numerous to list. Thank you for carrying our family through the failed-experiment tears, the newborn exhaustion, and the dissertation marathon. You are the best cheerleader and the best teammate; this degree is (at least) half yours.

Chapters 1 and 2 have been drawn, in part or in full, from multi-author publications with contributions from Jeff Knupp, Dr. Xiaofang Liu, Grace Cha, and Dr. Jay Chen. Funding sources are detailed in the Acknowledgements section of each chapter.

Table of Contents

List of Figures

Abstract

The endoplasmic reticulum (ER) is a dynamic network of membranous sheets and tubules that extends throughout the cell body and acts as a hub for protein synthesis and folding, protein quality control, phospholipid and steroid biosynthesis, calcium homeostasis, and organelle biogenesis, among other functions. To accomplish this wide range of functions, the ER exhibits remarkable structural diversity. Its continuous membrane is constantly shaped and remodeled by various morphogenic proteins, including reticulons (curvature-inducing proteins that support tubule formation), atlastins (fusogenic proteins that bring opposing tubules together), and lunapark (membrane proteins that stabilize the resulting tubular junctions). This dissertation examines two unexpected functions of the ER junctional sites: 1) as quality control storage sites for mislocalized nuclear proteins, and 2) as penetration sites for a nonenveloped virus.

The nuclear pore complex (NPC) is the large, modular channel mediating all cargo transport in and out of the nucleus; it is composed of 30 individual nucleoporins (Nups) assembled in strict stoichiometries. Mislocalization of Nups to the cytoplasm has been observed in many neurodegenerative diseases and some cancers, but the cellular response to this phenomenon is unclear. In this research, we describe a model system of Nup mislocalization and identify a discrete storage site at the ER membrane where excess Nups are routed (with the activity of the kinesin-1 motor and several ER morphogenic proteins). Furthermore, we show that the storage site sequesters Nups from re-localizing at the nuclear envelope and disrupting

nucleo-cytoplasmic transport. Thus, this ER junctional site serves a quality control function for nuclear pore proteins.

The second portion of this dissertation focuses on how ER junctions are exploited by a different large, proteinaceous cargo: SV40 polyomavirus virions. On their journey to the nucleus for replication, SV40 particles transit through the ER lumen, where they undergo a series of conformational changes to prepare them to penetrate the ER membrane at "foci" sites. Subsequently, the virus escapes into the cytosol and enters the nucleus to cause infection. Here we show that two prominent ER fusogenic proteins, ATL2 and ATL3, play critical, yet distinct roles in facilitating SV40 membrane penetration. ATL3 mobilizes to the virus-induced ER foci, where it engages an SV40-containing membrane penetration complex and promotes fusion of ER tubules via its GTPase activity. ATL2 does not mobilize to the foci or directly engage the virus; rather, it supports the reticulated ER morphology more broadly, allowing ATL3 to interact with the morphogenic complex. These findings show how a virus can hijack the ER-morphogenic activity of host proteins, reshaping the ER architecture to carry out its replication cycle.

Together, the chapters of this dissertation highlight how the basic junctional structure of the ER can support two disparate cellular processes: storage of mislocalized nucleoporins and membrane penetration of a nonenveloped virus. In both cases, the ER-morphogenic machinery enables the ER membrane to harbor large, proteinaceous particles at distinct perinuclear depots.

Chapter 1
The Endoplasmic Reticulum Is a Dynamic, Membranous Network That Functions in Protein Quality Control and Viral Pathogenesis

With permission from the publishers, portions of this chapter have been adapted from two previous publications:

Autophagy of the ER: the secretome finds the lysosome

Jeffrey Knupp[†], Madison L. Pletan[†], Peter Arvan, and Billy Tsai (2023).

The FEBS Journal, 290 (24), 5656-5673. https://doi.org/10.1111/febs.16986;

[†]co-first authors

and

Non-enveloped virus membrane penetration: New advances leading to new insights

Madison L. Pletan and Billy Tsai (2022)

PLoS Pathogens, 8 (12), e1010948. https://doi.org/10.1371/journal.ppat.1010948

1.1 Introduction

Extending from the nuclear envelope throughout the cytoplasm, the endoplasmic reticulum (ER) is a vast, interconnected organelle that supports a wide range of cellular activities. Canonically, the ER is primarily identified as a major site of protein biogenesis, folding, and modification: for example, within the ER lumen of a professional secretory cell such as a pancreatic beta cell, as many as 6000 molecules of the secretory protein proinsulin can be

synthesized per second.[1] Yet in addition to synthesizing an estimated one-third of the cellular proteome, the ER also supports protein translocation and secretion, phospholipid and steroid biosynthesis, calcium homeostasis, and organelle biogenesis. To understand how the ER successfully executes these diverse functions, we must first examine the structural diversity of this large organelle.

1.2 Basic structure of the endoplasmic reticulum subdomains

The endoplasmic reticulum network extends throughout the cell body and contains three continuous, yet morphologically and functionally distinct, subdomains: (1) the nuclear envelope, (2) ER sheets, and (3) ER tubules (Fig. 1.1).[2,3]

The nuclear envelope (NE) encloses the nuclear compartment, including the nuclear genome, and is comprised of the inner (INM) and outer (ONM) nuclear membranes. Between these membranes is the perinuclear space (PNS), a subdomain of the ER lumen.[4] The NE undergoes extensive remodeling over time, most notably during cell division, when the envelope must break down to allow the mitotic spindle to access the genome.[5] During anaphase, the NE rapidly reforms from the mitotic ER, where transmembrane NE proteins have been temporarily stored, and nuclear compartmentalization is re-established.[5-7] While the most basic function of this double membrane is to shield the nuclear genome from the cytoplasm, it is far more than a simple barrier: the NE also regulates nucleo-cytoplasmic transport, contributes to chromatin organization, and transduces signals.[4,8-10]

Though the NE is continuous with the perinuclear ER, it is characterized by enrichment of key nuclear proteins not typically found elsewhere in the ER.[4] One primary example is the nucleoporins (“Nups”), a group of 30 proteins that assemble into nuclear pore complexes

(NPCs), massive channels that bridge and fuse the ONM and INM.[11] Whereas the NE maintains nuclear compartmentalization, the NPCs govern transport of RNAs, transcription factors, and other crucial cargoes into and out of the nucleus.[11,12] Cargoes transit through a central channel lined with intrinsically disordered Nups, which interact to form a selectively permeable mesh barrier.[11,13] (For further discussion of the NPC, see Chapter 2.) Besides Nups, the NE also harbors a number of other unique proteins, including nesprins, the SUN family, emerin and other lamin-associated proteins, and more.[14] Some of these are scaffolding proteins that span the nuclear envelope and anchor to the cytoskeleton on one end and the nuclear lamina on the other, providing structural stability and transmission of mechanical forces.[15,16] Furthermore, some interact with transcription factors to influence gene expression.[17] Mislocalizations of various NE proteins have been linked to a variety of human diseases, including many aging-related and neurodegenerative diseases.[18,19]

Similar to the nuclear envelope, ER sheets are low-curvature double membranes surrounding ER lumen. They are predominantly located contiguous with the NE and stack to form cisternae, which are connected by twisted, helicoidal membrane "ramps."[3,20] The ratio of sheets to tubules in each cell varies by cell type and phase of the cell cycle.[21] Since protein biosynthesis primarily occurs at the ER sheets, professional secretory cells with high levels of protein production are dominated by ER sheets.[3]

The cytosolic faces of the ER sheets are enriched for ribosomes, creating the classic "rough ER" appearance by electron microscopy.[22,23] (In fact, the ribosomes themselves may contribute to the sheet morphology: some studies have suggested that the presence of ribosomes stabilizes the ER sheets, as stripping ribosomes with puromycin converts sheets to highly branched tubules.[21,24]) Consequently, the ER sheets are a prime site for protein biosynthesis via

co-translational translocation, the best-known function of the organelle. Briefly, the ribosome-mRNA complex is recruited to the Sec61 translocon channel on the ER membrane, where the ribosome feeds the nascent polypeptide chain into the ER.[25] After translation is complete, various ER luminal chaperones assist with initial protein folding and processing.[3] If the polypeptide in question is destined to become a membrane protein, its membrane insertion process may be mediated by the ER membrane protein complex (EMC), a multi-subunit complex that associates with the Sec61 translocon and drives co-translational membrane insertion of many multi-pass membrane proteins.[26,27] Once the newly synthesized protein has been properly folded and/or inserted, it exits the ER to continue along the secretory pathway.[3]

Finally, the ER tubules create the highly branched, "reticulated" morphology for which the endoplasmic reticulum was named. Whereas the ER sheets are composed of stacked layers of flat, parallel membrane bilayers linked by membrane helices, ER tubules have a high degree of membrane curvature, forming membrane tubes with a 50-100 nm diameter in mammalian cells.[28,29] (The thickness of the ER lumen cross-section is similar across sheets and these tubules.[29]) Recent work with super-resolution microscopy suggests that certain cell types may also exhibit ribbon-like, ultra-narrow ER tubules.[30] Regardless of their precise shape and diameter, ER tubules extend throughout the cell body to the periphery, remodel dynamically, and make contact with virtually every cellular organelle.[28,30,31] During mitosis, the ER morphology of some cell types shifts from a mixture of cisternae and tubules to all tubules, which some researchers have suggested may allow the cell to more evenly divide the structure between daughter cells.[22,32] Additionally, the presence of ER-morphogenic proteins is important for the re-formation of the nuclear envelope; the rate of NE formation is sensitive to the level of curvature-shaping proteins in the nearby ER.[32-34]

What machinery is responsible for shaping the ER membrane into highly curved and interconnected tubules? The first major ER-morphogenic proteins identified to shape both tubules and the curved edges of cisternae were the reticulon family and DP1/Yop1, integral membrane proteins conserved across eukaryotes.[35-37] Overexpression of these factors causes ER sheets to convert to tubules, and depletion causes the reverse.[33,36,38] Both the reticulons (RTNs) and DP1 rely on their membrane-embedded, hydrophobic double hairpin structures to stabilize local regions of high curvature.[35,38,39] For the RTN family, these hairpin structures are located at the C-terminus and comprise the reticulon homology domain (RHD).[40] The curvature-inducing RTNs cooperate with two other ER-morphogenic proteins, atlastins (ATLs) and lunapark (LNP), to form and maintain the "three-way junctions" where tubules intersect.[41] In the current model, RTNs initiate high membrane curvature, allowing for the formation of ER tubules. ATLs, a family of membrane-anchored GTPases, mediate the fusion of neighboring tubules: when ATLs on opposing membranes come into proximity, they dimerize and undergo a GTP-hydrolysis-dependent conformational change that allows the membranes to pull together and fuse.[42-44] Inhibition or depletion of ATLs causes the peripheral ER to form into long, unbranched tubules rather than the typically crisscrossed, reticulated network.[41] Once the membranes have initially been fused by ATL, the membrane protein LNP moves in to stabilize the nascent three-way junction.[45,46] While LNP is not essential for the formation of an ER tubular network, its absence causes a reduction in tubules and a corresponding increase in peripheral sheets.[41] Thus, RTNs, ATLs, and LNP work in cooperation to generate the three-way junctions characteristic of the peripheral ER (Fig 1.1).

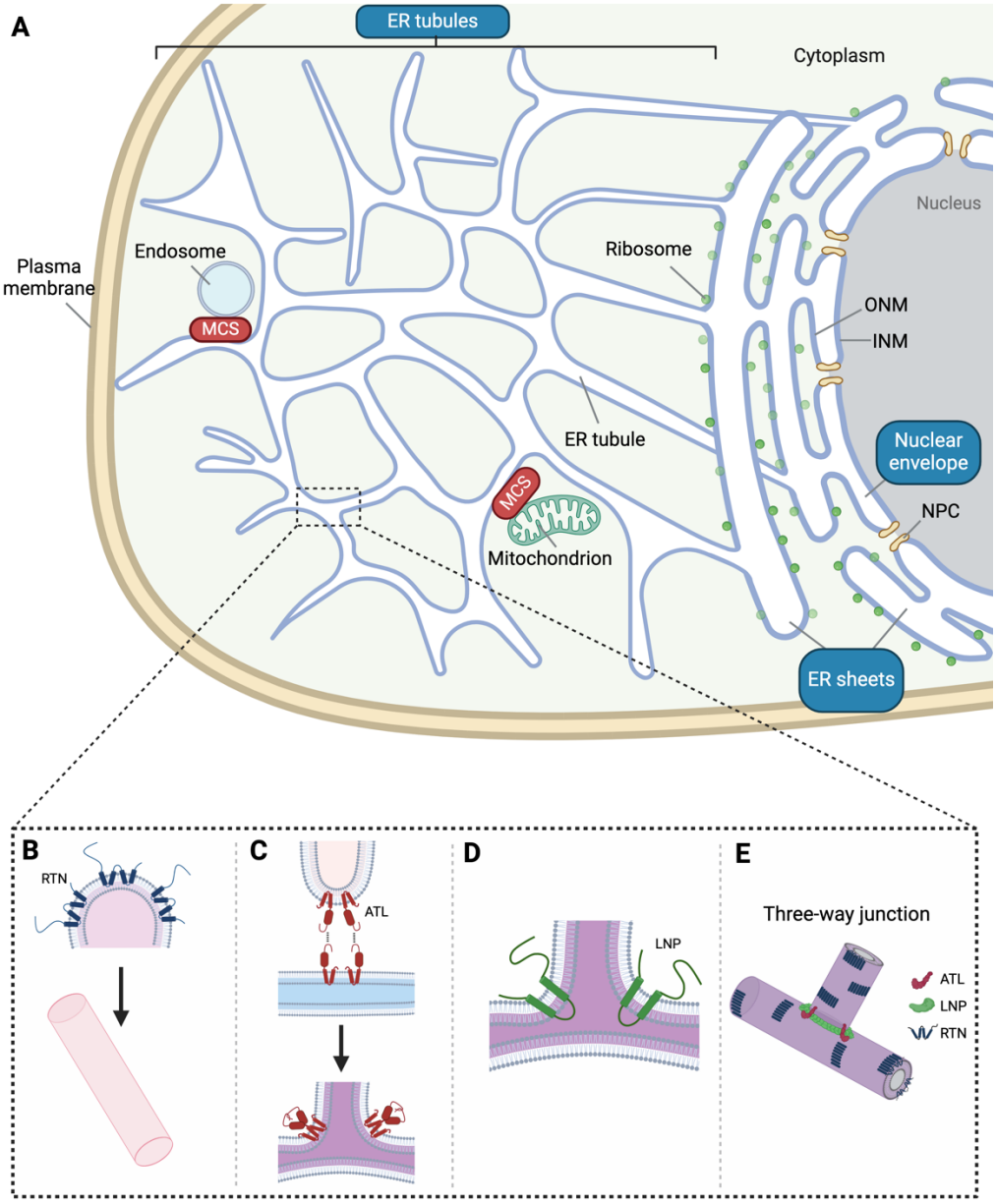

Figure 1.1: Overview of the ER structure and key peripheral morphogenic proteins

(A) The ER network is comprised of the nuclear envelope (including ONM and INM, fused at NPCs), perinuclear ER sheets (stacked in cisternae and studded with ribosomes), and peripheral ER tubules. (B-E) The ER-morphogenic proteins support formation of three-way junctions. (B) RTNs allow tubule formation by stabilizing membrane curvature. (C) ATLs dimerize and undergo a conformational shift, catalyzing membrane fusion of nearby tubules. (D) LNP is recruited to and stabilizes the junctions. (E) The final product of the membrane fusion activity is the three-way junction. Figure created with Biorender.com; portions adapted from Woo et al 2023 with permission.[47]

As we have already described, the ER subdomains carry out many functions beyond protein translation: shielding chromatin, regulating nucleo-cytoplasmic transport, influencing gene expression, folding and processing newly synthesized proteins, and inserting transmembrane proteins across membranes, to name a few. Several additional important functions of the ER are carried out at membrane contact sites (MCS, see Fig. 1.1). Since the peripheral ER extends throughout the cell body, ER membranes contact virtually every cellular organelle, including mitochondria, Golgi, endosomes, and peroxisomes.[22,48] At these dynamic contacts, the smooth ER membrane is in close apposition to the membrane of another organelle, tethered together by anchored proteins and/or lipids but not fully fusing.[49] Perhaps the best-characterized of the MCS are the ER-mitochondrial contact sites (EMCS), which play an important role in biological functions including Ca^{2+} signaling, lipid transfer, autophagy, and ROS signaling.[50] A growing body of research has examined the high-resolution structural details of various ER contact sites, their wide-ranging functional implications, and their role in human disease.[51-53]

1.3 Protein quality control at the endoplasmic reticulum

Given the central role of the ER in protein biosynthesis, it is not surprising that the organelle is also a hub of protein quality control pathways. Aberrant proteins may arise at any stage of the synthetic and processing pathway: genetic mutations, transcriptional errors, improper folding, incomplete or erroneous posttranslational modifications, and exposure to oxidative stressors may all result in proteins that are prone to aggregation.[54] Some mutant or misfolded proteins may not only lose their native function but also exercise a dominant-negative effect,

trapping properly folded proteins and preventing normal secretion.[54,55] To avoid these pitfalls and maintain proteostasis, it is imperative that the ER support robust protein quality control mechanisms. Two well-characterized pathways are ER-associated protein degradation (ERAD) and ER-coupled autophagy (ER-phagy; also known as ER-to-lysosome-associated degradation, or ERLAD), the details of which we outline briefly below.

In ERAD, misfolded proteins are targeted for proteasomal degradation in a ubiquitin-dependent pathway. ERAD substrates, including both soluble luminal and membrane proteins, are first recognized by an E3 ubiquitin ligase complex and retrotranslocated across the ER membrane to the cytosol.[56] Once exposed to the cytosol, the substrate is polyubiquitinated by an E3 ubiquitin ligase, extracted from the ER membrane, and targeted to the proteasome to be degraded (Fig 1.2A).[56] Historically, ERAD has been extensively studied in yeast, with 3 well-characterized branches classified by the ubiquitin ligase complexes used (Hrd1, Doa10, and Asi).[56,57] Mammalian cells have at least 10 known ubiquitin ligases, and the range of substrates is not known for all of them.[58]

In contrast to ERAD, ER-phagy is a subset of macro-autophagy that targets the contents of the ER for degradation by the lysosome. A simplified view of macro-autophagy can be boiled down to a handful of distinct steps, which include the following: (a) formation of the omegasome on the ER membrane, (b) maturation of the omegasome into the "phagophore" membrane (also called the isolation membrane), (c) phagophore elongation and closure to form the double-membrane organelle called the autophagosome, which contains the cargo destined to be degraded, and (d) fusion of the autophagosome with the lysosome to deliver its contents to the lytic lysosomal lumen.[59] ER-phagy can function during metabolic stress, degrading portions of the ER in bulk to provide necessary nutrients, or it may be used as a more selective protein

quality control pathway, restoring ER proteostasis from aggregates of misfolded or toxic proteins.[60,61] In the latter case, selectivity is achieved via interaction of ER-phagy substrates with critical ER membrane proteins, termed ER-phagy receptors. These receptors—acting in conjunction with their associated adaptors—function by recruiting the degradative cargo on the luminal side of the ER and binding to the autophagy machinery on the cytosolic side of the ER. In this manner, the receptors can deliver the cargo for lysosomal degradation (Fig 1.2B).[61] Although ER components have been found in the lysosomes since the earliest description of the autophagy process, how the ER is targeted to the lysosome during autophagy was not understood until the discovery of the first autophagy receptor FAM134B in 2015.[60] Since then, several other ER-phagy receptors have been identified, including Sec62, RTN3, CCPG1, ATL3, and Tex264.[62] Not surprisingly, either compromised or hyperactive ER-phagy can lead to disease outcomes, ranging from metabolic disease to neurodegenerative disease to certain cancers.[63]

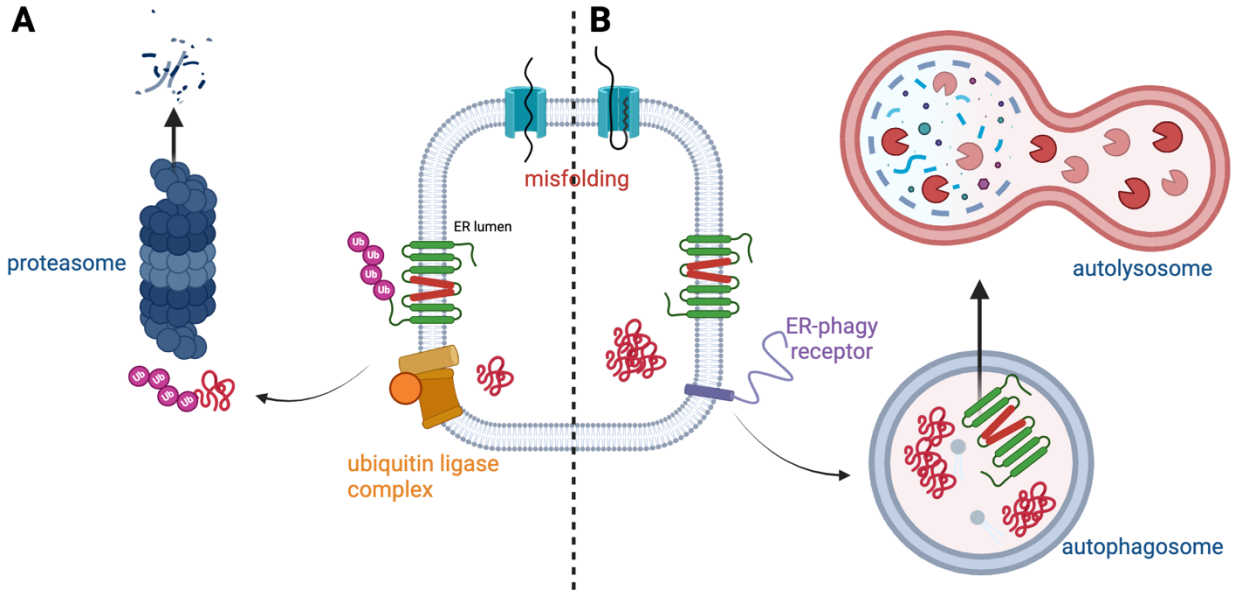

Figure 1.2: Simplified schematic of ERAD and ER-phagy pathways

(A) In ERAD, misfolded proteins are recognized by a ubiquitin ligase complex, retrotranslocated across the ER membrane, polyubiquitinated, and delivered to the proteasome for degradation. (B) In ER-phagy, misfolded protein

aggregates are recognized by an ER-phagy receptor, taken up into an autophagosome, and delivered to the lysosome for degradation.

Chapter 2 of this dissertation is focused on investigating quality control of nucleoporins (Nups; discussed in Section 1.2 above) at discrete sites in the ER. Because the NPC subcomplexes assemble in strict stoichiometries, it is crucial for cells to recognize and respond to misassembled and/or mislocalized Nups. The work described in this dissertation identifies a junctional storage site at the ER membrane for mislocalized Nups, where the long-lived Nups are sequestered to preserve partial functionality of the remaining NPCs. Thus, the protein quality control activity is not achieved by turnover (via either ERAD or ER-phagy), but by storage and sequestering of the excess proteins.

1.4 ER and viral pathogenesis

Many viruses rely heavily on the ER during their replication cycle: a few transit through the compartment *en route* to the nucleus, some simply use ER protein biosynthesis machinery to translate their genomes, and still others remodel significant portions of the ER membrane into full-fledged genome replication factories.[47,64] Understanding the cellular machinery hijacked by each virus is a crucial part of creating targeted therapeutics to disrupt the viral replication cycles, limiting infection. Below, we briefly discuss hallmark examples of ER-hijacking viruses, including both DNA and RNA viruses.

With the exception of nucleocytoplasmic large DNA viruses like the poxvirus family, all DNA viruses must eventually enter the nucleus in order to access the DNA replication machinery necessary to make copies of their genomes.[65] Relatively few DNA viruses transit through the ER

as part of their productive infectious pathway, but one notable exception is simian virus 40 (SV40), the prototype polyomavirus.[64] A nonenveloped virus with an icosahedral capsid, SV40 is endocytosed and targeted to the ER lumen, where it utilizes ER-resident oxidoreductase chaperones to perform partial uncoating of some of its major capsid protein.[47,66] It must then penetrate the ER membrane, no small feat given the virus's lack of a lipid envelope.[66] To accomplish this, SV40 remodels the ER membrane to form an "ER-focus" suborganellar structure, recruiting a suite of transmembrane proteins, molecular motors, and cytosolic factors to extract viral particles into the cytosol; nearly a dozen individual host components have been identified as indispensable for the penetration/extraction process.[67-70] SV40 thus represents a rare example of a DNA virus that remodels the ER membrane in a significant manner as part of its productive entry pathway.

Major ER morphological change is also a feature of the replication cycles of many RNA viruses; notably, flaviviruses and coronaviruses convert portions of the ER into suborganellar viral "factories." Flaviviruses, for instance, transit to the ER following receptor-mediated endocytosis and cytosolic uncoating. Upon co-translational translocation of the viral RNA message, some of the newly-synthesized viral non-structural proteins are used to remodel the ER membrane, forming ER-derived organelle-like structures where the viral genome replicates, though the precise morphology of these structures varies between viruses.[71] Following replication, the amplified viral genome is transferred to assembly sites also thought to be at the ER membrane.[72] Progeny nucleocapsids bud into the ER lumen, traffic to the Golgi apparatus for maturation, and are finally secreted for the next round of infection.[73] Similarly, during coronavirus infection, non-structural proteins translated from the viral RNA trigger formation of organelle-like double-membraned vesicles (DMVs) derived from ER membrane. These DMVs

serve as replication factories for the viral genome.[74] The newly-replicated genomes transit back to the ER, where they are translated to generate virus structural proteins that are in turn packaged into immature viral protein complexes. These complexes are finally transported through the ER-Golgi intermediate compartment (ERGIC) for maturation, assembly, and secretion.[75,76] The parallels between the flavivirus and coronavirus infection cycles are clear: both require extensive remodeling of the ER membrane in order to generate ER-derived replication organelles.

Chapter 3 of this dissertation elucidates SV40 infection, illuminating the precise molecular architecture of the SV40-induced "ER-foci." These structures in the ER support ER-to-cytosol membrane penetration of the virus essential during infection. Specifically, the work described in this dissertation will link the virus-induced penetration structure to the native ER morphology, demonstrating that the atlastin family of ER-fusion proteins are crucial in forming the ER-foci.

1.5 References

1. Schuit FC, Kiekens R, Pipeleers DG. Measuring the balance between insulin synthesis and insulin release. *Biochem Biophys Res Commun*. Aug 15 1991;178(3):1182-7. doi:10.1016/0006-291x(91)91017-7

2. Shibata Y, Hu J, Kozlov MM, Rapoport TA. Mechanisms shaping the membranes of cellular organelles. *Annu Rev Cell Dev Biol*. 2009;25:329-54. doi:10.1146/annurev.cellbio.042308.113324

3. Schwarz DS, Blower MD. The endoplasmic reticulum: structure, function and response to cellular signaling. *Cell Mol Life Sci*. Jan 2016;73(1):79-94. doi:10.1007/s00018-015-2052-6

4. Hetzer MW. The nuclear envelope. *Cold Spring Harb Perspect Biol*. Mar 2010;2(3):a000539. doi:10.1101/cshperspect.a000539

5. Ungricht R, Kutay U. Mechanisms and functions of nuclear envelope remodelling. *Nat Rev Mol Cell Biol*. Apr 2017;18(4):229-245. doi:10.1038/nrm.2016.153

6. Anderson DJ, Vargas JD, Hsiao JP, Hetzer MW. Recruitment of functionally distinct membrane proteins to chromatin mediates nuclear envelope formation in vivo. *J Cell Biol*. Jul 27 2009;186(2):183-91. doi:10.1083/jcb.200901106

7. Ulbert S, Platani M, Boue S, Mattaj IW. Direct membrane protein-DNA interactions required early in nuclear envelope assembly. *J Cell Biol*. May 22 2006;173(4):469-76. doi:10.1083/jcb.200512078

8. Reddy KL, Zullo JM, Bertolino E, Singh H. Transcriptional repression mediated by repositioning of genes to the nuclear lamina. *Nature*. Mar 13 2008;452(7184):243-7. doi:10.1038/nature06727

9. Koszul R, Kim KP, Prentiss M, Kleckner N, Kameoka S. Meiotic chromosomes move by linkage to dynamic actin cables with transduction of force through the nuclear envelope. *Cell*. Jun 27 2008;133(7):1188-201. doi:10.1016/j.cell.2008.04.050

10. De Magistris P, Antonin W. The Dynamic Nature of the Nuclear Envelope. *Curr Biol*. Apr 23 2018;28(8):R487-r497. doi:10.1016/j.cub.2018.01.073

11. Beck M, Hurt E. The nuclear pore complex: understanding its function through structural insight. *Nat Rev Mol Cell Biol*. Feb 2017;18(2):73-89. doi:10.1038/nrm.2016.147

12. Petrovic S, Mobbs GW, Bley CJ, Nie S, Patke A, Hoelz A. Structure and Function of the Nuclear Pore Complex. *Cold Spring Harb Perspect Biol*. Dec 1 2022;14(12)doi:10.1101/cshperspect.a041264

13. Frey S, Richter RP, Görlich D. FG-rich repeats of nuclear pore proteins form a three-dimensional meshwork with hydrogel-like properties. *Science*. Nov 3 2006;314(5800):815-7. doi:10.1126/science.1132516

14. Hahn L, Carvalho P. Making and breaking the inner nuclear membrane proteome. *Curr Opin Cell Biol*. Oct 2022;78:102115. doi:10.1016/j.ceb.2022.102115

15. Starr DA, Fridolfsson HN. Interactions between nuclei and the cytoskeleton are mediated by SUN-KASH nuclear-envelope bridges. *Annu Rev Cell Dev Biol*. 2010;26:421-44. doi:10.1146/annurev-cellbio-100109-104037

16. Hieda M. Signal Transduction across the Nuclear Envelope: Role of the LINC Complex in Bidirectional Signaling. *Cells*. Feb 4 2019;8(2)doi:10.3390/cells8020124

17. Heessen S, Fornerod M. The inner nuclear envelope as a transcription factor resting place. *EMBO Rep*. Oct 2007;8(10):914-9. doi:10.1038/sj.embor.7401075

18. Shin JY, Worman HJ. Molecular Pathology of Laminopathies. *Annu Rev Pathol*. Jan 24 2022;17:159-180. doi:10.1146/annurev-pathol-042220-034240

19. Liu J, Hetzer MW. Nuclear pore complex maintenance and implications for age-related diseases. *Trends Cell Biol*. Mar 2022;32(3):216-227. doi:10.1016/j.tcb.2021.10.001

20. Terasaki M, Shemesh T, Kasthuri N, et al. Stacked endoplasmic reticulum sheets are connected by helicoidal membrane motifs. *Cell*. Jul 18 2013;154(2):285-96. doi:10.1016/j.cell.2013.06.031

21. Puhka M, Vihinen H, Joensuu M, Jokitalo E. Endoplasmic reticulum remains continuous and undergoes sheet-to-tubule transformation during cell division in mammalian cells. *J Cell Biol*. Dec 3 2007;179(5):895-909. doi:10.1083/jcb.200705112

22. English AR, Zurek N, Voeltz GK. Peripheral ER structure and function. *Curr Opin Cell Biol*. Aug 2009;21(4):596-602. doi:10.1016/j.ceb.2009.04.004

23. West M, Zurek N, Hoenger A, Voeltz GK. A 3D analysis of yeast ER structure reveals how ER domains are organized by membrane curvature. *J Cell Biol*. Apr 18 2011;193(2):333-46. doi:10.1083/jcb.201011039

24. Puhka M, Joensuu M, Vihinen H, Belevich I, Jokitalo E. Progressive sheet-to-tubule transformation is a general mechanism for endoplasmic reticulum partitioning in dividing mammalian cells. *Mol Biol Cell*. Jul 2012;23(13):2424-32. doi:10.1091/mbc.E10-12-0950

25. Itskanov S, Park E. Mechanism of Protein Translocation by the Sec61 Translocon Complex. *Cold Spring Harb Perspect Biol*. Jan 3 2023;15(1)doi:10.1101/cshperspect.a041250

26. Bai L, You Q, Feng X, Kovach A, Li H. Structure of the ER membrane complex, a transmembrane-domain insertase. *Nature*. Aug 2020;584(7821):475-478. doi:10.1038/s41586-020-2389-3

27. Guna A, Volkmar N, Christianson JC, Hegde RS. The ER membrane protein complex is a transmembrane domain insertase. *Science*. Jan 26 2018;359(6374):470-473. doi:10.1126/science.aao3099

28. Hu J, Prinz WA, Rapoport TA. Weaving the web of ER tubules. *Cell*. Dec 9 2011;147(6):1226-31. doi:10.1016/j.cell.2011.11.022

29. Shibata Y, Voeltz GK, Rapoport TA. Rough sheets and smooth tubules. *Cell*. Aug 11 2006;126(3):435-9. doi:10.1016/j.cell.2006.07.019

30. Wang B, Zhao Z, Xiong M, Yan R, Xu K. The endoplasmic reticulum adopts two distinct tubule forms. *Proc Natl Acad Sci U S A*. May 3 2022;119(18):e2117559119. doi:10.1073/pnas.2117559119

31. Friedman JR, Voeltz GK. The ER in 3D: a multifunctional dynamic membrane network. *Trends Cell Biol*. Dec 2011;21(12):709-17. doi:10.1016/j.tcb.2011.07.004

32. Zhao G, Liu S, Arun S, Renda F, Khodjakov A, Pellman D. A tubule-sheet continuum model for the mechanism of nuclear envelope assembly. *Dev Cell*. May 22 2023;58(10):847-865.e10. doi:10.1016/j.devcel.2023.04.003

33. Anderson DJ, Hetzer MW. Reshaping of the endoplasmic reticulum limits the rate for nuclear envelope formation. *J Cell Biol*. Sep 8 2008;182(5):911-24. doi:10.1083/jcb.200805140

34. Kiseleva E, Morozova KN, Voeltz GK, Allen TD, Goldberg MW. Reticulon 4a/NogoA locates to regions of high membrane curvature and may have a role in nuclear envelope growth. *J Struct Biol*. Nov 2007;160(2):224-35. doi:10.1016/j.jsb.2007.08.005

35. Shibata Y, Shemesh T, Prinz WA, Palazzo AF, Kozlov MM, Rapoport TA. Mechanisms determining the morphology of the peripheral ER. *Cell*. Nov 24 2010;143(5):774-88. doi:10.1016/j.cell.2010.11.007

36. Voeltz GK, Prinz WA, Shibata Y, Rist JM, Rapoport TA. A class of membrane proteins shaping the tubular endoplasmic reticulum. *Cell*. Feb 10 2006;124(3):573-86. doi:10.1016/j.cell.2005.11.047

37. Hu J, Shibata Y, Voss C, et al. Membrane proteins of the endoplasmic reticulum induce high-curvature tubules. *Science*. Feb 29 2008;319(5867):1247-50. doi:10.1126/science.1153634

38. Shibata Y, Voss C, Rist JM, et al. The reticulon and DP1/Yop1p proteins form immobile oligomers in the tubular endoplasmic reticulum. *J Biol Chem*. Jul 4 2008;283(27):18892-904. doi:10.1074/jbc.M800986200

39. Shemesh T, Klemm RW, Romano FB, et al. A model for the generation and interconversion of ER morphologies. *Proc Natl Acad Sci U S A*. Dec 9 2014;111(49):E5243-51. doi:10.1073/pnas.1419997111

40. Zurek N, Sparks L, Voeltz G. Reticulon short hairpin transmembrane domains are used to shape ER tubules. *Traffic*. Jan 2011;12(1):28-41. doi:10.1111/j.1600-0854.2010.01134.x

41. Wang S, Tukachinsky H, Romano FB, Rapoport TA. Cooperation of the ER-shaping proteins atlastin, lunapark, and reticulons to generate a tubular membrane network. *Elife*. Sep 13 2016;5doi:10.7554/eLife.18605

42. Hu J, Shibata Y, Zhu PP, et al. A class of dynamin-like GTPases involved in the generation of the tubular ER network. *Cell*. Aug 7 2009;138(3):549-61. doi:10.1016/j.cell.2009.05.025

43. Orso G, Pendin D, Liu S, et al. Homotypic fusion of ER membranes requires the dynamin-like GTPase atlastin. *Nature*. Aug 20 2009;460(7258):978-83. doi:10.1038/nature08280

44. Rismanchi N, Soderblom C, Stadler J, Zhu PP, Blackstone C. Atlastin GTPases are required for Golgi apparatus and ER morphogenesis. *Hum Mol Genet*. Jun 1 2008;17(11):1591-604. doi:10.1093/hmg/ddn046

45. Chen S, Desai T, McNew JA, Gerard P, Novick PJ, Ferro-Novick S. Lunapark stabilizes nascent three-way junctions in the endoplasmic reticulum. *Proc Natl Acad Sci U S A*. Jan 13 2015;112(2):418-23. doi:10.1073/pnas.1423026112

46. Chen S, Novick P, Ferro-Novick S. ER network formation requires a balance of the dynamin-like GTPase Sey1p and the Lunapark family member Lnp1p. *Nat Cell Biol*. Jun 24 2012;14(7):707-16. doi:10.1038/ncb2523

47. Woo TT, Williams JM, Tsai B. How host ER membrane chaperones and morphogenic proteins support virus infection. *J Cell Sci*. Jul 1 2023;136(13)doi:10.1242/jcs.261121

48. Levine T, Loewen C. Inter-organelle membrane contact sites: through a glass, darkly. *Curr Opin Cell Biol*. Aug 2006;18(4):371-8. doi:10.1016/j.ceb.2006.06.011

49. Scorrano L, De Matteis MA, Emr S, et al. Coming together to define membrane contact sites. *Nat Commun*. Mar 20 2019;10(1):1287. doi:10.1038/s41467-019-09253-3

50. Sassano ML, Felipe-Abrio B, Agostinis P. ER-mitochondria contact sites; a multifaceted factory for Ca(2+) signaling and lipid transport. *Front Cell Dev Biol*. 2022;10:988014. doi:10.3389/fcell.2022.988014

51. Prinz WA, Toulmay A, Balla T. The functional universe of membrane contact sites. *Nat Rev Mol Cell Biol*. Jan 2020;21(1):7-24. doi:10.1038/s41580-019-0180-9

52. Wilson EL, Metzakopian E. ER-mitochondria contact sites in neurodegeneration: genetic screening approaches to investigate novel disease mechanisms. *Cell Death Differ*. Jun 2021;28(6):1804-1821. doi:10.1038/s41418-020-00705-8

53. Sassano ML, van Vliet AR, Agostinis P. Mitochondria-Associated Membranes As Networking Platforms and Regulators of Cancer Cell Fate. *Front Oncol*. 2017;7:174. doi:10.3389/fonc.2017.00174

54. Moreno-Gonzalez I, Soto C. Misfolded protein aggregates: mechanisms, structures and potential for disease transmission. *Semin Cell Dev Biol*. Jul 2011;22(5):482-7. doi:10.1016/j.semcdb.2011.04.002

55. Morimoto RI, Cuervo AM. Proteostasis and the aging proteome in health and disease. *J Gerontol A Biol Sci Med Sci*. Jun 2014;69 Suppl 1(Suppl 1):S33-8. doi:10.1093/gerona/glu049

56. Krshnan L, van de Weijer ML, Carvalho P. Endoplasmic Reticulum-Associated Protein Degradation. *Cold Spring Harb Perspect Biol*. Dec 1 2022;14(12)doi:10.1101/cshperspect.a041247

57. Zattas D, Hochstrasser M. Ubiquitin-dependent protein degradation at the yeast endoplasmic reticulum and nuclear envelope. *Crit Rev Biochem Mol Biol*. Jan-Feb 2015;50(1):1-17. doi:10.3109/10409238.2014.959889

58. Christianson JC, Carvalho P. Order through destruction: how ER-associated protein degradation contributes to organelle homeostasis. *Embo j*. Mar 15 2022;41(6):e109845. doi:10.15252/embj.2021109845

59. Yamamoto H, Zhang S, Mizushima N. Autophagy genes in biology and disease. *Nat Rev Genet*. Jun 2023;24(6):382-400. doi:10.1038/s41576-022-00562-w

60. Khaminets A, Heinrich T, Mari M, et al. Regulation of endoplasmic reticulum turnover by selective autophagy. *Nature*. Jun 18 2015;522(7556):354-8. doi:10.1038/nature14498

61. Chino H, Mizushima N. ER-Phagy: Quality Control and Turnover of Endoplasmic Reticulum. *Trends Cell Biol*. May 2020;30(5):384-398. doi:10.1016/j.tcb.2020.02.001

62. Yang M, Luo S, Wang X, et al. ER-Phagy: A New Regulator of ER Homeostasis. *Front Cell Dev Biol*. 2021;9:684526. doi:10.3389/fcell.2021.684526

63. Hübner CA, Dikic I. ER-phagy and human diseases. *Cell Death Differ*. Mar 2020;27(3):833-842. doi:10.1038/s41418-019-0444-0

64. Chen YJ, Bagchi P, Tsai B. ER functions are exploited by viruses to support distinct stages of their life cycle. *Biochem Soc Trans*. Oct 30 2020;48(5):2173-2184. doi:10.1042/bst20200395

65. Romero-Brey I, Bartenschlager R. Endoplasmic Reticulum: The Favorite Intracellular Niche for Viral Replication and Assembly. *Viruses*. Jun 7 2016;8(6)doi:10.3390/v8060160

66. Chen YJ, Liu X, Tsai B. SV40 Hijacks Cellular Transport, Membrane Penetration, and Disassembly Machineries to Promote Infection. *Viruses*. Oct 5 2019;11(10)doi:10.3390/v11100917

67. Bagchi P, Liu X, Cho WJ, Tsai B. Lunapark-dependent formation of a virus-induced ER exit site contains multi-tubular ER junctions that promote viral ER-to-cytosol escape. *Cell Rep*. Dec 7 2021;37(10):110077. doi:10.1016/j.celrep.2021.110077

68. Chen YJ, Williams JM, Arvan P, Tsai B. Reticulon protects the integrity of the ER membrane during ER escape of large macromolecular protein complexes. *J Cell Biol*. Feb 3 2020;219(2)doi:10.1083/jcb.201908182

69. Geiger R, Andritschke D, Friebe S, et al. BAP31 and BiP are essential for dislocation of SV40 from the endoplasmic reticulum to the cytosol. *Nat Cell Biol*. Sep 25 2011;13(11):1305-14. doi:10.1038/ncb2339

70. Ravindran MS, Engelke MF, Verhey KJ, Tsai B. Exploiting the kinesin-1 molecular motor to generate a virus membrane penetration site. *Nat Commun*. May 24 2017;8:15496. doi:10.1038/ncomms15496

71. Smit JM, Moesker B, Rodenhuis-Zybert I, Wilschut J. Flavivirus cell entry and membrane fusion. *Viruses*. Feb 2011;3(2):160-171. doi:10.3390/v3020160

72. Paul D, Bartenschlager R. Flaviviridae Replication Organelles: Oh, What a Tangled Web We Weave. *Annu Rev Virol*. Nov 2015;2(1):289-310. doi:10.1146/annurev-virology-100114-055007

73. Apte-Sengupta S, Sirohi D, Kuhn RJ. Coupling of replication and assembly in flaviviruses. *Curr Opin Virol*. Dec 2014;9:134-42. doi:10.1016/j.coviro.2014.09.020

74. Knoops K, Kikkert M, Worm SH, et al. SARS-coronavirus replication is supported by a reticulovesicular network of modified endoplasmic reticulum. *PLoS Biol*. Sep 16 2008;6(9):e226. doi:10.1371/journal.pbio.0060226

75. de Haan CA, Rottier PJ. Molecular interactions in the assembly of coronaviruses. *Adv Virus Res*. 2005;64:165-230. doi:10.1016/s0065-3527(05)64006-7

76. V'Kovski P, Kratzel A, Steiner S, Stalder H, Thiel V. Coronavirus biology and replication: implications for SARS-CoV-2. *Nat Rev Microbiol*. Mar 2021;19(3):155-170. doi:10.1038/s41579-020-00468-6

Chapter 2
An Endoplasmic-Reticulum-Associated Structure Sequesters Misassembled FG-Nups to Help Maintain NPC Function

2.1 Abstract

Misassembly of nucleoporins (Nups), central components of the nuclear pore complex (NPC), leads to Nup mislocalization outside of the nuclear envelope. Here we elucidate the fate of mislocalized Nups. To impair Nup assembly, we depleted the structural component Nup98 and found that nucleo-cytoplasmic transport of NPC remains largely intact. Under this condition, several phenylalanine-glycine (FG)-rich Nups no longer assemble at the nuclear membrane but instead accumulate at discrete puncta in the endoplasmic reticulum (ER) called foci. Formation of the foci harboring the misassembled FG-Nups requires the ER morphogenic proteins RTN3, ATL3, and LNP. Preventing accumulation of misassembled FG-Nups at the ER-foci impairs NPC nucleo-cytoplasmic transport, likely by allowing the misassembled FG-Nups to reach the nuclear envelope where they disrupt NPC function. Formation of the ER-foci is dependent on the kinesin-1 motor, which binds to the Nups. Our results suggest that the ER can sequester misassembled Nups to help maintain NPC function. Because Nup mislocalization is found in many age-related neurodegenerative diseases, our data should illuminate the molecular basis of these pathologic conditions.

2.2 Introduction

Nuclear pore complexes (NPCs) are massive, cylindrical complexes that mediate transport of proteins and nucleic acids in and out of the nucleus. Structurally, each NPC is composed of multiple copies of 30 nucleoporins ("Nups") arranged in eightfold radial symmetry.[1-3] During NPC biogenesis, which primarily occurs during interphase of the cell cycle, Nups must be incorporated into NPCs in precise stoichiometries.[4,5] Anchoring the NPC in the nuclear membrane are copies of the transmembrane Nups NDC1, GP210, and POM121.[6,7] The remaining Nups are peripheral membrane proteins organized in modular subcomplexes: the cytoplasmic filaments, cytoplasmic outer ring, inner ring, nuclear outer ring, and nuclear basket.[1,3,8] The ability of the NPC to mediate nucleo-cytoplasmic transport depends on its permeability barrier, which is composed of intrinsically disordered phenylalanine-glycine repeat containing Nups (termed "FG-Nups"). These Nups line the central channel of the pore and interact with each other to form a highly dynamic mesh, which facilitates selective cargo transport by the NPC.[9-11] Because the FG-Nups are prone to condensate formation, specific chaperones are required to maintain their solubility and prevent aggregation prior to NPC assembly.[12,13]

Despite the importance of proper NPC assembly and function, there is a significant gap in our understanding of Nup transport and quality control, especially in mammalian cells. Recent studies have begun to identify the chaperones and other cellular factors responsible for tightly controlling the stoichiometry of NPC biogenesis.[14,15] Importantly, if this assembly process is faulty, the misassembled NPCs must be identified and sequestered or recycled. In yeast cells, aberrant NPC intermediates are sequestered in a region of the nuclear envelope termed the storage of improperly assembled NPC compartment ("SINC"), thereby preventing the defective

complexes from being inherited by daughter cells.[16] Furthermore, recent studies in yeast suggest that structurally-compromised NPCs are subject to recognition, removal, and recycling via selective autophagy ("NPC-phagy").[17,18] Less is understood regarding how cells sense damage to mature NPCs, which may become clogged or leaky. Given that NPCs are extremely long-lived complexes, quality control mechanisms that repair aberrant NPCs could be energetically favorable for cells.[19] Consistent with this idea, cells have the ability to turn over individual member Nups within an NPC, and in fact do so at a higher rate within a subcomplex if that subcomplex is compromised.[20,21] Beyond this observation, little is known about quality control mechanisms that surveil and preserve NPC function.

Damage to the NPCs and resulting loss of nuclear compartmentalization is an established phenotype of aging cells.[22,23] One particularly striking phenotype—found in models of amyotrophic lateral sclerosis/frontotemporal dementia (ALS/FTD), Alzheimer's disease, and Huntington's disease—is mislocalization of many Nups outside the nuclear envelope.[24-29] In some cases, the mislocalized Nups form aggregates that colocalize with other pathological protein aggregates, but the functional significance of this phenotype continues to be disputed.[25] Although Nup mislocalization appears to be linked to disruption of NPC function, it is unclear precisely when Nup mislocalization occurs during disease progression and whether it is a cause or an effect of the disease. Additionally, the mechanism(s) of Nup mislocalization are completely mysterious, whether in healthy cells or disease models of neurodegeneration, cancer, and viral pathogenesis. Therefore, how cells recognize and respond to mislocalized Nups is a fundamental question that remains unanswered.

In this study, we depleted a select Nup (using an siRNA-dependent approach) to impair NPC assembly. Under this condition, the NPC function remains largely intact, coinciding with a

subset of Nups mislocalizing outside the nuclear envelope. We demonstrate that these mislocalized Nups accumulate at a discrete depot in the endoplasmic reticulum (ER). Mechanistically, formation of the ER-localized depot containing the mislocalized Nups requires specific ER morphogenic proteins, and transport of the mislocalized Nups to this depot depends on the kinesin-1 motor. Functionally, our data further suggest that sequestration of the Nups in the ER plays a role in maintaining proper nucleo-cytoplasmic transport of the remaining NPCs. These findings reveal a quality control strategy cells can deploy in order to preserve NPC functionality despite Nup mislocalization.

2.3 Results

2.3.1 Depletion of Nup98 causes FG-Nups to accumulate at discrete ER puncta called foci

To create a model system in which select Nups can be displaced from the NPC, we used the siRNA-mediated knockdown (KD) strategy to deplete Nup98, a component of multiple NPC subcomplexes (Fig. 2.1A).[30] We chose this approach because a previous report demonstrated that complete knock out of Nup98 causes several cytoplasmic Nups (Nups 214, 62, 88, and RanBP2) to form distinct cytoplasmic aggregates.[31] Although this report proposed that the aggregates are located in annulate lamellae —stacked ER-derived membranes that contain pore complexes[32]—it neither investigated the mechanism by which the aggregates are formed nor the functional significance of the aggregates.

We therefore replicated this observation of Nup aggregate formation by transiently knocking down Nup98 in COS-7 cells (Fig. 2.1A). To visualize the mislocalized Nups, we used an antibody (MAb414) against the FG-repeat domain found in several cytoplasmic Nups. While the FG-Nups clearly localized to the nuclear membrane in the control (scrambled siRNA, scr)

condition, in the Nup98 KD (Nup98 #1 siRNA) condition they are largely displaced to prominent perinuclear aggregates that we term "foci" (Fig. 2.1B, compare top to bottom; quantified in 2.1C).

Because the foci structure appeared proximal to the nucleus and because the nuclear and ER membranes are contiguous, we hypothesized that the displaced Nups are located at the ER. Indeed, the MAb414 foci (found under Nup98 KD) co-stained with the ER membrane marker Bap31 (Fig. 2.1B), consistent with the idea that the displaced Nups accumulate at the ER. To identify specific Nups that mobilized to the ER, we stained for Nup62 and Nup214—two established FG-Nups recognized by the Mab414 antibody[33]—and found that both proteins formed foci under Nup98 KD that also co-localized with the Bap31+ ER-foci (Fig. 2.1D and 2.1E). These findings indicate that Nup62 and Nup214 are two members of the FG-Nups that mobilize to and accumulate at the ER-foci when Nup98 is depleted.

We further evaluated this observation biochemically using a previously published protocol that partitioned cellular contents into a nuclear (Nuc, containing the nuclear marker histone H3) and a non-nuclear cytoplasmic (Non-Nuc, containing the ER marker Bap31) fraction[34]. Using this method, we found that under Nup98 KD, the majority of Nup62 shifted from the Nuc to Non-Nuc fraction (Fig. 2.1F, top blot), consistent with the imaging data demonstrating that in the absence of Nup98, select nuclear-localized FG-Nups are mislocalized and targeted to the ER.

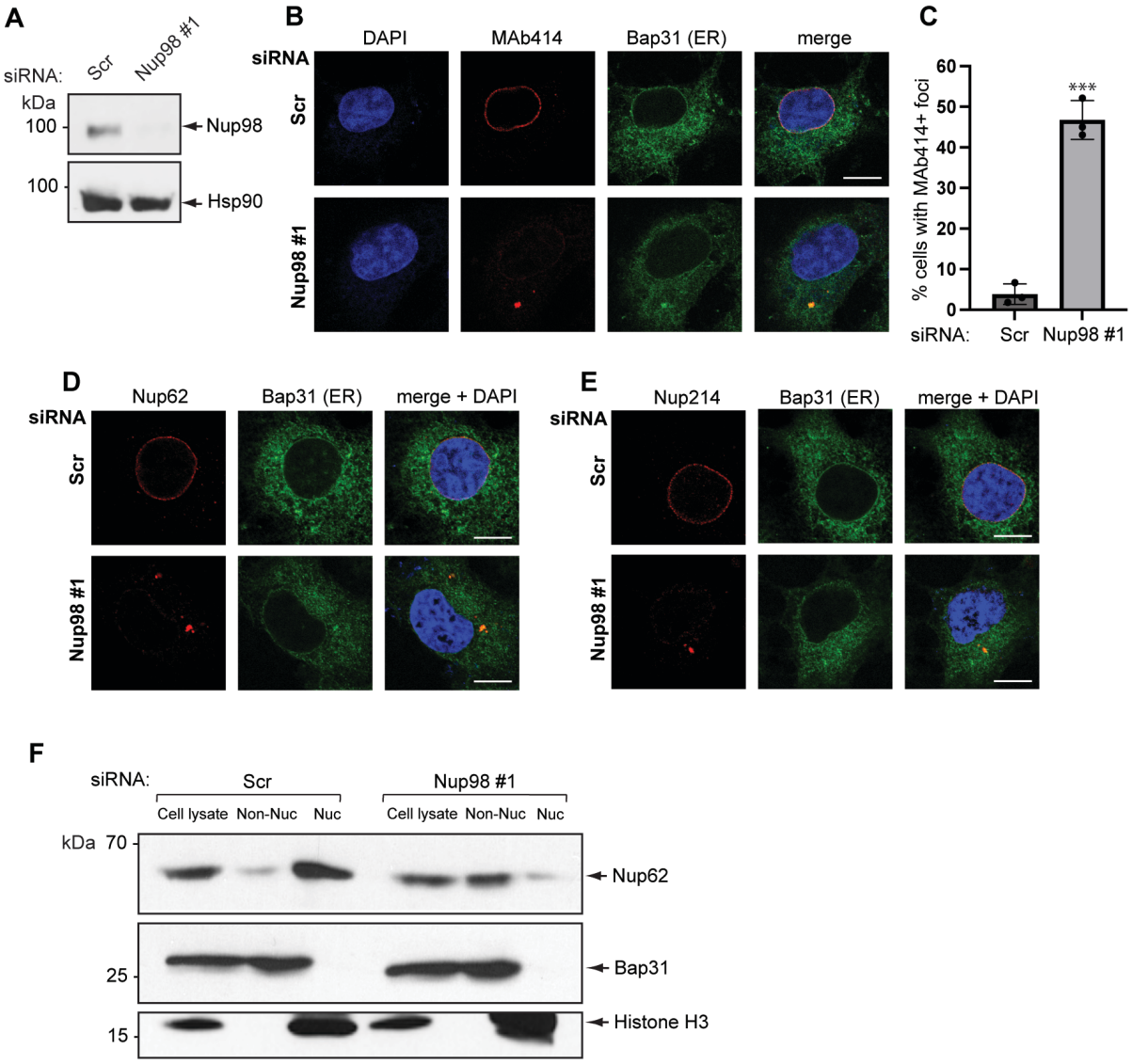

Figure 2.1: Depletion of Nup98 causes FG-Nups to form foci in the ER

(**A**) COS-7 cells transfected with scrambled control siRNA (Scr) or siRNA against Nup98 were lysed and the resulting whole cell lysates analyzed by SDS-PAGE and immunoblotting with the indicated antibodies. (**B**) and (**C**) COS-7 cells transfected with the indicated siRNAs were fixed and stained for FG-Nups (MAb414 antibody) and assessed by immunofluorescence microscopy. Scale bars, 10 µm. Presence of ER-foci was quantified by condition-blinded counting of MAb414- and Bap31-colocalized puncta (representative images shown). Graph represents mean +/- standard deviation (SD) from 3 independent experiments. The significance was determined via Student's two-tailed t test. ***, $p \leq 0.001$. (**D**) and (**E**) As in (B), except cells were stained with the indicated antibodies. (**F**) COS-7 cells were transfected with the indicated siRNAs, harvested, and subjected to nuclear fractionation (see Materials

and Methods) to yield a whole-cell lysate sample, a non-nuclear fraction, and a nuclear fraction. These fractions were subjected to SDS-PAGE and immunoblotting.

2.3.2 The FG-Nup foci phenotype is consistent across multiple Nup98 siRNAs.

To confirm the specificity of the Nup98 knockdown, we repeated the knockdowns using 3 different siRNAs. Each siRNA sequence yielded the same Bap31-colocalized FG-Nup foci phenotype (Fig. 2.2), indicating that this effect is specifically due to Nup98 depletion rather than off-target effects.

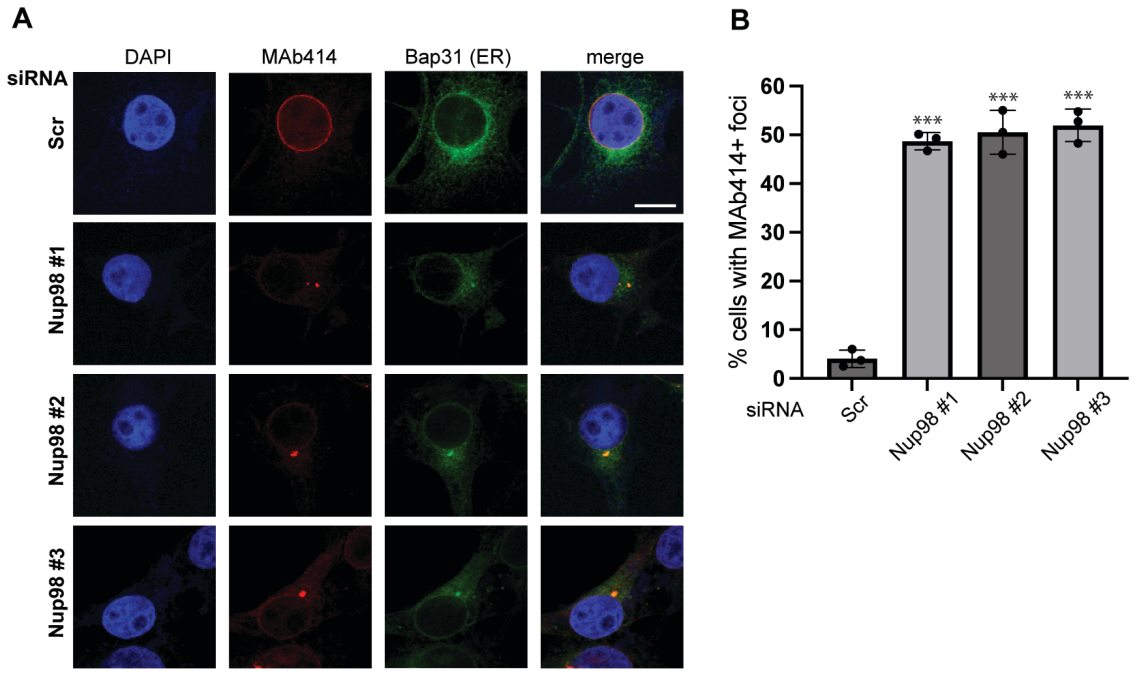

Figure 2.2: The FG-Nup foci phenotype is consistent across multiple Nup98 siRNAs

(A) and (B) COS-7 cells transfected with the indicated siRNAs were fixed and stained for FG-Nups (MAb414 antibody) and assessed by immunofluorescence microscopy. Scale bars, 10 µm. Presence of ER-foci was quantified by condition-blinded counting of MAb414- and Bap31-colocalized puncta. Graph represents mean +/- standard deviation (SD) from 3 independent experiments. The significance was determined via Student's two-tailed t test. ***, $p \leq 0.001$.

2.3.3 Misassembled Nups at the ER-foci are likely not targeted for proteasomal or lysosomal degradation

We first considered the possibility that the displaced Nups are routed to the ER-foci for degradation because they are no longer assembled into functional pores. There are multiple well-established pathways by which ER-associated proteins may be turned over, most notably ER-associated protein degradation (ERAD) which uses the ubiquitin-proteasome system, and ER-to-lysosome-associated degradation (ERLAD) that relies on the lysosome[35,36]. To test whether either of these pathways turns over the mislocalized Nups at the ER, we knocked down Nup98, then treated the cells with drug inhibitors of the proteasome (Fig. 2.3A, MG132 or epoxomicin) or the lysosome (Fig. 2.3B, chloroquine or BafA1). We reasoned that if the mislocalized Nups at the ER-foci were degraded by either of these pathways, addition of the inhibitors should increase the MAb414 signal at the ER-foci. However, none of the inhibitors caused such an increase. These data suggest that the mislocalized Nups are unlikely turned over by the proteasome or lysosome and may be routed to the ER-foci for storage (see below).

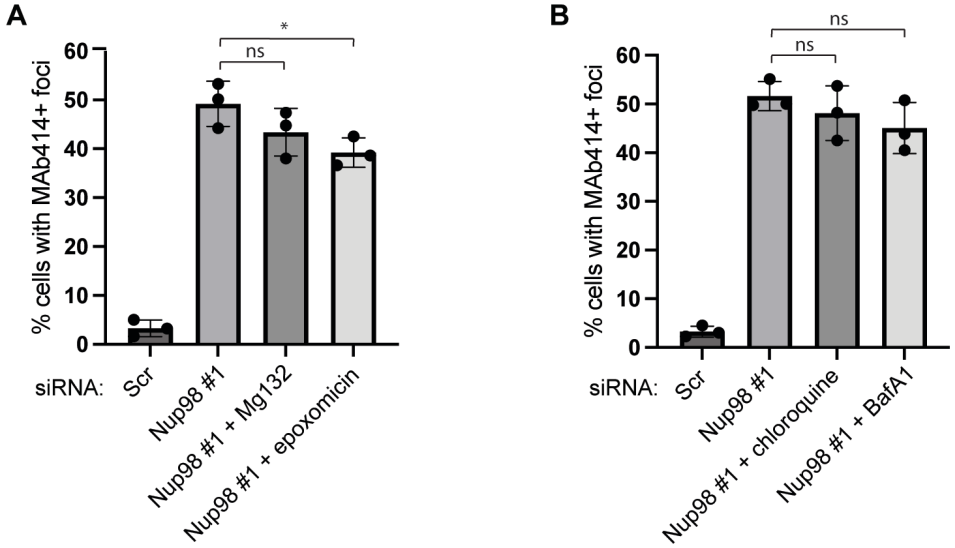

Figure 2.3: Misassembled Nups at the ER-foci are likely not targeted for proteasomal or lysosomal degradation

(**A**) and (**B**) COS-7 cells were transfected with the indicated siRNAs for 32 h, then treated with either DMSO (control) or the indicated chemical inhibitors for an additional 16 h. Cells were fixed, stained, and assessed by immunofluorescence microscopy to count MAb414- and Bap31-colocalized puncta.

2.3.4 Nup-containing ER-foci formation requires the ER membrane proteins RTN3, ATL3, and LNP

What cellular factors might promote formation of the ER-foci structure that store the misassembled Nups? We hypothesized that the ER membrane likely undergoes significant morphogenic remodeling in order to form these Nup-foci "storage depots". In this regard, multiple ER morphogenic proteins, including the reticulon (RTN), atlastin (ATL), and lunapark (LNP) ER-resident membrane proteins, have been shown to play critical roles in shaping the basic ER morphology.[37] We therefore asked whether any of these proteins are important for Nup ER-foci formation.

To test this possibility, we co-depleted the major ER morphogenic proteins under Nup98 KD (Fig. 2.4A). Strikingly, for the three morphogenic proteins—RTN3, ATL3, and LNP—double KD prevented formation of the Nup ER-foci (Fig. 2.4B, quantified in Fig. 2.4C). As a negative control, we found that depletion of another RTN family member, RTN4, under Nup98 KD did not affect ER-foci formation (quantified in Fig. 2.4C). Together, these results indicate that RTN3, ATL3, and LNP are functionally important for formation of the Nup ER-foci.

Intriguingly, blocking formation of the Nup ER-foci through KD of RTN3, ATL3, or LNP did not abolish the FG-Nup signal, nor were the Nups simply diffused throughout the cell. Instead, the Nup signal returned to the nuclear envelope and appeared similar to the control (scr-

treated) cells (Fig. 2.4B, compare rows 3-5 with 1). This apparent "rescue" of Nup localization was unanticipated because the cells still lacked Nup98 (Fig. 2.4A). Are the "re-localized" Nups forming functional NPCs?

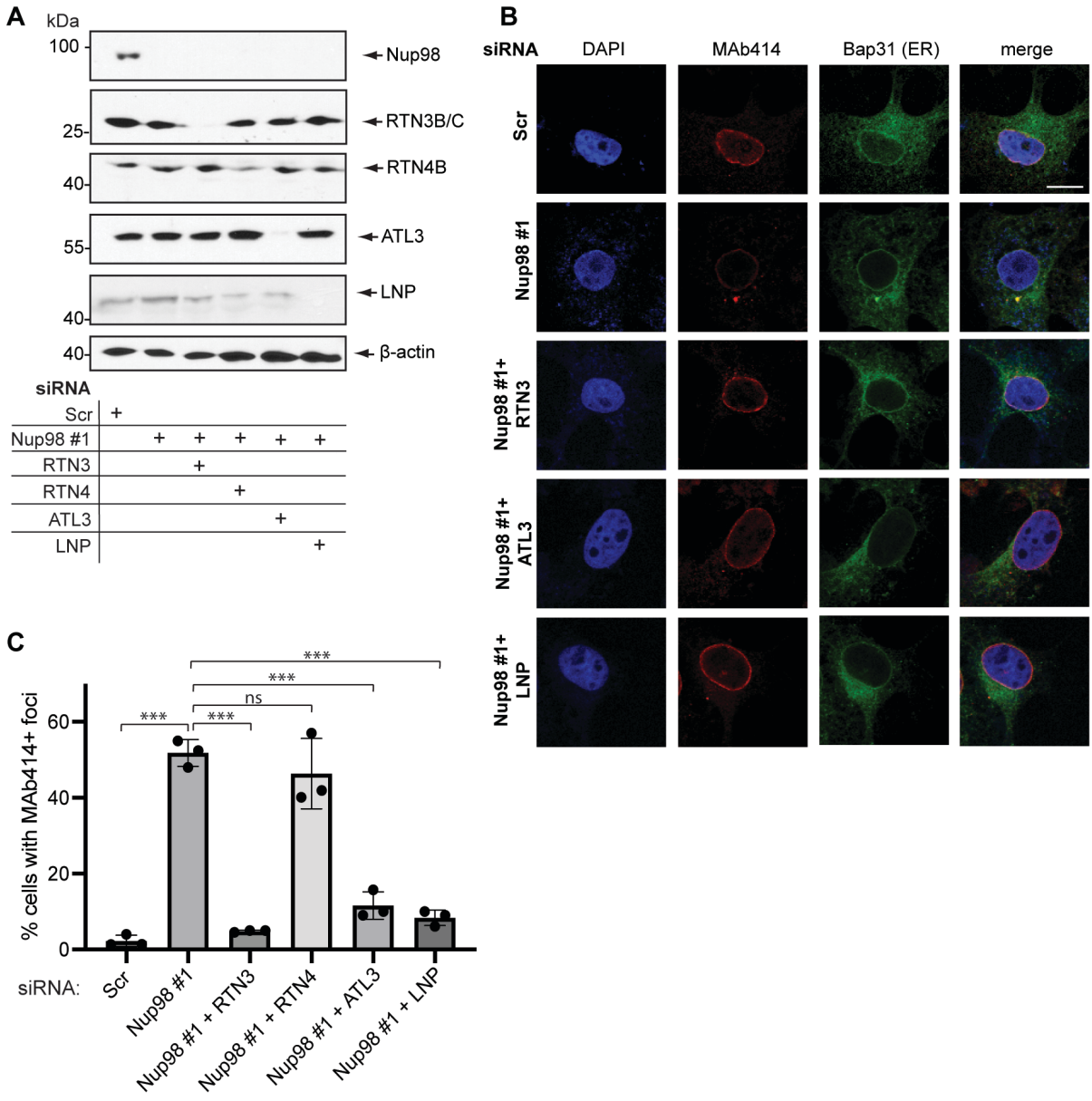

Figure 2.4: Nup-containing ER-foci formation requires the ER morphogenic membrane proteins RTN3, ATL3, and LNP

(**A**) COS-7 cells transfected with the indicated siRNAs were lysed and the resulting whole cell lysates analyzed by SDS-PAGE and immunoblotting with the indicated antibodies. (**B**) and (**C**) COS-7 cells transfected with the

indicated siRNAs were fixed and stained for FG-Nups (MAb414 antibody) and assessed by immunofluorescence microscopy. Scale bars, 10 μm. Presence of ER-foci was quantified by condition-blinded counting of MAb414- and Bap31-colocalized puncta. Graph represents mean +/- standard deviation (SD) from 3 independent experiments. The significance was determined via Student's two-tailed t test. ***, $p \leq 0.001$.

2.3.5 Preventing accumulation of misassembled FG-Nups at the ER-foci impairs nucleo-cytoplasmic transport

To probe the functional importance of Nup re-localization to the nuclear envelope when RTN3, ATL3, or LNP is depleted in Nup98 KD cells (Fig. 2.4A), we conducted a nuclear transport assay by transfecting cells with a reporter plasmid encoding mCherry tagged to a nuclear localization signal (NLS) sequence derived from the polyomavirus SV40 large T antigen (TAg) protein (mCherry-NLS; 28 kDa). In control cells with normal NPCs, the majority of cells (~90%) displayed bright mCherry signal exclusively in the nucleus (Fig. 2.5A, top row; quantified in Fig. 2.5B), indicating successful nuclear import. A similar amount of Nup98 KD cells also exhibited the mCherry signal in the nucleus (quantified in Fig. 2.5B), suggesting their NPCs retain a basal level of function sufficient to transport mCherry-NLS, despite being depleted of Nup98 and select FG-Nups.

However, under simultaneous KD of Nup98 and RTN3, ATL3, or LNP, a condition that prevented formation of the Nup-containing ER-foci (Fig. 2.4), only ~50% of the cells now exhibited the mCherry signal exclusively in the nucleus while the other ~50% of the cells have this signal in both the nucleus and cytoplasm (Fig. 2.5A, bottom row; quantified in Fig. 2.5B). These results suggest that although the double KD cells have the FG-Nups re-localized to the nuclear envelope, their NPC-mediated nuclear transport function are in fact perturbed. As a negative control, we found that co-depletion of RTN4 in Nup98 KD cells (which did not block

ER-foci formation, Fig. 2.4C) also did not decrease the percentage of cells displaying the mCherry-NLS signal exclusively in the nucleus (quantified in Fig. 2.5B). Additionally, single KD of any one ER morphogenic protein did not affect localization of mCherry-NLS in the nucleus (quantified in Fig. 2.5C). To evaluate if the impaired nuclear transport function under double KD of Nup98 and the ER morphogenic proteins (RTN3, ATL3, or LNP) might be due to loss of general cell viability, we use the well-established MTS cell viability assay and found that it was not (Fig. 2.5D).

To test whether nucleo-cytoplasmic transport is impaired with non-transfected cargoes, we took advantage of the SV40 large TAg itself (94 kDa), an NLS-containing protein stably expressed in COS-7 cells. In control cells, TAg staining was nearly exclusively observed in the nucleus (Fig. 2.5E, top row; quantified in Fig. 2.5F). Importantly, whereas ~35% of Nup98 KD cells displayed some TAg in the cytoplasm, even more cells (~60%) displayed some TAg in the cytoplasm under Nup98 + ER morphogenic protein double KD (Fig. 2.5E, bottom row; quantified in Fig. 2.5F), consistent with data using the mCherry-NLS transfected substrate. These results support the idea that blocking formation of the Nup ER-foci by KD of the ER morphogenic proteins worsens nucleo-cytoplasmic transport.

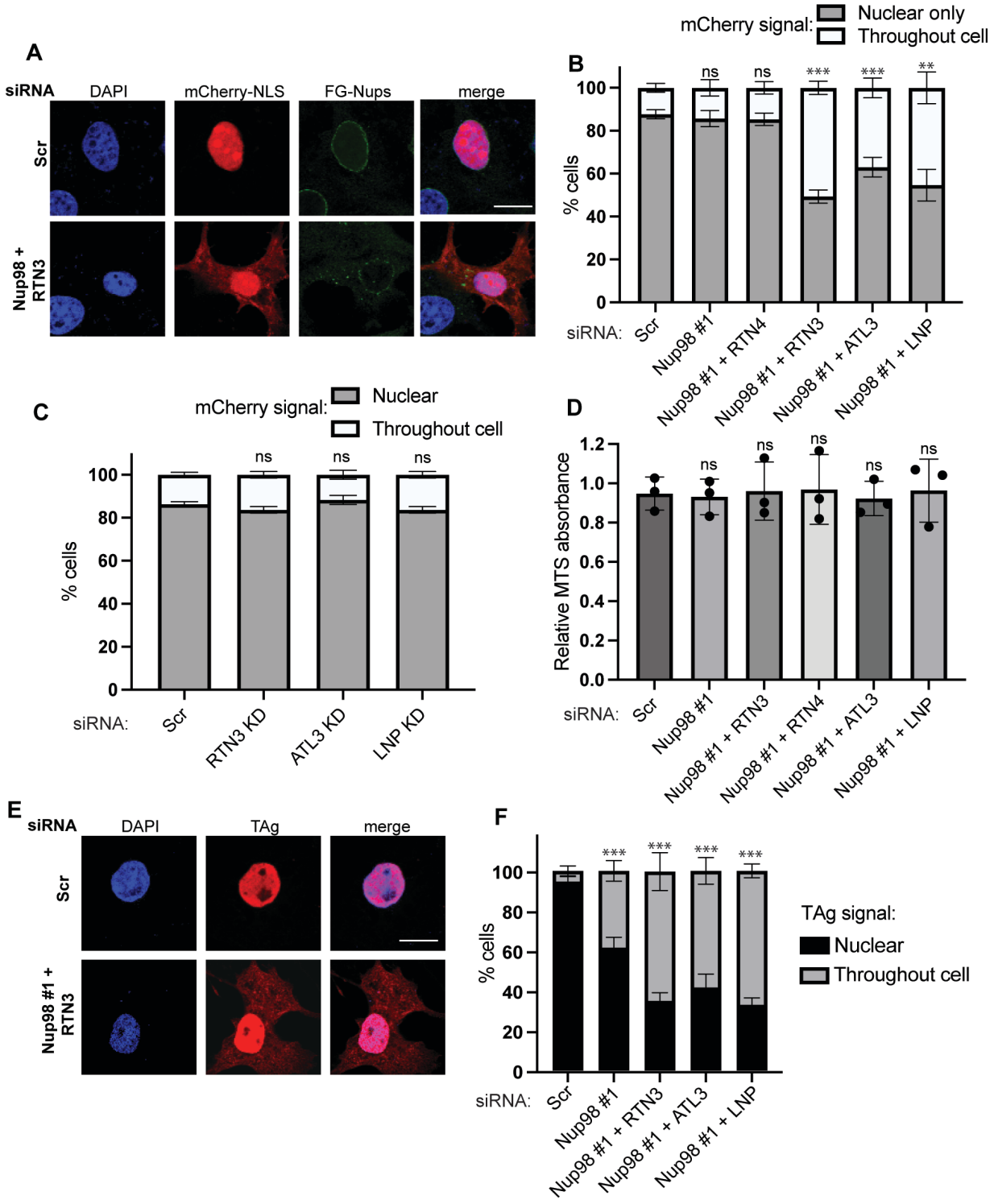

Figure 2.5: Preventing accumulation of misassembled FG-Nups at the ER-foci impairs nuclear import function

(**A**) and (**B**) COS-7 cells were transfected with either scrambled control or Nup98 + ER-morphogenic siRNAs (double KD) for 24 h, followed by 24 h of transfection with an mCherry-NLS construct. Cells were fixed and

stained, and the location of the mCherry signal was assessed. (**C**) As in (B), except cells were transfected with indicated siRNA (single knockdowns). (**D**) Cell viability under the knockdown conditions from (B) was assessed using an MTS absorbance assay (see Materials and Methods). (**E**) COS-7 cells were transfected with either scrambled control or Nup98 + ER-morphogenic siRNAs (double KD) for 48 h. Cells were fixed and stained, and the location of the large T antigen (TAg) signal was assessed. Graphs represent mean +/- standard deviation (SD) from 3 independent experiments. The significance was determined via Student's two-tailed t test. ***, $p \leq 0.001$; **, $p \leq 0.01$.

Together, our results indicate that preventing delivery and storage of the misassembled FG-Nups at the ER-foci selectively compromise NPC transport function, likely because the misassembled Nups are allowed to return to the nuclear membrane where they disrupt NPC function. Hence, our data suggest that sequestration of misassembled Nups is a critical quality control mechanism used to maintain basal NPC activity during assembly of this massive, multi-subunit protein complex.

2.3.6 The Nup-containing ER-focus is proximal to the MTOC and depends on intact microtubules for formation

The ER and microtubules are highly interdependent cellular structures. Because the displaced FG-Nups form discrete foci structure at the ER, we asked if formation of the ER-foci harboring the displaced Nups depends on microtubule-associated motor activities. We first investigated this by repeating the same Nup98 KD while staining for MAb414 (red), but this time co-staining for γ-tubulin (green) to visualize the microtubule organizing centers (MTOCs). Strikingly, almost every Nup focus we observed formed proximal to the cell's MTOC (representative images are shown in Fig. 2.6A). To directly test the role of microtubules in foci

formation, we performed Nup98 KD followed by nocodozole treatment to depolymerize the microtubule network. Compared to a vehicle control (DMSO) where the Nups formed large, distinct foci, the nocodozole-treated cells formed significantly fewer Bap31+/MAb414+ foci (Fig. 2.6B, compare top and bottom; quantified in Fig. 2.6C), suggesting that formation of the Nup foci at the ER is a microtubule-dependent process.

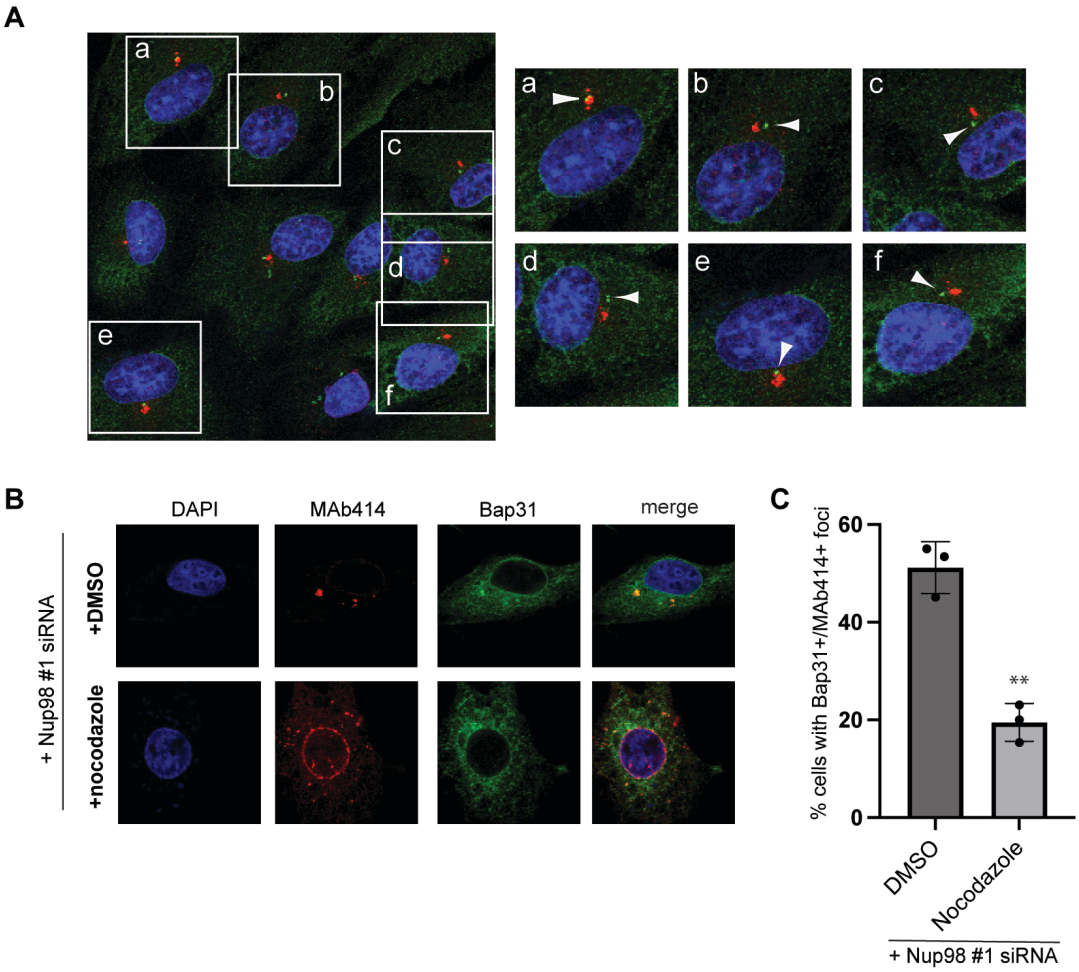

Figure 2.6: Nup foci are proximal to the MTOCs and dependent on intact microtubules

(**A**) COS-7 cells transfected with Nup98 siRNA were fixed, stained for FG-Nups (MAb414 antibody) and MTOC (arrowheads in insets, γ-tubulin antibody), and assessed by immunofluorescence microscopy. **(B)** Cells transfected with Nup98 siRNA for 24 h were treated with either DMSO control or nocodazole for an additional 24 h, then fixed and stained with the indicated antibodies. Scale bars, 10 µm. Presence of ER-foci was quantified by condition-

blinded counting of MAb414- and Bap31-colocalized puncta. Graph represents mean +/- standard deviation (SD) from 3 independent experiments. The significance was determined via Student's two-tailed t test. **, $p \leq 0.01$.

2.3.7 Formation of the Nup-containing ER-foci is dependent on kinesin-1

Because the ER-foci harboring the misassembled Nups are proximal to the MTOC and that an intact microtubule network is functionally important during foci formation (Fig. 2.6), we hypothesized that microtubule-associated molecular motors promote delivery of the unassembled Nups to the ER-foci. We first investigated the role of the major cellular kinesin, kinesin-1 (Kif5B), during Nup ER-foci formation as this motor is functionally linked to ER membrane transport and dynamics.[38] We depleted Nup98 and Kif5B alone or in combination (Fig. 2.7A). While Nup98 KD (using Nup98 #1 siRNA) alone resulted in formation of a large, intact, single focus (as expected), simultaneous KD of Nup98 and Kif5B (using Kif5B #1 siRNA) caused the FG-Nups to form many small and dispersed foci (Fig. 2.7B, compare inset in row 2 to 3; quantified in Fig. 2.7C); formation of these small foci was similarly observed using another siRNA against Kif5B (Kif5B #2 siRNA) under Nup98 KD (quantified in Fig. 2.7C). Importantly, Kif5B KD alone (using either siRNA but shown using Kif5B siRNA #1) did not affect FG-Nup localization compared to control (Fig. 2.7B, compare row 4 to row 1; quantified in Fig. 2.7C). These data strongly suggest that kinesin-1 is critical for Nup ER-foci formation.

Our model suggests that kinesin-1 may physically associate with the misassembled FG-Nups to transport these proteins to the ER-foci. To test this idea biochemically, we treated cells with siRNA, transfected the cells with mCherry-tagged Kif5B and performed immunoprecipitation of Nup62. Interestingly, we observed an interaction between Nup62 and

mCherry-Kif5B in both scrambled-treated control and Nup98 KD cells (Fig. 2.7D), indicating that kinesin associates with nucleoporins even under normal conditions.

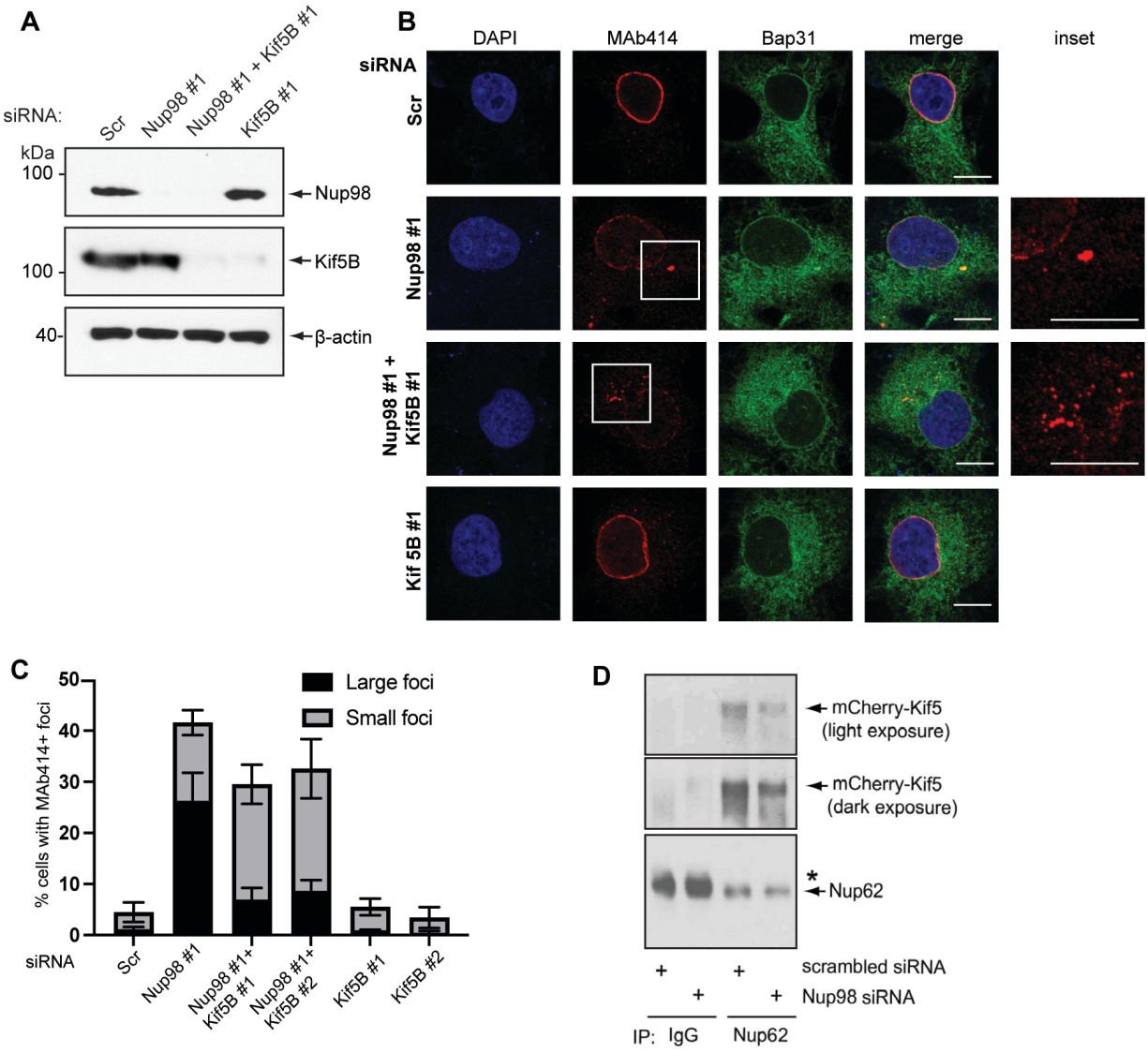

Figure 2.7: Nup foci formation is dependent on the kinesin-1 motor

(**A**) COS-7 cells transfected with the indicated siRNAs were lysed and the resulting whole cell lysates analyzed by SDS-PAGE and immunoblotting with the indicated antibodies. (**B**) COS-7 cells transfected with the indicated siRNAs were fixed and stained for FG-Nups (MAb414 antibody) and assessed by immunofluorescence microscopy. Scale bars, 10 µm. (**C**) Quantification of (B). Cells with a single distinct, Bap31-colocalized MAb414+ punctum were scored as "large foci," while cells with a cluster of multiple (3+) MAb414+ puncta in the perinuclear region

were scored as “small foci.” Graph represents mean +/- standard deviation (SD) from 3 independent experiments. (**D**) COS-7 cells were transfected with the indicated siRNAs for 24 h, followed by an additional 24 h of transfection with mCherry-Kif5B plasmid. The resulting whole cell lysates were subject to immunoprecipitation with Nup62 antibody and the precipitated material subjected to SDS-PAGE and immunoblotting with the indicated antibodies. * indicates nonspecific band.

2.4 Discussion

Though proper Nup trafficking, assembly, and function is crucial for nucleo-cytoplasmic transport across the nuclear membrane, many aspects of NPC quality control remain unclear. One unresolved question is how cells recognize and respond to mislocalized Nups, a phenotype observed in several neurodegenerative diseases, cancers, and viral infections.[25,39,40] In this manuscript, we elucidate one potential pathway by which cells traffic mislocalized Nups to discrete sites at the ER, where they are sequestered in order to help preserve NPC function.

Using a loss-of-function strategy, we depleted the key structural component Nup98 with siRNA, preventing a select number of other Nups from assembling into NPCs.[31] Both immunofluorescence microscopy and biochemical fractionation revealed that the Nups are displaced from the nuclear envelope. Strikingly, the mislocalized Nups are localized at large perinuclear foci that colocalize with the ER marker Bap31. These findings indicate that depletion of Nup98 causes select FG-Nups to be targeted to discrete sites at the ER membrane, rather than the nuclear membrane. Topologically, we expect the mislocalized Nups to be situated on the cytosolic surface (and not the luminal side) of the ER membrane.

We initially hypothesized that the Nups are routed to the ER for degradation: because the ER is a hub for protein turnover,[35,36] cells might sense the misassembled Nups and dispose of them via the ER. However, treating Nup98 KD cells with chemical inhibitors of the proteasome

and lysosome did not lead to a buildup of Nups at the ER-foci, as would be expected if the Nups were subject to proteasomal or lysosomal degradation. These findings raise the question of why cells would store excess Nups in the ER-foci, rather than simply recycling them. Nups are notoriously long-lived proteins, with turnover times among the longest in the cell.[19] Previous studies of annulate lamellae have suggested they act as holding sites for Nups that may be re-integrated into the nuclear envelope as part of functional NPCs.[41,42] Our finding that the displaced Nups are stored rather than degraded is therefore consistent with these past observations.

To pinpoint the specific cellular machinery necessary to build and maintain the Nup-storing ER-foci, we first examined the ER morphogenic proteins and determined that depletion of RTN3, ATL3, or LNP blocked Nup foci formation at the ER. One interpretation of these data is that the morphogenic proteins create highly reticulated areas of ER membrane more conducive to storing the large Nup aggregates. Recent studies of virus entry have revealed that for certain viruses that travel through the ER during infection, the RTNs, ATLs, and LNP all contribute to the formation of junctional sites where the large, proteinaceous viral particles gather and penetrate the ER membrane.[43-45] Our observation that morphogenic protein depletion significantly blocked Nup foci formation suggests that the mislocalized Nups may be collecting at a similar ER junctional site. Because super-resolution microscopy strategies were used to visualize some of these structures in viral infection,[43] a similar approach could be employed to further investigate the structural details of the Nup ER-foci structure.

Not only did double KD of Nup98 and either RTN3, ATL3, or LNP block Nup foci from forming in the ER, it also led to accumulation of FG-Nups at the nuclear envelope. While this might initially appear to be a “rescue” of normal Nup localization, a nuclear transport assay

using the well-established mCherry-NLS substrate revealed that these cells instead exhibited more defective nucleo-cytoplasmic transport when compared to the control and Nup98 single KD cells. Since the intrinsically disordered FG-Nups are known to phase separate and aggregate readily,[11,13] we envision a scenario where the Nups diffuse through the cell but aggregate with other Nups at the nuclear envelope. Because they are not correctly assembled into the NPC with proper stoichiometry, they would effectively clog the pores and hinder normal nucleo-cytoplasmic transport. We therefore propose a model in which the Nup ER-foci perform a dual function: 1) storage of misassembled Nups for possible future use, and 2) sequestration of excess Nups from the nuclear envelope to preserve NPC function (Fig. 2.8). This sequestration function represents a novel NPC quality control mechanism.

Interestingly, when we tested nucleo-cytoplasmic transport of the larger virus TAg cargo, we found that although the Nup98 single KD cells appeared more impaired in their transport when compared to control cells (~65% of control), the Nup98 and ER morphogenic protein double KD cells were even more defective (~40% of control). We speculate that the larger size of TAg (94 kDa) when compared to mCherry-NLS (28 kDa) may be more difficult for cells to import via the partially functional NPCs. Further work will be needed to ascertain the range of cargo sizes that the Nup98 KD NPCs can support.

We finally examined how FG-Nups are trafficked to the discrete ER-foci. Based on our observation that the Nup ER-foci are located proximal to MTOCs, we found that Nup ER-foci formation is dependent on intact microtubules and on the kinesin-1 motor specifically. Our biochemical analysis revealed that kinesin-1 interacts with Nup62 under both control and Nup98 KD conditions. This raises the possibility that kinesin-1 not only transports Nup62 (and possibly other FG-Nups) to the nuclear membrane under normal conditions, but also to the ER-foci under

Nup98 KD. The latter scenario depicts a motor-dependent mechanism by which mislocalized Nups are trafficked to the ER junctional storage sites, where they are sequestered to preserve NPC function (Fig. 2.8). We anticipate these results should further illuminate the molecular basis of various diseases associated with mislocalized Nup components.

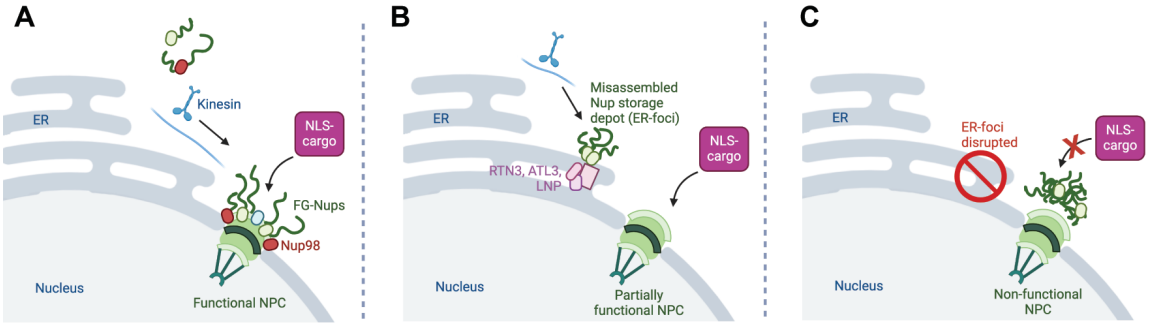

Figure 2.8: The Nup ER-foci function to preserve NPC function by sequestering excess Nups

(**A**) Under basal condition, Nups assemble properly into the NPCs, which support nucleo-cytoplasmic transport of cellular cargos. (**B**) When depleted of a key NPC structural component (Nup98), cells store excess Nups in ER-foci, allowing the remaining Nups to form partially functional NPCs. (**C**) However, when the Nup storage sites are destroyed (e.g. through compromised ER structure), excess Nups can no longer be sequestered, allowing them to migrate back and block normal nucleo-cytoplasmic transport. Figure created with Biorender.com.

2.5 Materials and Methods

2.5.1 Cells

COS-7 (CRL-1651) cells from ATCC were cultured in complete Dulbecco's modified Eagle medium (cDMEM) with 10% fetal bovine serum (FBS, Atlanta Biologicals, GA), 10 U/ml penicillin, and 10 µg/ml streptomycin (Thermo Fisher Scientific).

2.5.2 Antibodies

The antibodies used for this study were Nup98 (2598S, Cell Signaling Technology), Hsp90 (sc7947, Santa Cruz Biotechnology), MAb414 (ab24609, Abcam), Nup62 (NBP1-85091, Novus), Bap31 (Pierce MA3-002), Nup214 (ab7049, Abcam), histone H3 (9715S, Cell Signaling Technology), ATL2 (PA5-90788, Invitrogen), ATL3 (Proteintech 169211AP), RTN3 (12055-2-AP, Proteintech), RTN4 (sc-271878, Santa Cruz Biotechnology), LNP (NBP1-80637, Novus), and gamma tubulin (T5326, MilliporeSigma).

2.5.3 Reagents

Prolong diamond antifade mount with DAPI (4′,6-diamidino-2-phenylindole) mounting reagent was obtained from Thermo Fisher (Carlsbad, CA). Mg132 and nocodazole were obtained from Cayman Chemicals (Ann Arbor, MI). Chloroquine, BafA1, and epoximicin were obtained from Sigma Aldrich (St. Louis, MO). Opti-MEM and 0.25% trypsin were obtained from Invitrogen (Carlsbad, CA). Phosphate-buffered saline (PBS) (1x) was obtained from Gibco (Carlsbad, CA). Deoxy Big CHAP (DBC) and phenylmethylsulfonyl fluoride (PMSF) were obtained from EMD Millipore Chemicals (San Diego, CA).

2.5.4 siRNA transfection

All Star negative siRNA (Qiagen, Hilden, Germany) was used as a scrambled control for all knockdowns. siRNA targeting Nup98 was obtained from Sigma-Aldrich with the sequences: Nup98#1 GUGAAGGGCUAAAUAGGAA; Nup98#2 CUGGAGUUAGCACUAACAUAA; Nup98#3 CAGUGUAUUACUGCUAUGAAA. Sequences for siRNAs targeting KIF5B, ATL3,

RTN3, RTN4, and LNP were previously reported [43-46]. Reverse transfection at 40 nM was performed using Lipofectamine RNAiMAX (Thermo Fisher Scientific) for 48 h.

2.5.5 Plasmids and DNA transfection

The mCherry-tagged SV40 NLS construct was kindly provided by Chelsey Spriggs (University of Michigan). The generation of mCherry-tagged Kif5 was previously described [46]. Constructs were transfected into 50% confluent cells with Lipofectamine 2000 (Thermo Fisher, Carlsbad, CA) transfection reagent at a 1:4 ratio. Cells were transfected for 24 h before being fixed or harvested.

2.5.6 Immunofluorescence and confocal microscopy

Cells were seeded and grown on no. 1 glass coverslips, and all the following fixation and staining steps were performed at room temperature. Cells were washed 3x with PBS, fixed in 4% formaldehyde for 15 min, washed 3x with PBS, permeabilized in 0.2% Triton X-100 for 5 min, and blocked with 5% milk with 0.02% Tween-20 for 15 min. Incubation with primary antibodies was done in 5% milk with 0.02% Tween-20 for 1 h (varying antibody concentrations). Coverslips were washed 6x with milk. Incubation with Alexa Fluor secondary antibodies was done in 5% milk with 0.02% Tween-20 for 30 min. Finally, coverslips were washed 3x with milk and 3x with PBS before being mounted in Prolong diamond antifade mount with DAPI. All images were taken using a Zeiss LSM 780 confocal laser scanning microscope and processed and analyzed using FIJI software.

2.5.7 Nuclear fractionation

Separation of cytoplasmic and nuclear fractions was performed according to a modified previously published protocol [34]. Briefly, cells were resuspended in a lysis buffer consisting of 0.1% NP40 in PBS with 1mM PMSF. One third of the total volume was collected as whole cell lysate, and the remainder was centrifuged for 10 min at 13,000 rpm and 4°C. The supernatant (representing the cytosolic fraction) was collected, and the pellet was washed with lysis buffer and again centrifuged for 10 min at 13,000 rpm and 4°C. Finally, the pellet was resuspended with lysis buffer and lysed with the addition of sample buffer.

2.5.8 MTS assay

COS-7 cells were seeded in 96-well plates and reverse transfected with the indicated siRNAs for 48 h. At harvest, cells were treated with the MTS reagent (ab197010; MTS Assay Kit, Abcam) according to the manufacturer's protocol and incubated at 37°C under 5% CO2 for 1 h. After a brief vortex, absorbance (OD = 490 nm) was read for each well using a BioTek Synergy H1 Multimode Reader (Agilent) and analyzed with BioTek Gen5 software.

2.5.9 Co-immunoprecipitation

For immunoprecipitation of Nup62, COS-7 cells in 10 cm plates were lysed in HN buffer (150 mM NaCl, 50 mM Tris pH 7.4) with 1 mM PMSF and 1% Triton X-100 for 15 min on ice, then centrifuged at 16,000 x g for 10 min at 4°C. Supernatant was collected, and 5% input was reserved. Samples were rotated with 2 µg Nup62 antibody or rabbit IgG overnight at 4°C. The following day, 20 uL of protein A/G agarose beads per sample were washed 3x with lysis buffer

and added to each sample tube. Samples were rotated for 30 minutes at 4°C. The beads were again washed 3x with lysis buffer and eluted with 1x sample buffer.

2.6 Acknowledgements

This work was funded by grants from the National Institutes of Health to MP (F31 NS124088) and start-up funds from University of Michigan to BT.

2.7 References

1. Beck M, Hurt E. The nuclear pore complex: understanding its function through structural insight. *Nat Rev Mol Cell Biol*. Feb 2017;18(2):73-89. doi:10.1038/nrm.2016.147

2. Cronshaw JM, Krutchinsky AN, Zhang W, Chait BT, Matunis MJ. Proteomic analysis of the mammalian nuclear pore complex. *J Cell Biol*. Sep 2 2002;158(5):915-27. doi:10.1083/jcb.200206106

3. von Appen A, Kosinski J, Sparks L, et al. In situ structural analysis of the human nuclear pore complex. *Nature*. Oct 1 2015;526(7571):140-143. doi:10.1038/nature15381

4. Otsuka S, Tempkin JOB, Zhang W, et al. A quantitative map of nuclear pore assembly reveals two distinct mechanisms. *Nature*. Jan 2023;613(7944):575-581. doi:10.1038/s41586-022-05528-w

5. Doucet CM, Talamas JA, Hetzer MW. Cell cycle-dependent differences in nuclear pore complex assembly in metazoa. *Cell*. Jun 11 2010;141(6):1030-41. doi:10.1016/j.cell.2010.04.036

6. Bindra D, Mishra RK. In Pursuit of Distinctiveness: Transmembrane Nucleoporins and Their Disease Associations. *Front Oncol*. 2021;11:784319. doi:10.3389/fonc.2021.784319

7. Rabut G, Doye V, Ellenberg J. Mapping the dynamic organization of the nuclear pore complex inside single living cells. *Nat Cell Biol*. Nov 2004;6(11):1114-21. doi:10.1038/ncb1184

8. Goldberg MW, Wiese C, Allen TD, Wilson KL. Dimples, pores, star-rings, and thin rings on growing nuclear envelopes: evidence for structural intermediates in nuclear pore complex assembly. *J Cell Sci*. Feb 1997;110 (Pt 4):409-20. doi:10.1242/jcs.110.4.409

9. Sakiyama Y, Mazur A, Kapinos LE, Lim RY. Spatiotemporal dynamics of the nuclear pore complex transport barrier resolved by high-speed atomic force microscopy. *Nat Nanotechnol*. Aug 2016;11(8):719-23. doi:10.1038/nnano.2016.62

10. Bayliss R, Littlewood T, Stewart M. Structural basis for the interaction between FxFG nucleoporin repeats and importin-beta in nuclear trafficking. *Cell*. Jul 7 2000;102(1):99-108. doi:10.1016/s0092-8674(00)00014-3

11. Frey S, Richter RP, Görlich D. FG-rich repeats of nuclear pore proteins form a three-dimensional meshwork with hydrogel-like properties. *Science*. Nov 3 2006;314(5800):815-7. doi:10.1126/science.1132516

12. Kuiper EFE, Gallardo P, Bergsma T, et al. The chaperone DNAJB6 surveils FG-nucleoporins and is required for interphase nuclear pore complex biogenesis. *Nat Cell Biol*. Nov 2022;24(11):1584-1594. doi:10.1038/s41556-022-01010-x

13. Milles S, Huy Bui K, Koehler C, Eltsov M, Beck M, Lemke EA. Facilitated aggregation of FG nucleoporins under molecular crowding conditions. *EMBO Rep*. Feb 2013;14(2):178-83. doi:10.1038/embor.2012.204

14. Rouvière JO, Bulfoni M, Tuck A, Cosson B, Devaux F, Palancade B. A SUMO-dependent feedback loop senses and controls the biogenesis of nuclear pore subunits. *Nat Commun*. Apr 25 2018;9(1):1665. doi:10.1038/s41467-018-03673-3

15. Agote-Arán A, Lin J, Sumara I. Fragile X-Related Protein 1 Regulates Nucleoporin Localization in a Cell Cycle-Dependent Manner. *Front Cell Dev Biol*. 2021;9:755847. doi:10.3389/fcell.2021.755847

16. Webster BM, Colombi P, Jäger J, Lusk CP. Surveillance of nuclear pore complex assembly by ESCRT-III/Vps4. *Cell*. Oct 9 2014;159(2):388-401. doi:10.1016/j.cell.2014.09.012

17. Lee CW, Wilfling F, Ronchi P, et al. Selective autophagy degrades nuclear pore complexes. *Nat Cell Biol*. Feb 2020;22(2):159-166. doi:10.1038/s41556-019-0459-2

18. Tomioka Y, Kotani T, Kirisako H, et al. TORC1 inactivation stimulates autophagy of nucleoporin and nuclear pore complexes. *J Cell Biol*. Jul 6 2020;219(7)doi:10.1083/jcb.201910063

19. Daigle N, Beaudouin J, Hartnell L, et al. Nuclear pore complexes form immobile networks and have a very low turnover in live mammalian cells. *J Cell Biol*. Jul 9 2001;154(1):71-84. doi:10.1083/jcb.200101089

20. D'Angelo MA, Raices M, Panowski SH, Hetzer MW. Age-dependent deterioration of nuclear pore complexes causes a loss of nuclear integrity in postmitotic cells. *Cell*. Jan 23 2009;136(2):284-95. doi:10.1016/j.cell.2008.11.037

21. Hakhverdyan Z, Molloy KR, Keegan S, et al. Dissecting the Structural Dynamics of the Nuclear Pore Complex. *Mol Cell*. Jan 7 2021;81(1):153-165.e7. doi:10.1016/j.molcel.2020.11.032

22. Rempel IL, Crane MM, Thaller DJ, et al. Age-dependent deterioration of nuclear pore assembly in mitotic cells decreases transport dynamics. *Elife*. Jun 3 2019;8doi:10.7554/eLife.48186

23. Liu J, Hetzer MW. Nuclear pore complex maintenance and implications for age-related diseases. *Trends Cell Biol*. Mar 2022;32(3):216-227. doi:10.1016/j.tcb.2021.10.001

24. Grima JC, Daigle JG, Arbez N, et al. Mutant Huntingtin Disrupts the Nuclear Pore Complex. *Neuron*. Apr 5 2017;94(1):93-107.e6. doi:10.1016/j.neuron.2017.03.023

25. Coyne AN, Rothstein JD. Nuclear pore complexes - a doorway to neural injury in neurodegeneration. *Nat Rev Neurol*. Jun 2022;18(6):348-362. doi:10.1038/s41582-022-00653-6

26. Chou CC, Zhang Y, Umoh ME, et al. TDP-43 pathology disrupts nuclear pore complexes and nucleocytoplasmic transport in ALS/FTD. *Nat Neurosci*. Feb 2018;21(2):228-239. doi:10.1038/s41593-017-0047-3

27. Eftekharzadeh B, Daigle JG, Kapinos LE, et al. Tau Protein Disrupts Nucleocytoplasmic Transport in Alzheimer's Disease. *Neuron*. Sep 5 2018;99(5):925-940.e7. doi:10.1016/j.neuron.2018.07.039

28. Giampetruzzi A, Danielson EW, Gumina V, et al. Modulation of actin polymerization affects nucleocytoplasmic transport in multiple forms of amyotrophic lateral sclerosis. *Nat Commun*. Aug 23 2019;10(1):3827. doi:10.1038/s41467-019-11837-y

29. Zhang K, Donnelly CJ, Haeusler AR, et al. The C9orf72 repeat expansion disrupts nucleocytoplasmic transport. *Nature*. Sep 3 2015;525(7567):56-61. doi:10.1038/nature14973

30. Lin DH, Hoelz A. The Structure of the Nuclear Pore Complex (An Update). *Annu Rev Biochem*. Jun 20 2019;88:725-783. doi:10.1146/annurev-biochem-062917-011901

31. Wu X, Kasper LH, Mantcheva RT, Mantchev GT, Springett MJ, van Deursen JM. Disruption of the FG nucleoporin NUP98 causes selective changes in nuclear pore complex stoichiometry and function. *Proc Natl Acad Sci U S A*. Mar 13 2001;98(6):3191-6. doi:10.1073/pnas.051631598

32. Eymieux S, Blanchard E, Uzbekov R, Hourioux C, Roingeard P. Annulate lamellae and intracellular pathogens. *Cell Microbiol*. Aug 2021;23(8):e13328. doi:10.1111/cmi.13328

33. Shinkai Y, Kuramochi M, Miyafusa T. New Family Members of FG Repeat Proteins and Their Unexplored Roles During Phase Separation. *Front Cell Dev Biol*. 2021;9:708702. doi:10.3389/fcell.2021.708702

34. Suzuki K, Bose P, Leong-Quong RY, Fujita DJ, Riabowol K. REAP: A two minute cell fractionation method. *BMC Res Notes*. Nov 10 2010;3:294. doi:10.1186/1756-0500-3-294

35. Knupp J, Pletan ML, Arvan P, Tsai B. Autophagy of the ER: the secretome finds the lysosome. *Febs j*. Dec 2023;290(24):5656-5673. doi:10.1111/febs.16986

36. Lopata A, Kniss A, Löhr F, Rogov VV, Dötsch V. Ubiquitination in the ERAD Process. *Int J Mol Sci*. Jul 28 2020;21(15)doi:10.3390/ijms21155369

37. Wang S, Tukachinsky H, Romano FB, Rapoport TA. Cooperation of the ER-shaping proteins atlastin, lunapark, and reticulons to generate a tubular membrane network. *Elife*. Sep 13 2016;5doi:10.7554/eLife.18605

38. Woźniak MJ, Bola B, Brownhill K, Yang YC, Levakova V, Allan VJ. Role of kinesin-1 and cytoplasmic dynein in endoplasmic reticulum movement in VERO cells. *J Cell Sci*. Jun 15 2009;122(Pt 12):1979-89. doi:10.1242/jcs.041962

39. Simon DN, Rout MP. Cancer and the nuclear pore complex. *Adv Exp Med Biol*. 2014;773:285-307. doi:10.1007/978-1-4899-8032-8_13

40. Le Sage V, Mouland AJ. Viral subversion of the nuclear pore complex. *Viruses*. Aug 16 2013;5(8):2019-42. doi:10.3390/v5082019

41. Ren H, Xin G, Jia M, et al. Postmitotic annulate lamellae assembly contributes to nuclear envelope reconstitution in daughter cells. *J Biol Chem*. Jul 5 2019;294(27):10383-10391. doi:10.1074/jbc.AC119.008171

42. Hampoelz B, Mackmull MT, Machado P, et al. Pre-assembled Nuclear Pores Insert into the Nuclear Envelope during Early Development. *Cell*. Jul 28 2016;166(3):664-678. doi:10.1016/j.cell.2016.06.015

43. Bagchi P, Liu X, Cho WJ, Tsai B. Lunapark-dependent formation of a virus-induced ER exit site contains multi-tubular ER junctions that promote viral ER-to-cytosol escape. *Cell Rep*. Dec 7 2021;37(10):110077. doi:10.1016/j.celrep.2021.110077

44. Chen YJ, Williams JM, Arvan P, Tsai B. Reticulon protects the integrity of the ER membrane during ER escape of large macromolecular protein complexes. *J Cell Biol*. Feb 3 2020;219(2)doi:10.1083/jcb.201908182

45. Pletan M, Liu X, Cha G, Chen YJ, Knupp J, Tsai B. The atlastin ER morphogenic proteins promote formation of a membrane penetration site during non-enveloped virus entry. *J Virol*. Aug 31 2023;97(8):e0075623. doi:10.1128/jvi.00756-23

46. Ravindran MS, Engelke MF, Verhey KJ, Tsai B. Exploiting the kinesin-1 molecular motor to generate a virus membrane penetration site. *Nat Commun*. May 24 2017;8:15496. doi:10.1038/ncomms15496

Chapter 3

The Atlastin ER Morphogenic Proteins Promote Formation of a Membrane-Penetration Site During Non-Enveloped Virus Entry

With permission from the publisher, this chapter has been adapted from a previous publication:

The Atlastin ER morphogenic proteins promote formation of a membrane-penetration site during non-enveloped virus entry

Madison Pletan, Xiaofang Liu, Grace Cha, Yu-Jie Chen, Jeffrey Knupp, and Billy Tsai (2023). Journal of Virology, 97 (8), e0075623. https://doi.org/10.1128/jvi.00756-23.

3.1 Abstract

During entry, non-enveloped viruses penetrate a host membrane to cause infection, although how this is accomplished remains enigmatic. Polyomaviruses (PyVs) are non-enveloped DNA viruses that penetrate the endoplasmic reticulum (ER) membrane to reach the cytosol *en route* to the nucleus for infection. To penetrate the ER membrane, the prototype PyV SV40 induces formation of ER-escape sites, called foci, composed of repeating units of multi-tubular ER junctions where the virus is thought to exit. How SV40 triggers formation of the ER-foci harboring these multi-tubular ER junctions is unclear. Here we show that the ER morphogenic ATL2 and ATL3 membrane proteins play critical roles in SV40 infection. Mechanistically, ATL3 mobilizes to the ER-foci where it deploys its GTPase-dependent

membrane fusion activity to promote formation of multi-tubular ER junctions within the ER-foci. ATL3 also engages a SV40-containing membrane penetration complex. By contrast, ATL2 does not reorganize to the ER-foci. Instead, it supports the reticular ER morphology critical for the integrity of the ATL3-dependent membrane complex. Our findings illuminate how two host factors play distinct roles in formation of an essential membrane-penetration site for a non-enveloped virus.

3.2 Introduction

Viruses are potent pathogens that induce debilitating human diseases. To cause infection, they deliver their nucleic acid across a cellular membrane into the cytosol (or nucleus) of their host cell. For enveloped viruses surrounded by a lipid bilayer, this requires fusion of the viral and host membranes, resulting in delivery of the viral particle across the limiting membrane.[1] In contrast, non-enveloped viruses cannot invade host cells by a fusion mechanism as they lack a lipid bilayer. Hence the precise mechanism whereby a non-enveloped virus crosses a membrane remains mysterious.[2-4]

Polyomaviruses (PyVs) are non-enveloped DNA viruses responsible for many human diseases, including nephropathy and hemorrhagic cystitis caused by the BK PyV, a fatal demyelinating disease called progressive multifocal leukoencephalopathy triggered by JC PyV, and an aggressive skin cancer called Merkel cell carcinoma (MCC) caused by Merkel cell PyV.[5-8] Because the cell entry mechanism of the prototype PyV simian virus 40 (SV40) is similar to human PyVs, elucidating SV40 cell entry has illuminated our understanding of human PyV infections.[9] Structurally, SV40 is composed of 72 pentamers of the coat protein VP1 that encloses its DNA genome,[10] with each pentamer encasing an internal hydrophobic protein VP2

or VP3.[11] Three forces stabilize the viral architecture: the VP1 C-terminus invades a neighboring VP1 pentamer to provide inter-pentamer support, presence of intra-/inter-pentamer disulfide bonds stabilize the viral structure, and calcium ions bound to the virus further strengthen its structure.[11,12] When assembled, each SV40 particle is 50 nm in diameter.[10]

To infect cells, SV40 undergoes receptor-mediated endocytosis, reaching the endosomes and then the endoplasmic reticulum (ER).[13-15] In the ER lumen, redox-active protein disulfide isomerase (PDI) chaperones reduce and isomerize the viral disulfide bonds and unfold the VP1 C-terminal arms.[16-19] These reactions partially destabilize SV40, exposing the hydrophobic proteins VP2 and VP3.[20] This generates a hydrophobic viral particle that inserts into the ER membrane.[21] To escape from the ER, SV40 remodels the membrane to form suborganellar structures – called "foci" – which act as the ER-to-cytosol membrane penetration site for the viral particle.[22-27] In the final step, the membrane-inserted virus recruits cytosolic extraction machinery to pull it into the cytosol, where it further disassembles and then transits to the nucleus to cause infection.[28-33] Despite this basic model, major gaps remain in our understanding of ER membrane penetration of SV40. In particular, a key question is how the virus exploits host factors to construct the ER-foci structure so that it can successfully eject into the cytosol.

Using high-resolution microscopy, we recently discovered that the virus-induced ER-foci harbor repeating units of multi-ER tubules that coalesce, forming junctional sites where the virus is thought to penetrate into the cytosol.[27] Importantly, the ER membrane protein lunapark (LNP) reorganizes to the ER-foci during SV40 infection to stabilize these multi-tubular ER junctions,[27] reminiscent of the normal function of LNP in stabilizing three-way junctions of the web-like reticular ER morphology.[34,35] Additionally, we reported that the ER morphogenic proteins reticulon3 (RTN3) and reticulon4 (RTN4) mobilize to the ER-foci where they deploy their

established membrane-curvature activity to protect the ER membrane integrity during ER-to-cytosol membrane penetration of SV40.[36]

Beyond LNP and the RTNs, whether other ER "morphogenic" factors are hijacked by SV40 to help construct the ER-foci is unknown. In this manuscript, we report that the ER morphogenic membrane proteins atlastin2 (ATL2) and atlastin3 (ATL3) are important in SV40-triggered ER-foci formation and infection. ATL3 reorganizes to the ER-foci where it uses its GTPase-dependent membrane fusion activity to support generation of multi-tubular ER junctions harbored within the ER-foci. It also associates with LNP, RTN, and SV40, forming an ER membrane-penetration protein complex. By contrast, ATL2 does not reorganize to the ER-foci. Rather, ATL2 supports general reticular ER morphology, which is necessary for the integrity of the ATL3-LNP membrane complex that forms the SV40 foci. Our findings thus illuminate how two related host factors play critical but distinct roles during formation of a membrane-penetration site required for entry of a non-enveloped virus.

3.3 Results

3.3.1 ATL2 and ATL3 are important for SV40 infection

We previously reported that the SV40 ER-foci, which are essential for ER-to-cytosol penetration of the viral particles leading to infection, harbor many coalesced multi-tubular ER junctions.[27] This prompted us to examine the role of the Atlastins in formation of the ER-foci, since this family of ER membrane proteins normally promotes fusion of ER tubules to generate three-way junctions,[35,37-39] reminiscent of the structure of the SV40-induced foci. To test the role of Atlastins in SV40 infection, we used a siRNA-mediated knockdown (KD) approach in simian

CV-1 cells, which are used classically to study SV40. Of the three known ATL proteins (ATL1, ATL2 and ATL3), ATL1 is expressed in the central nervous system, while ATL2 and ATL3 are broadly expressed across many cell types and tissues.[35,37] We therefore focused on the roles of ATL2 and ATL3 during SV40 infection. Accordingly, CV-1 cells were depleted of ATL2 or ATL3 (or both) using their respective siRNAs (Fig. 3.1A, compare lanes 2-4 to 1). Under this KD condition, we monitored appearance of the virally-encoded large T antigen in the cells, which is expressed only when the virus successfully reaches the host nucleus, in order to evaluate infection. Importantly, under ATL2 or ATL3 KD, SV40 infection was markedly reduced when compared to the control (scrambled siRNA, scr) condition (Fig. 3.1B); a similar block in virus infection was also found under the ATL2+3 double KD condition (Fig. 3.1B). These findings suggest ATL2 and ATL3 play important roles during SV40 infection.

We used a rescue approach to ensure that the block in SV40 infection resulting from the ATL2 or ATL3 siRNAs is due to depletion of the intended host protein and not to off-target effects. In these experiments, cells incubated with the scr or ATL2 siRNA were transfected with either a control (GFP-Sec61) or rescue (siRNA-resistant Myc-ATL2) construct, then infected with SV40. Only cells expressing GFP-Sec61 or Myc-ATL2 were assessed for large T-antigen expression. Importantly, expression of Myc-ATL2 largely restored the block in SV40 infection due to the ATL2 siRNA (Fig. 3.1C; compare third to second bar). Likewise, expression of Myc-ATL3 robustly rescued the block in SV40 infection due to the ATL3 siRNA (Fig. 3.1D, compare third to second bar). These results indicate that the block in SV40 infection is due to loss of the intended host target, demonstrating ATL2 and ATL3 promote SV40 infection.

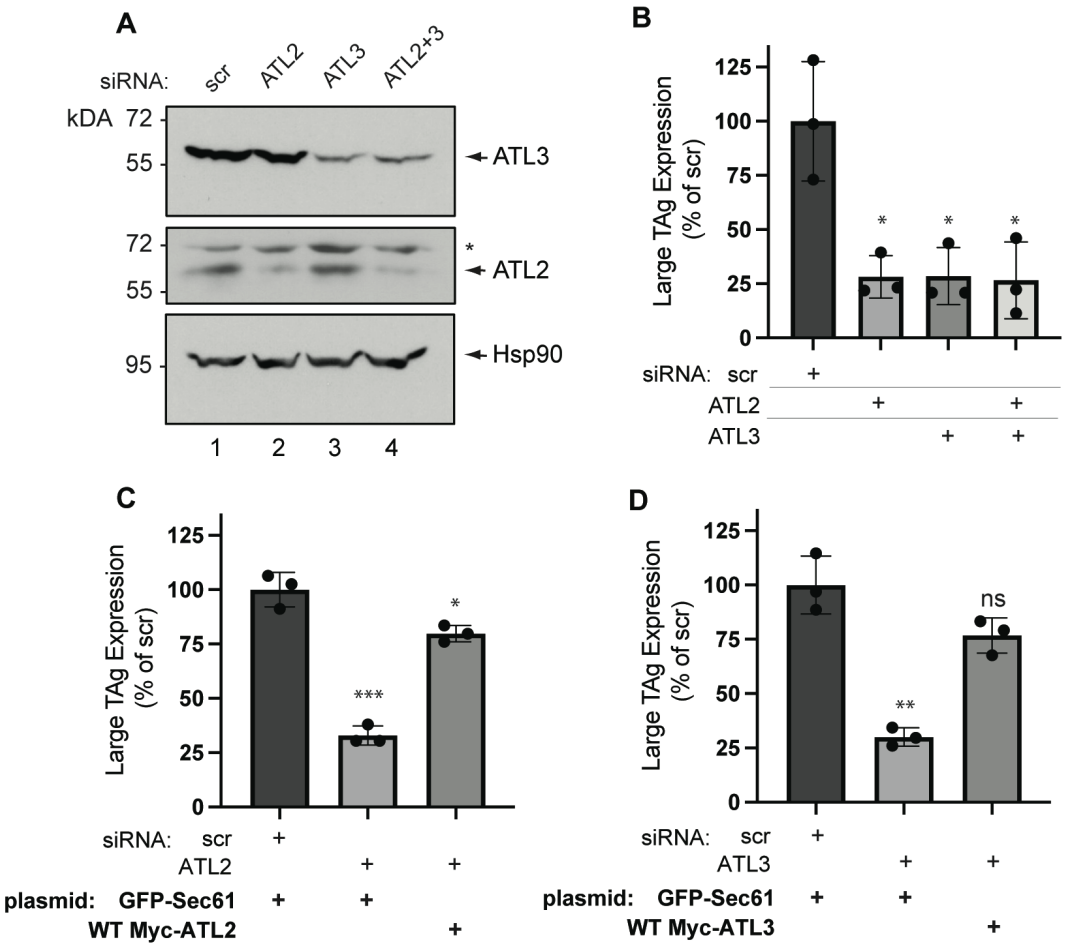

Figure 3.1: ATL2 and ATL3 are important for SV40 infection

(**A**) CV-1 cells were transfected with scrambled control siRNA (scr) or siRNA against ATL2, ATL3, or both. After 48 h of transfection, cell extracts were assessed by SDS-PAGE and immunoblotting with the indicated antibodies. * indicates unidentified protein. (**B**) CV-1 cells transfected with the indicated siRNA were infected with SV40 (MOI ~0.3), fixed, and stained for large T antigen (TAg). TAg expression was scored by immunofluorescence microscopy. Data were normalized to the mean of the scrambled controls. (**C**) and (**D**) As in (B), except cells were transfected with the indicated constructs after the initial siRNA transfection. Cells were fixed and stained for TAg and Myc, and at least 100 GFP/Myc dual-expressing cells were counted in each condition for each biological replicate. Graphs represent mean +/- standard deviation (SD) from 3 independent experiments. The significance was determined via Student's two-tailed *t* test. *, $P \leq 0.05$; **, $P \leq 0.01$; ***, $P \leq 0.001$.

3.3.2 ATL2 and ATL3 are critical for SV40-induced ER-foci formation

Since ATL2 and ATL3 are ER morphogenic proteins that are important in SV40 infection, we reasoned that they might play a role in virus-induced ER-foci formation. As previously reported, in control (scr-treated) cells, incubation with SV40 induces reorganization of select ER membrane proteins (including Bap31) to distinct puncta called foci (Fig. 3.2A, compare second to first row; see white arrows in merge).[23] By contrast, under ATL2, ATL3, or ATL2+3 (double) KD, we found the percentage of cells harboring virus-triggered ER-foci decreased markedly (Fig. 3.2A, compare third, fourth, and fifth rows to second row; quantified in 3.2B).

The ER morphology of ATL3-depleted cells is largely indistinguishable from control cells (Fig. 3.2A, compare fourth to second row; also see Fig. 3.5B, compare third to first row), although depletion of ATL2 caused the ER to appear more elongated and extended when compared to control cells (Fig. 3.2A, compare third to second row; also see Fig. 3.5B, compare second to first row). This modest effect of ER morphology under ATL2 KD is consistent with a previous report.[39]

While this data suggests that ATL2 and ATL3 promote SV40 ER-foci formation, it is possible the ATLs support an upstream step in viral entry. We therefore asked whether depletion of the ATL proteins perturbs SV40 arrival to the ER from the cell surface. To test this, we used a well-established biochemical assay designed to isolate ER-localized SV40 from infected cells (see Materials and Methods). Using this assay, we found that KD of ATL2 or ATL3 did not decrease the ER-localized VP1 level when compared to scr-treated cells (Fig. 3.2C, first panel, compare lane 3 and 4 to 1; the VP1 band intensity in the ER-localized fraction is quantified in Fig. 3.2D). By contrast, cells treated with brefeldin A (BFA), a drug that blocks retrograde cargo

transport from the cell surface to the ER, did reduce the ER-localized VP1 level when compared to scr-treated cells, as expected (Fig. 3.2C, first panel, compare lane 2 to 1; the VP1 band intensity is quantified in Fig. 3.2D). These findings strongly suggest that transport of SV40 from the cell surface to the ER is not affected under ATL2 or ATL3 KD, despite the modest effect of depleting ATL2 on ER morphology. Together, the data demonstrate that after reaching the ER, SV40 exploits that actions of ATL2 and ATL3 to promote ER-foci formation, consistent with the function of these two proteins in overall SV40 infection (Fig. 3.1).

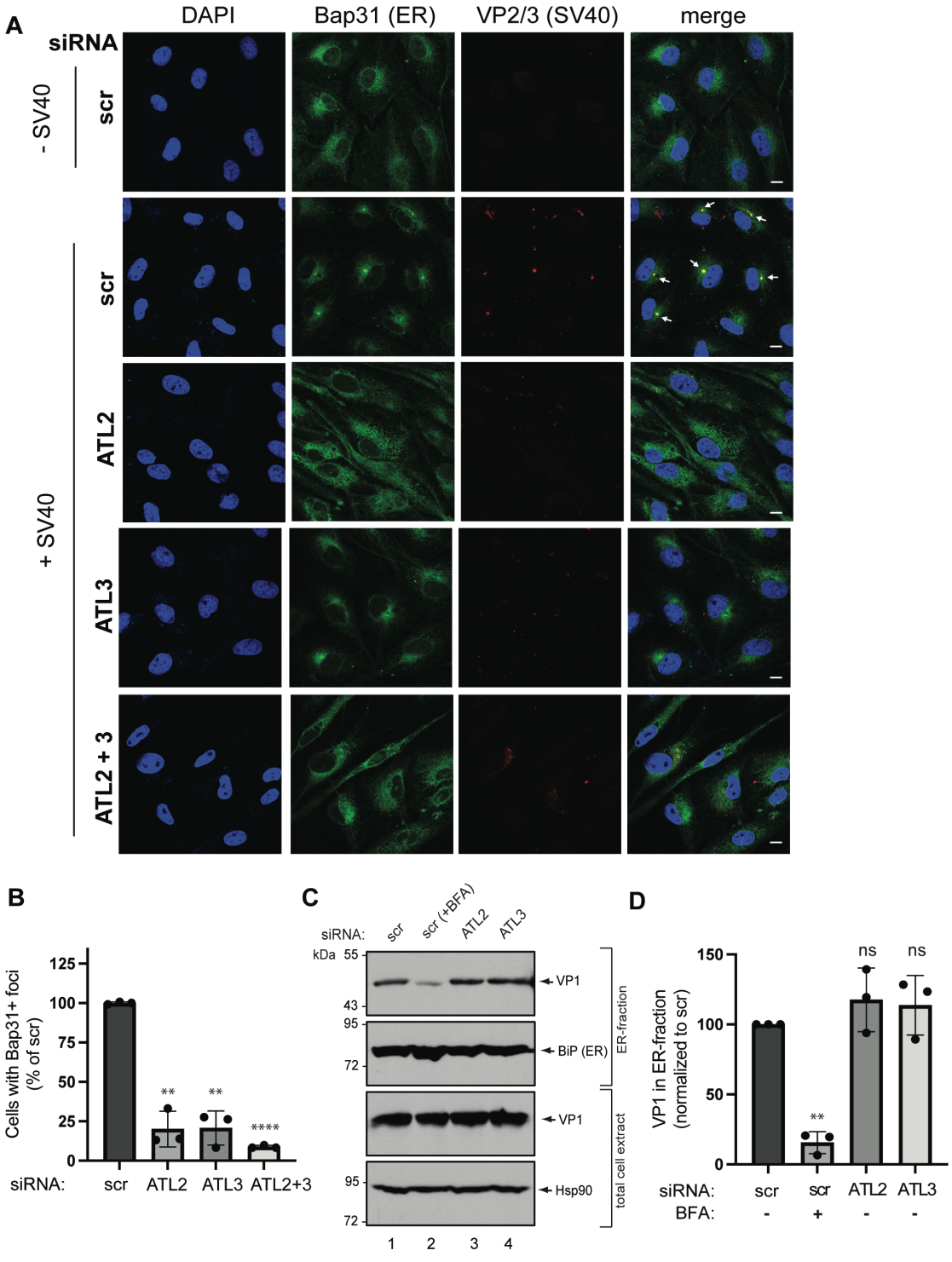

Figure 3.2: ATL2 and ATL3 are critical for SV40-induced ER-foci formation

(**A**) CV-1 cells transfected with the indicated siRNA were infected (or left uninfected) with SV40 (MOI ~10), fixed, stained with the indicated antibodies, counterstained with DAPI, and subjected to confocal immunofluorescence

microscopy. Scale bars, 10 μm. (**B**) Quantification of (A). Cells were scored as positive if at least one Bap31 focus was present in the cell. Data were normalized to the scrambled control. (**C**) CV-1 cells were transfected with the indicated siRNA. After transfection, either DMSO control or brefeldin A (BFA) was added to the cells and infected with SV40 (MOI ~5). Cells were then harvested and subjected to a fractionation assay (see Materials and Methods) to isolate an ER-containing fraction. This fraction, and the total cell extract, were subjected to SDS-PAGE and immunoblotting with the indicated antibodies. (**D**) Quantification of relative VP1 band intensities in the ER-fractions of (C). Bands were quantified with FIJI software, normalized relative to the total levels of VP1, and expressed as a percentage of the band intensity of the scrambled control. Graphs represent mean +/- SD from 3 independent experiments. The significance was determined via Student's two-tailed *t* test. **, $P \leq 0.01$; ****, $P \leq 0.0001$.

3.3.3 The GTPase-dependent membrane fusion activity of ATL2 and ATL3 are crucial for SV40 infection

ATLs mediate homotypic membrane fusion of ER tubules to form three-way junctions that gives rise to the reticular ER morphology.[35,38,40,41] This membrane fusion activity depends strictly on the GTPase activity of ATL, which is contained within its cytosolic domain.[38,41,42] Because multi-tubular ER junctions are found in the SV40-induced ER-foci structure,[27] we hypothesized that the GTPase activity of ATL2 and ATL3 is important in SV40 infection. To test this, we used a GTPase-defective ATL2 or ATL3 mutant protein in the KD-rescue strategy established in Fig. 3.1. Importantly, we found expression of Myc-tagged WT ATL2 (WT Myc-ATL2), but not the corresponding GTPase-defective K107A ATL2 mutant (K107A Myc-ATL2),[35] restored SV40 infection under ATL2 KD (Fig. 3.3A; representative expression in Fig. 3.3B). Similar to the ER morphology phenotype noted under ATL2 KD (Figs. 3.2A and 3.5B), expression of GTPase-defective ATL2 also resulted in an elongated, unbranched ER morphology

(Fig. 3.3B), consistent with previous reports.[35] Likewise, expression of Myc-tagged WT ATL3 (WT Myc-ATL3), but not the GTPase-defective K47A ATL3 mutant (K47A Myc-ATL3),[35] rescued SV40 infection under ATL3 KD (Fig. 3.3C; representative expression in Fig. 3.3D). These findings indicate that the GTPase-dependent membrane fusion activity of ATL2 and ATL3 are crucial in promoting SV40 infection.

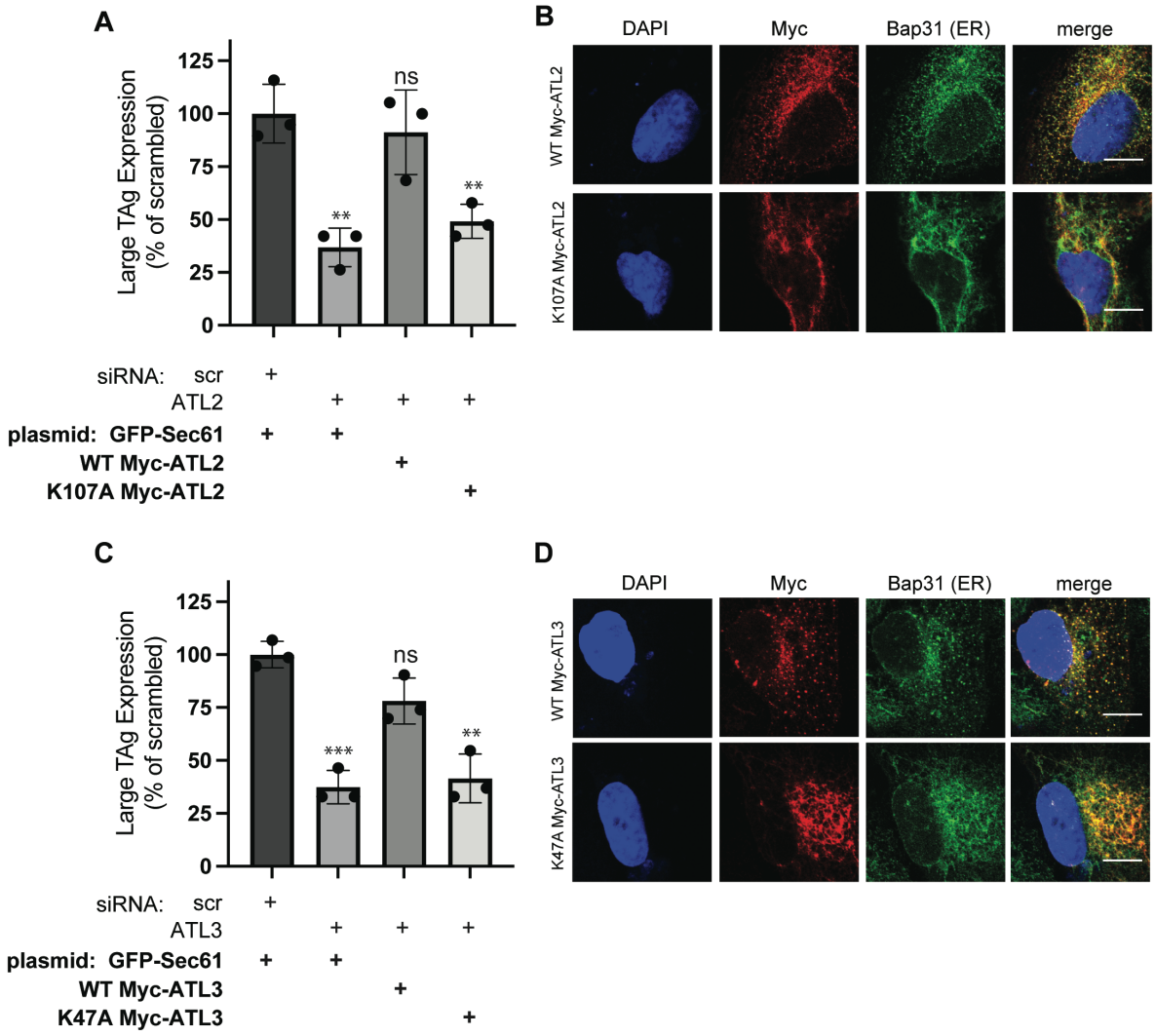

Figure 3.3: The GTPase-dependent membrane fusion activity of ATL2 and ATL3 are crucial for SV40 infection

(**A**) and (**C**) CV-1 cells were transfected with the indicated siRNA, then transfected with the indicated constructs. Cells were then infected with SV40 (MOI ~0.3), fixed, stained for TAg and Myc, then assessed for infection via confocal microscopy as in Fig. 3.1. At least 100 GFP/Myc dual-expressing cells were counted in each condition for each biological replicate. Data were normalized to the mean of the scrambled controls. Graphs represent mean +/- SD from 3 independent experiments. The significance was determined via Student's two-tailed *t* test. **, $P \leq 0.01$; ***, $P \leq 0.001$. (**B**) and (**D**) CV-1 cells were transfected with the indicated constructs, fixed, stained for Myc and Bap31, and counterstained with DAPI. Scale bars, 10 μm.

3.3.4 ATL3 mobilizes to the SV40-induced ER-foci to participate in an ER membrane penetration complex

A simple model to explain how SV40 infection requires the membrane fusion activity of ATL3 (Fig. 3.3) is that ATL3 reorganizes to the ER-foci where it catalyzes membrane fusion of the coalescing multi-ER tubules to generate junctional sites where SV40 escapes into the cytosol.[27] Consistent with this idea, by microscopy, we found endogenous ATL3 mobilizes to the Bap31+ ER-foci (Fig. 3.4A); quantification revealed that approximately 75% Bap31+ foci colocalize with distinct ATL3+ foci (Fig. 3.4B). This result is consistent with the hypothesis that ATL3 mobilizes to the SV40 membrane penetration structure, promoting membrane fusion of ER tubules to form the junctional sites.

We have previously reported two other ER morphogenic proteins—RTN and LNP—mobilize to the SV40 ER-foci to form and maintain this membrane penetration structure.[27,36] Mechanistically, RTN deploys its membrane-curvature-stabilizing activity to relieve the mechanistic stress caused by the viral particles;[36] LNP is later recruited to stabilize the multi-tubular junctions within the ER-foci.[27] Since ATL3 strongly mobilizes to the foci, we postulated that ATL3 associates with these two key critical foci-forming proteins. Co-immunoprecipitation

(coIP) experiments performed in CV-1-derived COS-7 cells showed that precipitation of FLAG-tagged LNP (FLAG-LNP), but not the control HA+FLAG-tagged GFP (HA-FLAG-GFP), pulled down endogenous ATL3 but not ATL2 (Fig. 3.4C, compare lane 4 to 3). (COS-7 cells were used due to their higher transfection efficiency when compared to the CV-1 cells.) Similarly, immunoprecipitation of HA-tagged RTN4B (HA-RTN4B) but not HA-FLAG-GFP precipitated endogenous ATL3 but not ATL2 (Fig. 3.4D, compare lane 2 to 1). (RTN4B is a RTN4 isoform lacking the cytosolic domain.) These findings demonstrate that ATL3 physically associates with LNP and RTN4B, two other ER membrane proteins critical for SV40 ER-foci formation and infection.

Because the ATL3-LNP-RTN4B membrane protein complex is responsible for generating and maintaining the ER-foci structure that supports SV40 ER-to-cytosol escape, we then asked if this ER membrane protein complex interacts with SV40 itself. Indeed, our coIP analysis using virus-infected cells revealed that precipitation of HA-RTN4B (but not HA-FLAG-GFP) pulled down SV40 VP1, and ATL3 as expected (Fig. 3.4E, compare lane 2 to 1). Thus, ATL3 not only associates with other ER morphogenic proteins essential in promoting ER-foci formation and maintenance, but also interacts with SV40 as part of a virus membrane-penetration complex.

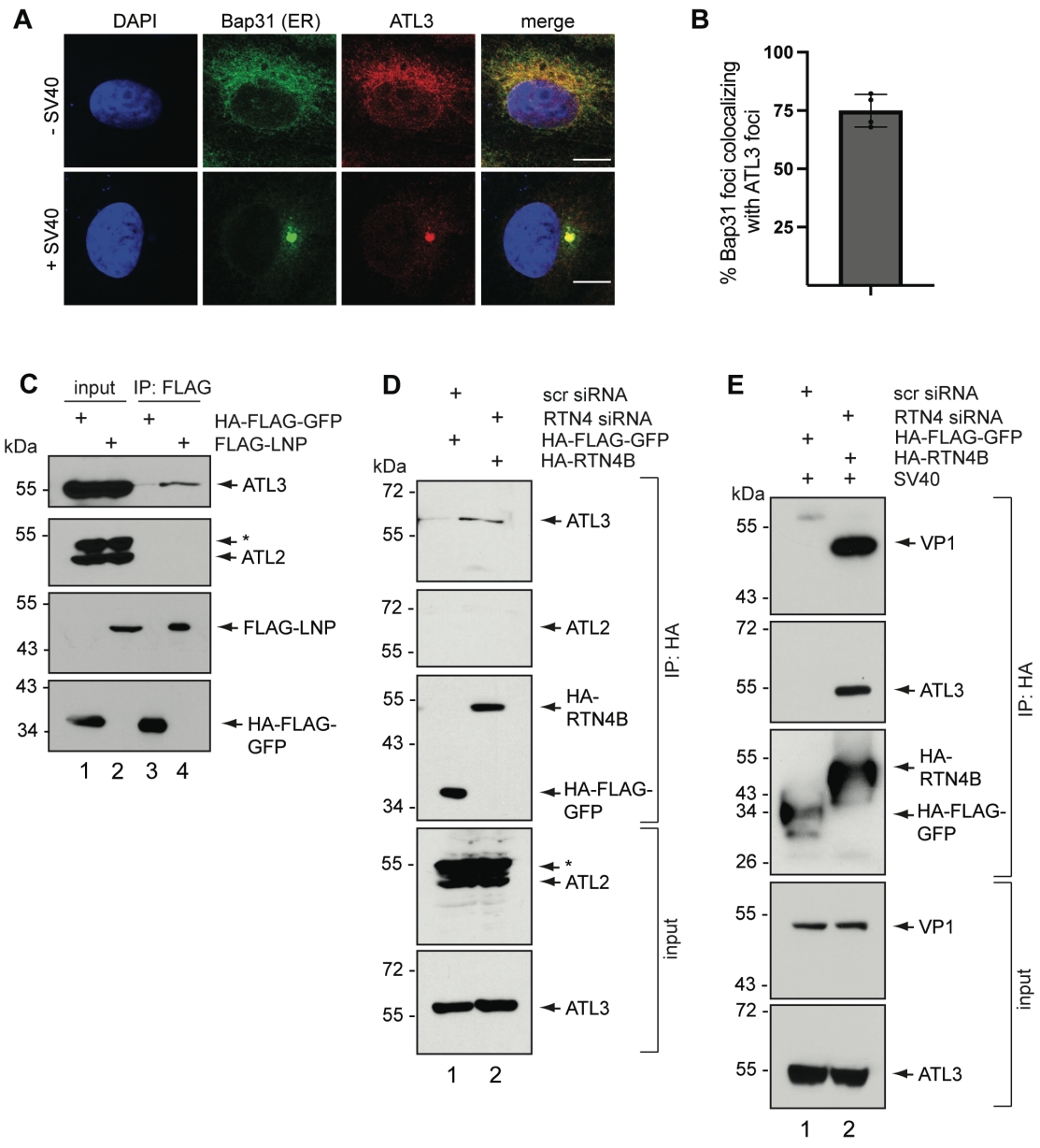

Figure 3.4: ATL3 mobilizes to the SV40-induced ER-foci to participate in an ER membrane-penetration complex

(**A**) CV-1 cells were infected (or left uninfected) with SV40 (MOI ~50), fixed, stained with the indicated antibodies, and then counterstained with DAPI. Scale bars, 10 μm. (**B**) Quantification of (A): a Bap31+ focus was scored as positive if it colocalized with an ATL3+ focus. Graph represents mean +/- SD from 4 independent experiments. (**C**) COS-7 cells were transfected with the indicated constructs and the cell extracts were subject to immunoprecipitation with FLAG M2 antibody-conjugated beads. Immunoprecipitated material was subjected to SDS-PAGE and immunoblotting with the indicated antibodies. Input represents 2.5% of the total sample used for

immunoprecipitation. * indicates unidentified protein. (**D**) COS-7 cells were transfected with the indicated siRNAs and then transfected with the indicated constructs. Cell extracts were subject to immunoprecipitation with HA antibody-conjugated beads. Immunoprecipitated material was subjected to SDS-PAGE and immunoblotting with the indicated antibodies. Input represents 2.5% of the total sample used for immunoprecipitation. * indicates unidentified protein. (**E**) As in (D), except cells were infected with SV40 (MOI ~10) after transfection of the indicated plasmids. Cell extracts were cross-linked using DSP, then subjected to immunoprecipitation with HA antibody-conjugated beads. Input represents 1% of the total sample used for immunoprecipitation.

3.3.5 ATL2 knockdown alters ER morphology and selectively impairs ATL3-LNP interaction

Since ATL3 mobilizes to the SV40 ER-foci, we next examined whether endogenous ATL2 also reorganizes to the foci. Surprisingly, we found that it did not (Fig. 3.5A), in contrast to ATL3. This phenotype was repeatedly observed using two additional ATL2 antibodies (see Materials and Methods). Furthermore, as shown above, ATL2 does not physically associate with either LNP (Fig. 3.4C) or RTN (Fig. 3.4D), two morphogenic proteins that mobilize to the ER-foci and are crucial for foci formation. What then might be the functional significance of ATL2 during SV40-induced ER-foci formation? We found that cells depleted of ATL2 displayed elongated ER morphology (Fig. 3.2A). Indeed, at higher magnification, examination of the ER morphology (via staining of the Bap31 ER membrane protein) confirmed that ATL2 KD cells display longer, less reticulated ER structure compared to either control or ATL3 KD (Fig. 3.5B).

Given this moderate alteration in ER morphology, we asked whether depletion of ATL2 causes global ER stress, preventing cells from supporting viral infection. We tested this by checking the levels of spliced Xbp1, a well-established assay for ER stress[36]: the presence of the spliced form of mRNA encoding the transcription factor Xbp1 (Xbp1s) is used to assess ER stress induction and can be detected by RT-PCR analysis. ATL2 knockdown, with or without

SV40 infection, did not lead to splicing of Xbp1 (Fig. 3.5C, compare lanes 3 and 4 to lanes 2 and 1), whereas positive control cells treated with dithiothreitol (DTT) did exhibit Xbp1 splicing (Fig. 3.5C, compare lanes 5 to 1) as expected. Therefore, although depletion of ATL2 did cause ER elongation, this alteration in morphology did not result in global ER stress induction. Rather, ATL2 KD appears to more specifically prevent SV40 from reorganizing ER components into the foci. This is consistent with our finding that ATL2 is necessary for the foci formation step of SV40 entry (Fig. 3.2).

Importantly, although depletion of ATL2 did not lead to global ER stress, we detected a marked impairment in the interaction between ATL3 and LNP under this condition. Specifically, under ATL2 knockdown, the level of endogenous LNP (but not RTN4B) that co-precipitated with endogenous ATL3 was significantly reduced (Fig. 3.5D, compare lane 4 to 3). Since we posit that the ATL3-LNP complex forms and stabilizes the foci (Fig. 3.4C),[27] this finding demonstrates that the integrity of a key foci component is compromised by ATL2 depletion. This result provides one possible explanation for why ATL2 is critical for foci formation.

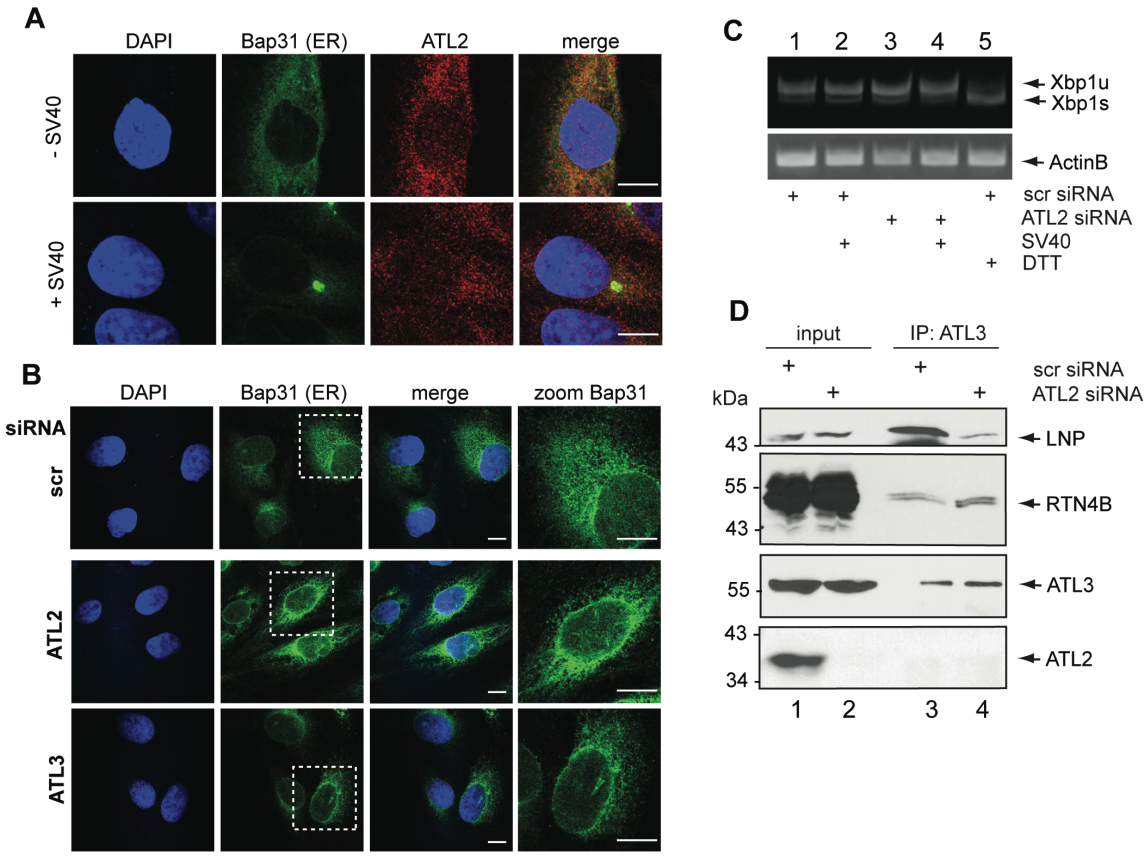

Figure 3.5: ATL2 knockdown alters ER morphology and selectively impairs ATL3-LNP interaction

(**A**) CV-1 cells were infected (or left uninfected) with SV40 (MOI ~50), fixed, stained with the indicated antibodies, and then counterstained with DAPI. (**B**) CV-1 cells were transfected with the indicated siRNA, fixed, stained with Bap31 antibody, counterstained with DAPI, and then examined using confocal immunofluorescence. Scale bars, 10 μm. (**C**) CV-1 cells were transfected with the indicated siRNAs, mock infected or infected (MOI ~50), then treated with DTT or DMSO control. RNA was extracted and reverse transcribed; the resulting cDNA was subjected to PCR amplification and gel electrophoresis. Xbp1u is unspliced Xpb1, while Xbp1s is spliced Xbp1. (**D**) COS-7 cells were transfected with the indicated siRNAs and the cell extracts were subject to immunoprecipitation with antibody against endogenous ATL3. Immunoprecipitated material was subjected to SDS-PAGE and immunoblotting with the indicated antibodies. Input represents 2.5% of the total sample used for immunoprecipitation.

3.3.6 Overexpression of ATL3 compensates for ATL2 knockdown, restoring both ER morphology and SV40 infection

Because ATL2 and ATL3 have distinct roles during virus-induced ER-foci formation, we asked if they can compensate for each other during SV40 infection. To test this, we performed "cross-rescue" experiments and found that whereas expression of WT ATL2 cannot rescue the block in SV40 infection under ATL3 KD (Fig. 3.6A), expression of WT ATL3 can restore the block in SV40 infection under ATL2 KD (Fig. 3.6B). The latter observation is likely because expressing WT ATL3 in ATL2-depleted cells restored normal ER morphology (Fig. 3.6C, compare third to second row; GFP-Sec61 serves as a transfection control). Together, these results suggest that during SV40 infection, ATL3 executes a role that cannot be substituted by ATL2, while ATL2 participates in a step that can at least be partially compensated by ATL3.

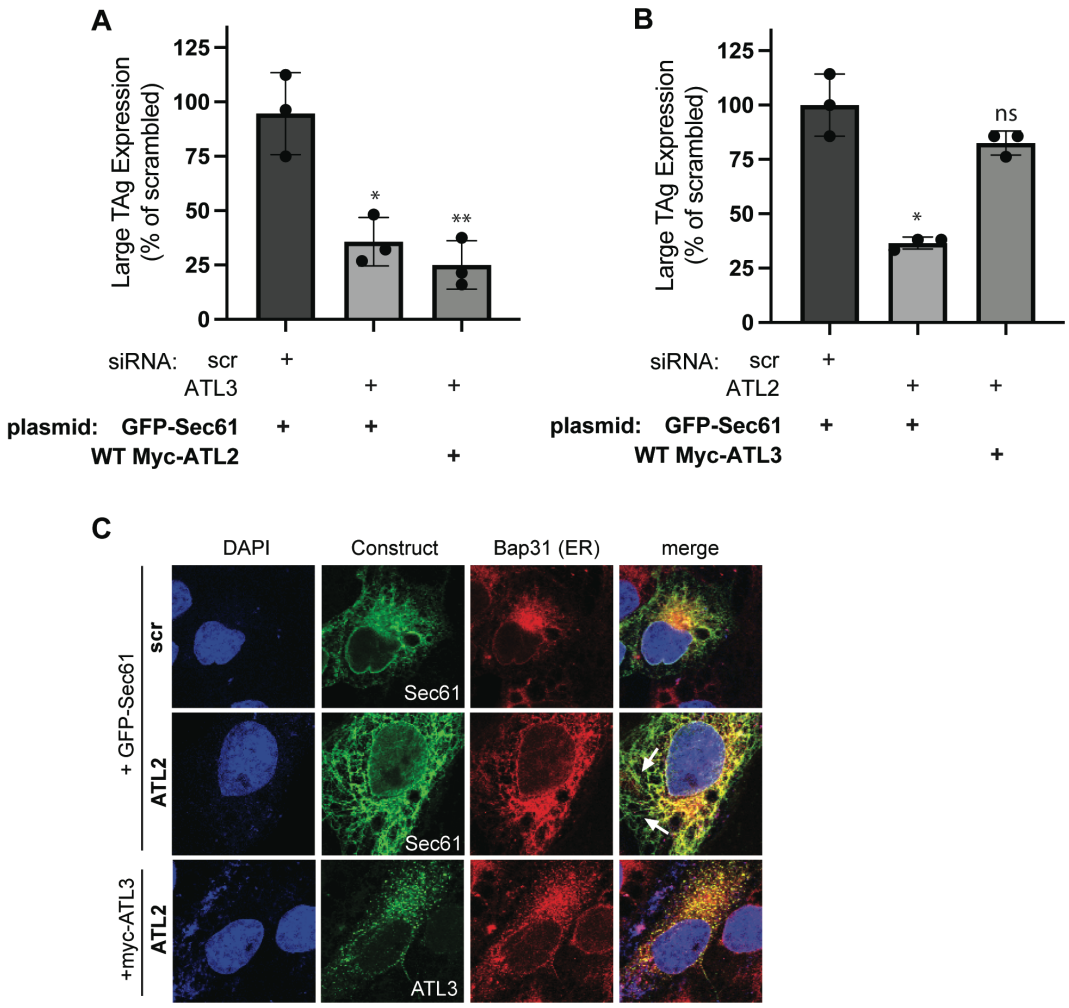

Figure 3.6: Overexpression of ATL3 compensates for ATL2 knockdown, restoring both ER morphology and SV40 infection

(**A**) and (**B**) CV-1 cells were transfected with the indicated siRNA and then transfected with the indicated constructs. Cells were then infected with SV40 (MOI ~0.3), fixed, stained for TAg and Myc, and then assessed for infection via confocal microscopy as in Fig. 3.1. At least 100 GFP/Myc dual-expressing cells were counted in each condition for each biological replicate. Data were normalized to the mean of the scrambled controls. Graphs represent mean +/- SD from 3 independent experiments. The significance was determined via Student's two-tailed *t* test. *, $P \leq 0.05$; **, $P \leq 0.01$. (**C**) CV-1 cells were transfected with the indicated siRNAs and then transfected with the indicated constructs. Cells were fixed, stained for Myc and Bap31, and counterstained with DAPI. Scale bars, 10 μm.

3.4 Discussion

How a non-enveloped virus penetrates a biological membrane to cause infection remains enigmatic. In the case of the non-enveloped prototype PyV SV40, the virus induces formation of a sub-organellar focus structure at the ER membrane through which the viral particle penetrates to reach the cytosol *en route* to the nucleus for infection. Using super-resolution FIB-SEM microscopy, we recently reported that the ER-foci structure harbors repeating units of multi-ER tubular junctional sites where SV40 penetrates to reach the cytosol.[27] These junctional sites are likely highly destabilized and are therefore ideally suited for penetration by a viral particle.[43] Despite these insights, the molecular basis by which SV40 hijacks host components to construct the ER-foci is not entirely clear. In this manuscript, we identify a role of the ATL ER morphogenic proteins in construction of this SV40 membrane-penetration site.

Using a loss-of-function (siRNA-mediated) KD approach coupled with a rescue strategy, we showed that ATL2 and ATL3 play critical roles in supporting virus infection. Because concurrent KD of ATL2 and ATL3 did not lead to a stronger block in virus infection when compared to the single KD condition, ATL2 and ATL3 likely act along the same pathway. Under the same ATL KD condition, SV40-induced ER-foci formation was markedly impaired without affecting virus arrival to the ER from the cell surface, suggesting that these two ATL proteins play important functions in construction of the ER-escape structure necessary for infection.

Mechanistically, we demonstrate that the GTPase-dependent membrane fusion activity of ATL2 and ATL3 are required for SV40 infection. One interpretation of this result is that during virus infection, both ATL2 and ATL3 mobilize to the ER-foci where they mediate membrane fusion of the coalescing multi-ER tubules, thereby generating junctional sites where the virus escapes into the cytosol. This scenario is reminiscent of the normal cellular function of the ATL

proteins, where they deploy the GTPase-dependent membrane fusion activity to generate three-way junctions that gives rise to the web-like reticular ER morphology.[35,38,40,41] Importantly, we find that ATL3 but not ATL2 mobilizes to the ER-foci during SV40 infection. Thus, SV40 induces ATL3 to reorganize to the ER-foci where its membrane fusion activity is used to promote fusion of the multi-ER tubules to generate the junctional sites (Fig. 3.7). Our observation that ATL3 depletion markedly blocked ER-foci formation suggests that fusion of the coalescing multi-ER tubules plays a critical role is stabilizing the ER-foci structure.

In contrast to ATL3, ATL2 does not reorganize into the foci structure yet is important for ER-foci formation, raising the possibility that ATL2 acts at a step upstream of ER-foci formation. How might ATL2 participate in ER-foci formation without mobilizing to the foci structure? One possibility is that ATL2-mediated, GTPase-dependent membrane fusion of ER tubules plays a more prominent role in establishing and/or maintaining general ER morphology than ATL3 (Fig. 3.7) – an intact ER morphology is in turn crucial for SV40 to generate the ER-foci. Consistent with this idea, the ER appears more extended and elongated under ATL2 (but not ATL3) KD, and more disrupted under expression of GTPase-deficient ATL2 (but not ATL3). This finding is in agreement with a previous report suggesting a prominent role of ATL2 in establishing the ER morphology.[39] ATL1 and ATL2 were reported to be significantly more fusogenic than ATL3,[41] consistent with ATL2 playing a more dominant role in establishing the reticular ER morphology. Importantly, we found that although no ER stress induction was observed under ATL2 knockdown, depletion of ATL2 did impair the integrity of the ATL3-LNP complex. This result likely accounts, in part, for why ATL2 is critical during SV40-induced ER-foci formation. Intriguingly, in the context of an overexpression system, both the block in SV40 infection and impaired ER morphology due to ATL2 depletion can be restored by the exogenous

expression of ATL3, suggesting that ATL3 has the capacity to functionally replace ATL2. This is consistent with a recent finding reporting that in cells lacking ATL1, ATL2, and ATL3, overexpression of ATL3 is sufficient to restore the reticular ER morphology.[44]

A key conundrum is how SV40 triggers reorganization of ATL3, as well as the other two ER morphogenic proteins RTN and LNP,[27,36] to the ER-foci. Our biochemical analysis revealed that ATL3 engages RTN and LNP, consistent with a previous report showing that ATL3 recruits LNP to stabilize three-way junctions.[44] Furthermore, we show that the ATL3-RTN protein complex binds to SV40. Taken together, these data suggest a model (Fig. 3.7) in which SV40, upon reaching the ER, associates with the ATL3-RTN membrane complex, inducing reorganization of this morphogenic protein complex into the foci structure. LNP is then recruited to stabilize the junctions. Here ATL3 both promotes membrane fusion of the ER tubules and recruits LNP, leading to formation of stable multi-tubular junctional sites where SV40 penetrates to reach the cytosol.

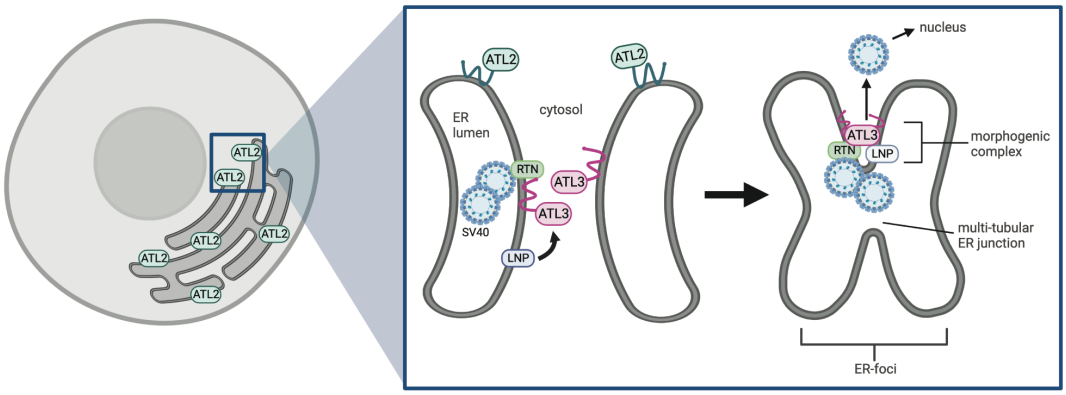

Figure 3.7: Model depicting the roles of ATL2 and ATL3 during SV40-induced ER-foci formation

During entry, SV40 is targeted from the cell surface to the ER. Here, ER-resident host factors impart conformational changes to the virus, generating a hydrophobic SV40 particle that initiates the ER-to-cytosol membrane penetration

process. In this manuscript, we found that this viral entry pathway is dependent on ATL2, which serves to establish and maintain the reticular structure of the ER. During membrane penetration itself, SV40 engages the ER morphogenic proteins RTN and ATL3, which recruit LNP, and the virus reorganizes to the ER-foci with this morphogenic protein complex. Importantly, the interaction between LNP and ATL3 is dependent on ATL2. Thus, both ATL2 and ATL3 promote formation of a multi-tubular ER junction site where the virus penetrates to reach the cytosol. Figure created in Biorender.com.

Finally, it is important to stress that the actions of the ATL ER membrane proteins in regulation of the virus life cycle are not exclusive to non-enveloped DNA viruses. For instance, in the case of the enveloped RNA flaviviruses, ATL2 was reported to support formation of the replication organelle while ATL3 was shown to participate in virus maturation and secretion.[45] Moreover, for the HIV retrovirus, ATL1 is thought to play a role in virus replication.[46] Hence, our findings here underscore the versatility of the ATL morphogenic factors in supporting distinct steps of the viral life cycle across wide-ranging virus families.

3.5 Materials and Methods

3.5.1 Cells

CV-1 (CCL-70) and COS-7 (CRL-1651) cells were obtained from ATCC. Because CV-1 cells are susceptible to SV40 infection and are historically used to study SV40 entry, CV-1 cells were used for infection and ER-foci formation studies (Figs. 1-4). For co-immunoprecipitation studies requiring a higher transfection efficiency (Fig. 3.5), COS-7 cells were used, as they are derived from CV-1 cells but transfect more efficiently. All cells were cultured in complete Dulbecco's modified Eagle medium (cDMEM) supplemented with 10% fetal bovine serum

(FBS, Atlanta Biologicals, GA), 10 U/ml penicillin, and 10 μg/ml streptomycin (Thermo Fisher Scientific).

3.5.2 Antibodies and reagents

The antibodies used for this study were SV40 large T antigen (Santa Cruz sc-147), Hsp90 (Santa Cruz sc-13119), Myc (Sigma c3956), Bap31 (Pierce MA3-002), ATL3 (Proteintech 169211AP), ATL2 (Thermo Fisher PA5-111729, PA5-113190, PA5-90788), BiP (Abcam ab21685), polyclonal VP1 (Abcam ab53977), VP2/3 (Abcam ab53983), FLAG (Millipore Sigma-Aldrich F1365), and HA (Roche 11867423001). Fugene HD was obtained from Promega (Madison, WI). FLAG M2 antibody-conjugated beads, Triton X-100, 2-Mercaptoethanol and brefeldin A (BFA) were obtained from Sigma-Aldrich (St. Louis, MO). HA antibody-conjugated beads, dithiobis-succinimidyl-propionate (DSP), and Prolong diamond antifade mount with DAPI (4′,6-diamidino-2-phenylindole) mounting reagent were obtained from Thermo Fisher (Carlsbad, CA). Opti-MEM and 0.25% trypsin were obtained from Invitrogen (Carlsbad, CA). Phosphate-buffered saline (PBS) (1x) was obtained from Gibco (Carlsbad, CA). Digitonin, Deoxy Big CHAP (DBC) and phenylmethylsulfonyl fluoride (PMSF) were obtained from EMD Millipore Chemicals (San Diego, CA).

3.5.3 siRNA transfection

All Star negative siRNA (Qiagen, Hilden, Germany) served as a scrambled control in all siRNA experiments. siRNAs targeting ATL2, ATL3, and RTN4 were synthesized by Sigma-Aldrich with the following target sequences: siATL2:

GGAGCUAUCCUUAUGAACAUUCAUA; siATL3: CAGGUUCAUAUCCAGAGGAAU; siRTN4: GUUCAGAAGUACAGUAAUU. CV-1 cells were reverse-transfected with each siRNA at 20 nM using Lipofectamine RNAiMAX (Thermo Fisher Scientific) for 48 h.

3.5.4 Plasmids

FLAG-HA-GFP (AddGene plasmid #22612) was kindly provided by Wade Harper (Harvard). Myc-tagged Atlastin (wild-type ATL2, K107A ATL2, wild-type ATL3, and K47A ATL3) and GFP-Sec61 constructs were kindly provided by Tom Rapoport (Harvard). A construct expressing wild-type LNP was also provided by Tom Rapoport and cloned with a C-terminal FLAG tag. The generation of an siRNA-resistant RTN4B construct was previously described [36]. To generate a siRNA-resistant construct of wild-type and K107A ATL2 for this study, the following silent mutations (underlined) of the ATL2 siRNA were introduced via polymerase chain reaction (PCR): GGAGCTATCC<u>A</u>TA<u>C</u>GA<u>G</u>CATTCATA.

3.5.5 DNA transfection

In CV-1 cells, the indicated constructs were transfected into 50% confluent cells using the FuGENE HD (Promega, Madison, WI) transfection reagent at a 1:4 ratio. In COS-7 cells, Lipofectamine 2000 (Thermo Fisher, Carlsbad, CA) was used as the transfection reagent. DNA was allowed to express 24-48 h before cells were fixed or harvested.

3.5.6 Preparation of SV40

Growth and purification of SV40 virions using the OptiPrep gradient (Sigma) has been previously described [47].

3.5.7 Immunofluorescence and confocal microscopy

After being grown on no. 1 glass coverslips, cells were washed with PBS 3x, fixed with 4% formaldehyde for 15 min, washed with PBS 3x, permeabilized in 0.2% Triton X-100 for 5 min, and blocked with 5% milk with 0.02% Tween-20 for 15 min (all steps at 25 °C). Cells were then incubated with primary antibodies in 5% milk with 0.02% Tween-20 for 1 h at 25 °C. Cells were washed 6x with milk and incubated in 5% milk with 0.02% Tween-20 with Alexa Fluor secondary antibodies for 30 min at 25 °C. Coverslips were finally washed 3x with milk and 3x with PBS before being mounted with Prolong diamond antifade mount with DAPI. Cells were imaged using a Zeiss LSM 780 confocal laser scanning microscope, and images were processed and analyzed using FIJI software.

3.5.8 Large T antigen assay

Expression of Large T antigen was used to assess levels of SV40 infection. CV-1 cells (5 x 10^4) were seeded on coverslips in 12-well plates and transfected with the indicated siRNA at 20 nM for 48 h. For knockdown-rescue experiments, after 24 h of siRNA transfection as described above, the CV-1 cells were washed and transfected with the indicated constructs for 24 h. 48 h after siRNA transfection, cells were infected with SV40 (MOI ~0.3) for 24 h, fixed, and stained using antibodies against SV40 TAg. To assess SV40 infection in cells without DNA transfection, at least 250 cells were counted per condition per biological replicate. To assess

SV40 infection in rescue experiments, at least 100 transfected cells were counted per condition per biological replicate.

3.5.9 Virus-induced ER-foci formation

Number of Bap31-positive puncta was used to assess formation of virus-induced ER-foci, as described previously [23]. Briefly, CV-1 cells were seeded on glass coverslips in 12-well plates and transfected with the indicated siRNA. 48 h post-transfection, cells were infected with SV40 (MOI ~10) for 16 h, fixed, and stained using antibodies against Bap31. To assess viral foci formation, at least 100 cells were counted per condition.

3.5.10 ER-arrival assay

Fractionation of cells into cytosolic, ER, and membrane fractions was used to assess SV40 arrival to the ER, as described previously [47]. In brief, CV-1 cells were seeded on 6 cm plates and transfected with 20 nM scrambled, ATL2, or ATL3 siRNA for 48 h. After 46 h transfection, cells were treated with either 5 ug/uL brefeldin A or DMSO control. After 48 h transfection (2 hours of drug treatment), cells were infected with SV40 (MOI ~5) for 16 h. Cells were then semi-permeabilized by using 0.1% digitonin on ice for 10 mins and centrifuged at 16,000 x g for 10 mins. The resulting supernatant fraction represented the cytosol fraction, while the pellet fraction represented the membrane fraction. The membrane fraction was further treated with 1% Triton X-100 and centrifuged at 16,000 x g for 10 mins, where the resulting supernatant fraction contains ER-localized SV40 [47].

3.5.11 Co-immunoprecipitation

For immunoprecipitation of FLAG-LNP (Fig. 3.5A), COS-7 cells in 10 cm plates were lysed in HN buffer (150 mM NaCl, 50 mM Tris pH 7.4) with 1 mM PMSF and 1% DBC for 15 min on ice, then centrifuged at 16,000 x g for 10 min at 4°C. Supernatant was collected and input (2.5%) removed. 20 uL of anti-FLAG M2 magnetic beads were added to the remainder of each supernatant, and the samples were rotated at 4°C overnight. The beads were washed 3x with lysis buffer and eluted with 3x FLAG peptide at 25°C. For immunoprecipitation of HA-RTN4B in non-infected cells (Fig. 3.5B), the same protocol was followed, except 20 uL of anti-HA magnetic beads were used in place of anti-FLAG beads, and proteins were eluted with 1x sample buffer. For immunoprecipitation of HA-RTN4B in SV40-infected cells (Fig. 3.5C), COS-7 cells were grown in 15 cm plates (2 plates per condition). Cells were infected with SV40 (MOI ~10) for 16 h. Cells were then washed 2x with HBSS, incubated with 50 mM DSP crosslinker for 45 min at 25°C, quenched with 50 mM Tris pH 7.4 for 15 min at 25 °C, and washed 1x with PBS. Following this, cells were lysed in HN buffer with 1 mM PMSF and 1% Triton X-100 for 15 min on ice, then centrifuged at 16,000 x g for 10 min at 4°C. Supernatant was collected and input (1%) removed. 40 uL of anti-HA magnetic beads were added to the remainder of each supernatant, and the samples were rotated at 4°C overnight. The beads were washed and eluted with 1x sample buffer.

3.5.12 Xbp1 splicing

CV-1 cells were transfected with either scrambled or ATL2 siRNA for 48 h. As a positive control, one sample was treated for 2h with 1 mM DTT to induce Xbp1 splicing. Cells were harvested and the total RNA was extracted using the RNeasy Mini Kit (Qiagen; 74104). The

cDNA was then synthesized from the extracted RNA using the iScript Reverse Transcription kit (BioRad; 1708841). Xbp1 fragments were finally amplified using the following primers: 5'-CGCGGATCCGAATGTGAGGCCAGTGG-3' and 5'-GGGGCTTGGTATATATGTGG-3'. To examine the splicing event, the amplified fragments were separated on an acrylamide gel and images acquired with a UVP BioDoc-It Imaging system.

3.6 Acknowledgements

This work was funded by grants from the National Institutes of Health to MP (F31 NS124088) and BT (RO1 AI064296).

With permission from the publisher, this chapter has been adapted from an original publication: *The Atlastin ER morphogenic proteins promote formation of a membrane-penetration site during non-enveloped virus entry. Madison Pletan, Xiaofang Liu, Grace Cha, Yu-Jie Chen, Jeffrey Knupp, and Billy Tsai (2023). Journal of Virology, 97 (8), e0075623.* *https://doi.org/10.1128/jvi.00756-23*.

3.7 Author Contributions

Data contributions for each figure are as follows:

Madison Pletan

Figures 1A, 1B, 1C, 1D, 2A, 2B, 2C, 2D, 3A, 3B, 3C, 3D, 4A, 4B, 4C, 4D, 5A, 5B, 5D, 6A, 6B, 6C

Xiaofang Liu

Figures 1B, 2B, 4B

Grace Cha

Figures 3A, 6A, 6B

Yu-Jie Chen

Figure 4E

Jeffrey Knupp

Figure 5C

3.8 References

1. Weissenhorn W, Dessen A, Calder LJ, Harrison SC, Skehel JJ, Wiley DC. Structural basis for membrane fusion by enveloped viruses. *Mol Membr Biol*. Jan-Mar 1999;16(1):3-9. doi:10.1080/096876899294706

2. Kumar CS, Dey D, Ghosh S, Banerjee M. Breach: Host Membrane Penetration and Entry by Nonenveloped Viruses. *Trends Microbiol*. Jun 2018;26(6):525-537. doi:10.1016/j.tim.2017.09.010

3. Moyer CL, Nemerow GR. Viral weapons of membrane destruction: variable modes of membrane penetration by non-enveloped viruses. *Curr Opin Virol*. Jul 2011;1(1):44-9. doi:10.1016/j.coviro.2011.05.002

4. Tsai B. Penetration of nonenveloped viruses into the cytoplasm. *Annu Rev Cell Dev Biol*. 2007;23:23-43. doi:10.1146/annurev.cellbio.23.090506.123454

5. DeCaprio JA, Garcea RL. A cornucopia of human polyomaviruses. *Nat Rev Microbiol*. Apr 2013;11(4):264-76. doi:10.1038/nrmicro2992

6. Jiang M, Abend JR, Johnson SF, Imperiale MJ. The role of polyomaviruses in human disease. *Virology*. Feb 20 2009;384(2):266-73. doi:10.1016/j.virol.2008.09.027

7. Pinto M, Dobson S. BK and JC virus: a review. *J Infect*. Jan 2014;68 Suppl 1:S2-8. doi:10.1016/j.jinf.2013.09.009

8. Krump NA, You J. From Merkel Cell Polyomavirus Infection to Merkel Cell Carcinoma Oncogenesis. *Front Microbiol*. 2021;12:739695. doi:10.3389/fmicb.2021.739695

9. Howley PM, Livingston DM. Small DNA tumor viruses: large contributors to biomedical sciences. *Virology*. Feb 20 2009;384(2):256-9. doi:10.1016/j.virol.2008.12.006

10. Liddington RC, Yan Y, Moulai J, Sahli R, Benjamin TL, Harrison SC. Structure of simian virus 40 at 3.8-A resolution. *Nature*. Nov 28 1991;354(6351):278-84. doi:10.1038/354278a0

11. Chen XS, Stehle T, Harrison SC. Interaction of polyomavirus internal protein VP2 with the major capsid protein VP1 and implications for participation of VP2 in viral entry. *EMBO J*. Jun 15 1998;17(12):3233-40. doi:10.1093/emboj/17.12.3233

12. Stehle T, Gamblin SJ, Yan Y, Harrison SC. The structure of simian virus 40 refined at 3.1 A resolution. *Structure*. Feb 15 1996;4(2):165-82. doi:10.1016/s0969-2126(96)00020-2

13. Tsai B, Gilbert JM, Stehle T, Lencer W, Benjamin TL, Rapoport TA. Gangliosides are receptors for murine polyoma virus and SV40. *EMBO J*. Sep 1 2003;22(17):4346-55. doi:10.1093/emboj/cdg439

14. Anderson HA, Chen Y, Norkin LC. Bound simian virus 40 translocates to caveolin-enriched membrane domains, and its entry is inhibited by drugs that selectively disrupt caveolae. *Mol Biol Cell*. Nov 1996;7(11):1825-34. doi:10.1091/mbc.7.11.1825

15. Kartenbeck J, Stukenbrok H, Helenius A. Endocytosis of simian virus 40 into the endoplasmic reticulum. *J Cell Biol*. Dec 1989;109(6 Pt 1):2721-9. doi:10.1083/jcb.109.6.2721

16. Schelhaas M, Malmstrom J, Pelkmans L, et al. Simian Virus 40 depends on ER protein folding and quality control factors for entry into host cells. *Cell*. Nov 2 2007;131(3):516-29. doi:10.1016/j.cell.2007.09.038

17. Magnuson B, Rainey EK, Benjamin T, Baryshev M, Mkrtchian S, Tsai B. ERp29 triggers a conformational change in polyomavirus to stimulate membrane binding. *Mol Cell*. Oct 28 2005;20(2):289-300. doi:10.1016/j.molcel.2005.08.034

18. Walczak CP, Tsai B. A PDI family network acts distinctly and coordinately with ERp29 to facilitate polyomavirus infection. *J Virol*. Mar 2011;85(5):2386-96. doi:10.1128/JVI.01855-10

19. Inoue T, Dosey A, Herbstman JF, Ravindran MS, Skiniotis G, Tsai B. ERdj5 Reductase Cooperates with Protein Disulfide Isomerase To Promote Simian Virus 40 Endoplasmic Reticulum Membrane Translocation. *J Virol*. Sep 2015;89(17):8897-908. doi:10.1128/JVI.00941-15

20. Norkin LC, Anderson HA, Wolfrom SA, Oppenheim A. Caveolar endocytosis of simian virus 40 is followed by brefeldin A-sensitive transport to the endoplasmic reticulum, where the virus disassembles. *J Virol*. May 2002;76(10):5156-66. doi:10.1128/jvi.76.10.5156-5166.2002

21. Rainey-Barger EK, Magnuson B, Tsai B. A chaperone-activated nonenveloped virus perforates the physiologically relevant endoplasmic reticulum membrane. *J Virol*. Dec 2007;81(23):12996-3004. doi:10.1128/JVI.01037-07

22. Geiger R, Andritschke D, Friebe S, et al. BAP31 and BiP are essential for dislocation of SV40 from the endoplasmic reticulum to the cytosol. *Nat Cell Biol*. Sep 25 2011;13(11):1305-14. doi:10.1038/ncb2339

23. Walczak CP, Ravindran MS, Inoue T, Tsai B. A cytosolic chaperone complexes with dynamic membrane J-proteins and mobilizes a nonenveloped virus out of the endoplasmic reticulum. *PLoS Pathog*. Mar 2014;10(3):e1004007. doi:10.1371/journal.ppat.1004007

24. Bagchi P, Walczak CP, Tsai B. The endoplasmic reticulum membrane J protein C18 executes a distinct role in promoting simian virus 40 membrane penetration. *J Virol*. Apr 2015;89(8):4058-68. doi:10.1128/JVI.03574-14

25. Ravindran MS, Bagchi P, Inoue T, Tsai B. A Non-enveloped Virus Hijacks Host Disaggregation Machinery to Translocate across the Endoplasmic Reticulum Membrane. *PLoS Pathog*. Aug 2015;11(8):e1005086. doi:10.1371/journal.ppat.1005086

26. Ravindran MS, Engelke MF, Verhey KJ, Tsai B. Exploiting the kinesin-1 molecular motor to generate a virus membrane penetration site. *Nat Commun*. May 24 2017;8:15496. doi:10.1038/ncomms15496

27. Bagchi P, Liu X, Cho WJ, Tsai B. Lunapark-dependent formation of a virus-induced ER exit site contains multi-tubular ER junctions that promote viral ER-to-cytosol escape. *Cell Rep*. Dec 7 2021;37(10):110077. doi:10.1016/j.celrep.2021.110077

28. Dupzyk A, Williams JM, Bagchi P, Inoue T, Tsai B. SGTA-Dependent Regulation of Hsc70 Promotes Cytosol Entry of Simian Virus 40 from the Endoplasmic Reticulum. *J Virol*. Jun 15 2017;91(12)doi:10.1128/JVI.00232-17

29. Dupzyk A, Tsai B. Bag2 Is a Component of a Cytosolic Extraction Machinery That Promotes Membrane Penetration of a Nonenveloped Virus. *J Virol*. Aug 1 2018;92(15)doi:10.1128/JVI.00607-18

30. Ravindran MS, Spriggs CC, Verhey KJ, Tsai B. Dynein Engages and Disassembles Cytosol-Localized Simian Virus 40 To Promote Infection. *J Virol*. Jun 15 2018;92(12)doi:10.1128/JVI.00353-18

31. Clever J, Yamada M, Kasamatsu H. Import of simian virus 40 virions through nuclear pore complexes. *Proc Natl Acad Sci U S A*. Aug 15 1991;88(16):7333-7. doi:10.1073/pnas.88.16.7333

32. Spriggs CC, Badieyan S, Verhey KJ, Cianfrocco MA, Tsai B. Golgi-associated BICD adaptors couple ER membrane penetration and disassembly of a viral cargo. *J Cell Biol*. May 4 2020;219(5)doi:10.1083/jcb.201908099

33. Spriggs CC, Cha G, Li J, Tsai B. Components of the LINC and NPC complexes coordinately target and translocate a virus into the nucleus to promote infection. *PLoS Pathog*. Sep 2022;18(9):e1010824. doi:10.1371/journal.ppat.1010824

34. Chen S, Desai T, McNew JA, Gerard P, Novick PJ, Ferro-Novick S. Lunapark stabilizes nascent three-way junctions in the endoplasmic reticulum. *Proc Natl Acad Sci U S A*. Jan 13 2015;112(2):418-23. doi:10.1073/pnas.1423026112

35. Wang S, Tukachinsky H, Romano FB, Rapoport TA. Cooperation of the ER-shaping proteins atlastin, lunapark, and reticulons to generate a tubular membrane network. *Elife*. Sep 13 2016;5doi:10.7554/eLife.18605

36. Chen YJ, Williams JM, Arvan P, Tsai B. Reticulon protects the integrity of the ER membrane during ER escape of large macromolecular protein complexes. *J Cell Biol*. Feb 3 2020;219(2)doi:10.1083/jcb.201908182

37. Zhu PP, Patterson A, Lavoie B, et al. Cellular localization, oligomerization, and membrane association of the hereditary spastic paraplegia 3A (SPG3A) protein atlastin. *J Biol Chem*. Dec 5 2003;278(49):49063-71. doi:10.1074/jbc.M306702200

38. Hu J, Shibata Y, Zhu PP, et al. A class of dynamin-like GTPases involved in the generation of the tubular ER network. *Cell*. Aug 7 2009;138(3):549-61. doi:10.1016/j.cell.2009.05.025

39. Hu X, Wu F, Sun S, Yu W, Hu J. Human atlastin GTPases mediate differentiated fusion of endoplasmic reticulum membranes. *Protein Cell*. Apr 2015;6(4):307-311. doi:10.1007/s13238-015-0139-3

40. Orso G, Pendin D, Liu S, et al. Homotypic fusion of ER membranes requires the dynamin-like GTPase atlastin. *Nature*. Aug 20 2009;460(7258):978-83. doi:10.1038/nature08280

41. Rismanchi N, Soderblom C, Stadler J, Zhu PP, Blackstone C. Atlastin GTPases are required for Golgi apparatus and ER morphogenesis. *Hum Mol Genet*. Jun 1 2008;17(11):1591-604. doi:10.1093/hmg/ddn046

42. Bian X, Klemm RW, Liu TY, et al. Structures of the atlastin GTPase provide insight into homotypic fusion of endoplasmic reticulum membranes. *Proc Natl Acad Sci U S A*. Mar 8 2011;108(10):3976-81. doi:10.1073/pnas.1101643108

43. Georgiades P, Allan VJ, Wright GD, et al. The flexibility and dynamics of the tubules in the endoplasmic reticulum. *Sci Rep*. Nov 28 2017;7(1):16474. doi:10.1038/s41598-017-16570-4

44. Zhou X, He Y, Huang X, Guo Y, Li D, Hu J. Reciprocal regulation between lunapark and atlastin facilitates ER three-way junction formation. *Protein Cell*. Jul 2019;10(7):510-525. doi:10.1007/s13238-018-0595-7

45. Neufeldt CJ, Cortese M, Scaturro P, et al. ER-shaping atlastin proteins act as central hubs to promote flavivirus replication and virion assembly. *Nat Microbiol*. Dec 2019;4(12):2416-2429. doi:10.1038/s41564-019-0586-3

46. Shen W, Liu B, Liu Z, Feng J, Liu C, Kong X. Host protein atlastin-1 promotes human immunodeficiency virus (HIV-1) replication. *Virol Sin*. Aug 2017;32(4):338-341. doi:10.1007/s12250-017-3998-3

47. Inoue T, Tsai B. A large and intact viral particle penetrates the endoplasmic reticulum membrane to reach the cytosol. *PLoS Pathog*. May 2011;7(5):e1002037. doi:10.1371/journal.ppat.1002037

Chapter 4
Conclusion and Future Directions

4.1 Overview

The endoplasmic reticulum (ER) is a structurally and functionally diverse organelle that extends throughout the cell body and plays a crucial role in maintaining cellular proteostasis, as described in Chapter 1. Various morphogenic proteins serve to curve the ER membrane into tubules (reticulons, RTNs), fuse the tubules together (atlastins, ATLs), and stabilize the resulting 3-way junctions (lunapark, LNP), creating the highly reticulated peripheral ER network. In this dissertation, I demonstrated how these ER junctional sites serve two unexpected functions: 1) sequestering mislocalized nucleoporins as a nuclear pore complex (NPC) quality control mechanism, and 2) supporting the entry pathway of the polyomavirus simian virus 40 (SV40).

4.2 Nuclear protein quality control

One major gap in our understanding of protein quality control was *what cellular mechanisms and machinery protect the stoichiometry and structural integrity of NPCs in mammalian cells*. Since NPC subcomplexes assemble in strict stoichiometries, cells rely on chaperones to mediate NPC biogenesis and surveillance mechanisms to monitor existing NPCs.[1,2] These surveillance mechanisms are best understood in yeast cells, where misassembled or defective NPCs are known to be sequestered at the nuclear envelope and targeted for selective autophagy (termed "NPC-phagy").[3-5] Recent proteomics studies of yeast NPCs have revealed

that some level protein exchange occurs for most Nups, albeit at a very slow rate for components of the inner, outer, and membrane rings; this protein exchange can partially ameliorate damage to individual Nups.[6] In mammalian cells, where Nups may be even longer-lived, less is understood about quality control mechanisms that respond to Nup damage, misassembly, and mislocalization.[7] This topic is of particular interest in the context of aging-related and neurodegenerative disease, as cells from these disease models often exhibit Nup mislocalization and NPC damage or leakiness.[7,8]

4.2.1 Key findings: mislocalized Nups are sequestered at storage sites on the ER membrane

In study described in Chapter 2, we used a siRNA knockdown approach to deplete the key structural protein Nup98, thus disrupting the NPC and forcing mislocalization of a subset of peripheral FG-Nups.[9] Rather than their normal localization lining the nuclear envelope, these Nups formed large, discrete, perinuclear foci colocalizing with the ER marker Bap31. Though these mislocalized Nup aggregates would seem poised for turnover at the ER, we found no evidence that they are subject to autophagy or ERAD. This finding begs the question: why do cells store the Nups at the ER?

To address this question, we sought to disrupt the Nup storage sites by co-depleting the cells of the ER morphogenic proteins RTN3, ATL3, and LNP, which we had identified to be important for the Nup foci formation. Surprisingly, destroying the Nup-foci allowed the "mislocalized" Nups to re-accumulate at the nuclear envelope, apparently reversing the foci phenotype. We next tested the functionality of this re-localization using a nuclear transport assay with mCherry-NLS and large T antigen as substrates. This assay revealed that in the Nup98/ER-morphogenic-protein-depleted cells (where the NPCs are compromised and the Nup storage sites

are disrupted), nucleo-cytoplasmic transport is more impaired when compared to control or Nup98-depleted cells. We speculate that this deficiency may be caused by the misassembled FG-Nups, which are known to aggregate easily[10]; it is possible that they are blocking proper nuclear import by aggregating at the pores. This finding points to a potential purpose for Nup storage at the ER: sequestration of Nups away from the NPCs may prevent them from exerting a dominant negative effect on nucleo-cytoplasmic transport. Analogous to a city that hauls waste from individual houses to a central waste-collection site, the cell may transport excess Nups to a central ER storage site to prevent harm at the nuclear envelope.

The final portion of this research delved into the transport mechanisms behind Nup foci formation. After observing that the Nup foci always formed proximal to MTOCs, we established that intact microtubules and kinesin-1 motors are necessary for trafficking of the misassembled FG-Nups to the ER. Without kinesin-1, the Nups formed small, dispersed foci rather than a single large focus next to the MTOC. (For further discussion of the potential significance of this finding, see Sections 4.4 and 4.5.) Our further observation that kinesin-1 interacts with the misassembled Nup62 under both control and Nup98-depleted conditions suggests that the motor plays a role in trafficking Nup62 under basal and compromised conditions.

4.3 Polyomavirus pathogenesis at the ER

Following receptor-mediated endocytosis and endosomal trafficking, SV40 polyomavirus is delivered to the ER, an infection step unusual for DNA virus entry. The virus takes advantage of ER-resident oxidoreductases to undergo important conformational changes to its major capsid protein, exposing the hydrophobic minor capsid proteins beneath.[11,12] The newly hydrophobic virion can then hijack additional ER proteins to form “foci” membrane penetration sites, where it

can insert itself into the membrane and recruit cytosolic extraction machinery that extracts it into the cytosol.[13] Entrance into the nucleus from the cytosol, which enables SV40 to cause infection, completes its entry journey. Recent studies have exploited high-resolution microscopy strategies to study the virus-induced ER-foci, unveiling that their basic structure consists of flower-like multi-tubular junctions.[14] This fascinating glimpse into the mysterious sub-organellar structure highlighted a key question: *what ER-morphogenic proteins might be involved in stabilizing these complex, highly curved and reticulated membrane regions*?

Previous work in our lab to address this question had identified the RTNs and LNP as important proteins for virus-induced foci formation. Both proteins were shown to mobilize to the ER-foci, where they stabilized membrane curvature/integrity and tubular junctions, respectively.[14,15] The extent to which other ER-morphogenic proteins were hijacked by SV40 to form the foci was still unclear. Since nonenveloped viral penetration of membranes is an ongoing topic of interest in the field, this research question could also shed light on the entry pathways of nonenveloped viruses beyond polyomavirus.

4.3.1 Key findings: SV40 penetration at the ER hijacks the atlastin machinery

As described in Chapter 3, we began to investigate the role of the ATL family in SV40-induced foci formation. By depleting ATL2 and ATL3 with siRNA and performing functional rescue experiments, we established that both ATLs are important for viral pathogenesis, most likely within the same pathway since single and double KD resulted in a similar level of block in virus infection. We further observed that under either ATL2 or ATL3 KD, virions were able to successfully transit to the ER (as shown by a biochemical arrival assay), but there were significantly fewer SV40-induced ER-foci. This pinpointed the mechanistic

involvement of ATL2 and ATL3 at the ER-escape step. Using GTPase-deficient point-mutant constructs, we demonstrated that the GTPase-dependent membrane fusion activity of the ATLs is necessary for infection.

To delve into the mechanistic details of how SV40 utilizes the ER-morphogenic proteins to reshape the peripheral ER, we performed co-immunoprecipitations of the proteins under infected and noninfected conditions. These experiments revealed interactions between ATL3 and RTN, as well as between ATL3 and LNP, even in the absence of SV40. Moreover, under infected conditions, SV40 also interacts with the ATL3-RTN protein complex. This finding was bolstered by immunofluorescence data showing that ATL3 is strongly recruited to the SV40 foci during infection. Taken together, these data suggest that SV40 hijacks an existing ATL3-RTN protein complex at the ER to reshape the membrane into multi-tubular junctions, following which ATL3 recruits LNP to stabilize the foci.

While ATL3 is recruited to the ER-foci and interacts with SV40, ATL2 does not exhibit this relocalization during infection. This surprising contrast between the atlastins raised the question: *how does ATL2 support foci formation if it is not recruited to the foci?* To answer this question, we first noted that ATL2 depletion causes a markedly extended, unbranched ER morphology compared to ATL3 depletion. We therefore considered the possibility that ATL2 plays a more global role in establishing and maintaining general ER morphology, thus allowing the virus to traverse and reshape the ER successfully. While ATL2 depletion did not induce severe ER stress (based on the highly-sensitive, PCR-based Xbp1 splicing assay), it did prevent the interaction of ATL3 with LNP by co-immunoprecipitation. This disruption could partly account for the indirect role of ATL2 in SV40 foci formation and infection. Finally, we observed that overexpression of ATL3 may cross-rescue ATL2 depletion, but the reverse is not true. This

again underscores the specificity of ATL3 involvement: while the more general ATL2 fusogenic activity may be replaced by excess ATL3, ATL2 is unable to perform the specific binding and recruitment activity of ATL3. Our study thus expands our understanding of the individual roles of the ATL family members, a relatively understudied topic.

4.4 Convergence of SV40 penetration with Nup storage

This dissertation discusses how the peripheral ER supports two unexpected—and seemingly unrelated—processes: quality control of nuclear proteins and penetration of a nonenveloped virus. Yet both of these stories center on large, proteinaceous complex being trafficked to the ER, utilizing ER-morphogenic proteins, and forming distinct, Bap31-colocalized perinuclear foci at the ER membrane. Furthermore, the kinesin-dependent Nup foci formation was strongly reminiscent of previous work our lab published on kinesin-dependent SV40 foci formation. In this story, we reported that under kinesin-1 depletion, SV40 particles formed small, dispersed foci rather than large, coalesced foci—an identical phenotype to the one observed with the Nup foci under Nup98/Kif5B double KD.[16]

Curious whether these two biological processes were actually taking place at the same cellular site, we performed a "crossover" experiment by knocking down Nup98 followed by infecting the cells with SV40. We then stained for FG-Nups, SV40 VP2/3, and Bap31 to visualize any resulting foci (see Materials & Methods in Chapter 3 for siRNA treatment protocol and Chapter 4 for foci assay and fixation/staining/immunofluorescence protocol). Confocal microscopy of these cells showed strong colocalization between all 3 foci markers: rather than forming separate foci, the misassembled FG-Nups and SV40 were appearing at the same sites in the ER membrane (Fig. 4.1).

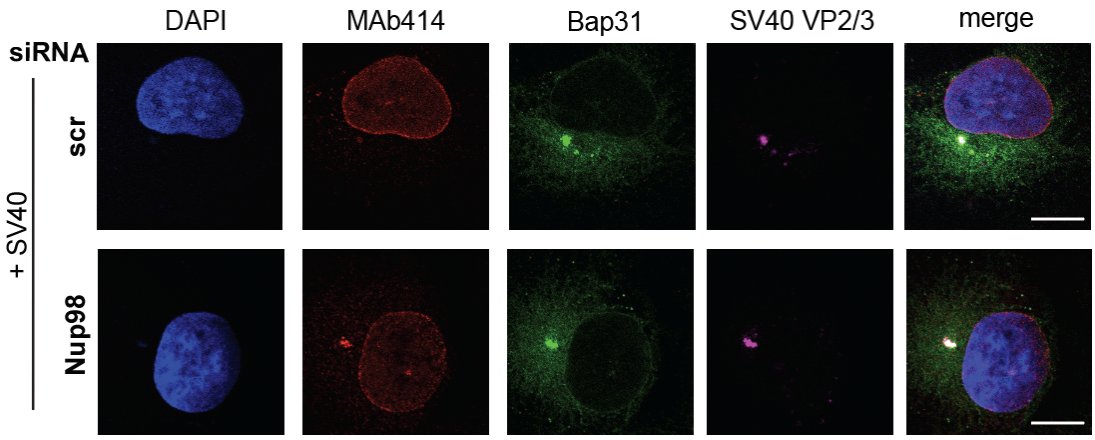

Figure 4.1: The SV40-penetration foci and the mislocalized FG-Nups foci colocalize at the ER

CV-1 cells were transfected with the indicated siRNAs for 24 h, infected with SV40 for 16 h, and stained for FG-Nups (MAb414), ER membrane markers (Bap31), and virus (VP2/3). Scale bars, 10 µm.

Since the two types of foci harness much of the same cellular machinery (including the kinesin motor, RTN3, ATL3, and LNP), we consider two possible explanations for this striking colocalization. First, perhaps one of the proteinaceous cargoes recruits the machinery to a single perinuclear location to form a focus, and the other cargo is also recruited to that site. For example, if the Nup focus has already begun to form by the time the SV40 virions start the membrane penetration process (~32 h after cell seeding and ~8 h after infection), the SV40 virions may naturally be recruited to the ER-morphogenic complex at that nascent focus. Second, perhaps the "foci" represent pre-existing regions of the ER membrane with increased surface area due to the highly-reticulated, multi-tubular junctional structure – this property enables the foci to more readily harbor large, proteinaceous particles. In this model, the SV40 virions are not inducing dramatic ER remodeling as has been postulated, but rather harnessing the structural

characteristics of a pre-existing site. Indeed, one putative function of this site would be protein quality control, as we demonstrate with mislocalized Nups.

4.5 Future directions

4.5.1 What is the significance of the overlapping foci?

As shown in Section 4.4 above, we observe an intriguing convergence of the Nup foci with the SV40 foci at the ER membrane, and it is unclear whether this points to a pre-existing site with highly reticulated, multi-tubular structures. Previous studies have used scanning electron microscopy (SEM) and 3D focused ion beam scanning electron microscopy (FIB-SEM) to probe the structure of virus-induced ER-foci[14]; these techniques could be used to examine cells containing Nup foci as well as normal cells to identify perinuclear, ER-morphogenic-protein dense regions. As the host cell penetration and extraction machinery hijacked by SV40 has been extensively documented,[11] it would also be interesting to examine whether these proteins are also recruited or involved in Nup foci formation.

Additionally, it is likely that the ER tubular junctions support cargoes beyond SV40 and mislocalized Nups. Indeed, previous work from our lab showed that the reticulon family protects ER membrane integrity by relieving mechanical stress in the presence of large misfolded prohormone aggregates *en route* for lysosomal degradation.[15] Given the range of protein aggregates frequently harbored within the ER lumen, it could be fruitful to test the importance of the ER-morphogenic proteins in supporting similar aggregates.[17]

4.5.2 Do the storage sites represent true annulate lamellae?

In their initial findings that knockout of Nup98 causes Nup mislocalization, Wu and colleagues provided TEM images exhibiting ER-derived annulate-lamellae (AL)-like patterns, concluding that the mislocalized Nup aggregates are harbored in AL.[9] To investigate if this observation extends to our Nup98 KD system, we intend to repeat similar microscopy-based studies to identify the characteristic AL patterns in the KD cells. If the Nup foci do indeed represent true AL, our research may shed more light on this mysterious organelle, leading to more research questions regarding cells that have prominent AL basally. Is the kinesin-1 motor involved in typical AL biogenesis? Do typical AL form proximal to the MTOCs? Does AL formation rely on the activity of ER-morphogenic proteins (as the AL are known to be embedded in stacked layers of ER-derived membranes)? All these questions remain unanswered for the "last frontier in cellular organelles."[18]

4.5.3 What is the ultimate fate of the mislocalized Nups?

Due to the technical limitations of cell growth and siRNA knockdown timelines, our study of Nup foci did not examine the fate of the misassembled FG-Nup foci past ~72 h, where they appeared persistent and static. Treatment with proteasomal and lysosomal inhibitors also did not cause a buildup of the ER-localized Nups, suggesting that they are not subject to degradation by ERAD or ER-phagy. We therefore posited that cells store the Nups indefinitely at the ER, perhaps with the purpose of re-integrating them in new, functional nuclear pores in the future (as has been proposed for AL functionality).[19,20] Do the Nups remain at the ER in perpetuity, or are they eventually reused in NPCs or turned over?

Answering this question could require use of a Nup98 KO cell line, which could be transfected with an inducibly tagged FG-Nup whose subcellular location could be tracked via

live-cell imaging.[21] Tagging a single "pulse" of Nups would enable researchers to pinpoint the journey and fate of those specific mislocalized Nups. This could also provide more information regarding the role and fates of AL in new cell types.

4.5.4 What other viruses might take advantage of the ER morphogenic proteins?

SV40 is not the only virus to hijack the ER morphogenic proteins in order to carry out its infectious pathway. A recent publication from our lab revealed that severe acute respiratory syndrome coronavirus-2 (SARS-CoV-2) utilizes both RTN3 and RTN4 to promote formation of double-membrane vesicles for its replication.[22] Similarly, in flavivirus infection, ATL2 and ATL3 are thought to play roles in viral replication and maturation/secretion, respectively.[23] However, the full extent to which the remaining ER-morphogenic proteins may be involved in replication for these viruses is not known. Furthermore, given the wide range of viruses that rely on the ER for some aspect of their infectious cycle, it is possible that many more viruses exploit the atlastins and their shaping partners to manipulate host cell membranes.[24,25] Understanding how various viruses rely on and hijack the ER could illuminate possible therapies to treat these infectious agents.

4.6 Final remarks

In sum, my dissertation research reveals the extraordinary adaptability and versatility of the ER in supporting two distinct cellular processes: harboring of a nuclear protein and penetration of a nonenveloped virus. In Chapter 2, I describe a novel protein quality control mechanism by which the ER sequesters excess and potentially harmful Nups, preventing them

from disrupting nucleo-cytoplasmic transport. I also identify several key cellular machinery components necessary to build and maintain this ER storage site. In Chapter 3, I elucidate how pieces of the same machinery—notably, ATL2 and ATL3—are exploited by the virus SV40 to build a multi-tubular ER penetration site for its entry pathway. In this study, I outline the mechanistic basis for ATL2 and ATL3's overlapping but distinct roles in fusing ER tubules and recruiting other important proteins to form the viral foci. Fundamentally, my research illustrates how basic aspects of cell biology, such as ER architecture, can be harnessed for disparate processes, both preserving the cell (in the case of protein quality control) and harming the cell (in the case of viral infection). By studying the mechanisms and interactions of highly-conserved yet critical ER proteins, basic cell biology research can illuminate many wide-ranging lessons about unexpected diseases.

4.7 References

1. Agote-Arán A, Lin J, Sumara I. Fragile X-Related Protein 1 Regulates Nucleoporin Localization in a Cell Cycle-Dependent Manner. *Front Cell Dev Biol*. 2021;9:755847. doi:10.3389/fcell.2021.755847

2. Rouvière JO, Bulfoni M, Tuck A, Cosson B, Devaux F, Palancade B. A SUMO-dependent feedback loop senses and controls the biogenesis of nuclear pore subunits. *Nat Commun*. Apr 25 2018;9(1):1665. doi:10.1038/s41467-018-03673-3

3. Lee CW, Wilfling F, Ronchi P, et al. Selective autophagy degrades nuclear pore complexes. *Nat Cell Biol*. Feb 2020;22(2):159-166. doi:10.1038/s41556-019-0459-2

4. Tomioka Y, Kotani T, Kirisako H, et al. TORC1 inactivation stimulates autophagy of nucleoporin and nuclear pore complexes. *J Cell Biol*. Jul 6 2020;219(7)doi:10.1083/jcb.201910063

5. Webster BM, Colombi P, Jäger J, Lusk CP. Surveillance of nuclear pore complex assembly by ESCRT-III/Vps4. *Cell*. Oct 9 2014;159(2):388-401. doi:10.1016/j.cell.2014.09.012

6. Hakhverdyan Z, Molloy KR, Keegan S, et al. Dissecting the Structural Dynamics of the Nuclear Pore Complex. *Mol Cell*. Jan 7 2021;81(1):153-165.e7. doi:10.1016/j.molcel.2020.11.032

7. D'Angelo MA, Raices M, Panowski SH, Hetzer MW. Age-dependent deterioration of nuclear pore complexes causes a loss of nuclear integrity in postmitotic cells. *Cell*. Jan 23 2009;136(2):284-95. doi:10.1016/j.cell.2008.11.037

8. Coyne AN, Rothstein JD. Nuclear pore complexes - a doorway to neural injury in neurodegeneration. *Nat Rev Neurol*. Jun 2022;18(6):348-362. doi:10.1038/s41582-022-00653-6

9. Wu X, Kasper LH, Mantcheva RT, Mantchev GT, Springett MJ, van Deursen JM. Disruption of the FG nucleoporin NUP98 causes selective changes in nuclear pore complex stoichiometry and function. *Proc Natl Acad Sci U S A*. Mar 13 2001;98(6):3191-6. doi:10.1073/pnas.051631598

10. Milles S, Huy Bui K, Koehler C, Eltsov M, Beck M, Lemke EA. Facilitated aggregation of FG nucleoporins under molecular crowding conditions. *EMBO Rep*. Feb 2013;14(2):178-83. doi:10.1038/embor.2012.204

11. Chen YJ, Liu X, Tsai B. SV40 Hijacks Cellular Transport, Membrane Penetration, and Disassembly Machineries to Promote Infection. *Viruses*. Oct 5 2019;11(10)doi:10.3390/v11100917

12. Speckhart K, Williams JM, Tsai B. How DNA and RNA Viruses Exploit Host Chaperones to Promote Infection. *Viruses*. May 21 2021;13(6)doi:10.3390/v13060958

13. Woo TT, Williams JM, Tsai B. How host ER membrane chaperones and morphogenic proteins support virus infection. *J Cell Sci*. Jul 1 2023;136(13)doi:10.1242/jcs.261121

14. Bagchi P, Liu X, Cho WJ, Tsai B. Lunapark-dependent formation of a virus-induced ER exit site contains multi-tubular ER junctions that promote viral ER-to-cytosol escape. *Cell Rep*. Dec 7 2021;37(10):110077. doi:10.1016/j.celrep.2021.110077

15. Chen YJ, Williams JM, Arvan P, Tsai B. Reticulon protects the integrity of the ER membrane during ER escape of large macromolecular protein complexes. *J Cell Biol*. Feb 3 2020;219(2)doi:10.1083/jcb.201908182

16. Ravindran MS, Engelke MF, Verhey KJ, Tsai B. Exploiting the kinesin-1 molecular motor to generate a virus membrane penetration site. *Nat Commun*. May 24 2017;8:15496. doi:10.1038/ncomms15496

17. Knupp J, Pletan ML, Arvan P, Tsai B. Autophagy of the ER: the secretome finds the lysosome. *Febs j*. Dec 2023;290(24):5656-5673. doi:10.1111/febs.16986

18. Kessel RG. Annulate lamellae: a last frontier in cellular organelles. *Int Rev Cytol*. 1992;133:43-120. doi:10.1016/s0074-7696(08)61858-6

19. Hampoelz B, Mackmull MT, Machado P, et al. Pre-assembled Nuclear Pores Insert into the Nuclear Envelope during Early Development. *Cell*. Jul 28 2016;166(3):664-678. doi:10.1016/j.cell.2016.06.015

20. Ren H, Xin G, Jia M, et al. Postmitotic annulate lamellae assembly contributes to nuclear envelope reconstitution in daughter cells. *J Biol Chem*. Jul 5 2019;294(27):10383-10391. doi:10.1074/jbc.AC119.008171

21. England CG, Luo H, Cai W. HaloTag technology: a versatile platform for biomedical applications. *Bioconjug Chem*. Jun 17 2015;26(6):975-86. doi:10.1021/acs.bioconjchem.5b00191

22. Williams JM, Chen YJ, Cho WJ, Tai AW, Tsai B. Reticulons promote formation of ER-derived double-membrane vesicles that facilitate SARS-CoV-2 replication. *J Cell Biol*. Jul 3 2023;222(7)doi:10.1083/jcb.202203060

23. Neufeldt CJ, Cortese M, Scaturro P, et al. ER-shaping atlastin proteins act as central hubs to promote flavivirus replication and virion assembly. *Nat Microbiol*. Dec 2019;4(12):2416-2429. doi:10.1038/s41564-019-0586-3

24. Chen YJ, Bagchi P, Tsai B. ER functions are exploited by viruses to support distinct stages of their life cycle. *Biochem Soc Trans*. Oct 30 2020;48(5):2173-2184. doi:10.1042/bst20200395

25. Inoue T, Tsai B. How viruses use the endoplasmic reticulum for entry, replication, and assembly. *Cold Spring Harb Perspect Biol*. Jan 1 2013;5(1):a013250. doi:10.1101/cshperspect.a013250